Supplement of Atmos. Meas. Tech., 11, 6231–6257, 2018
https://doi.org/10.5194/amt-11-6231-2018-supplement

Atmospheric Measurement Techniques
Open Access
EGU

Supplement of

The Fifth International Workshop on Ice Nucleation phase 2 (FIN-02): laboratory intercomparison of ice nucleation measurements

Paul J. DeMott et al.

Correspondence to: Paul J. DeMott (paul.demott@colostate.edu)

S.1 Direct sampling instrument systems

Online INP measurement systems are cloud chambers or instruments using continuous flow systems to assess INPs. Most have been reported on in the literature or will be in the near future, and some have a record of reported data of more than 20 years. Most of these systems are documented to the extent that they could easily be reproduced, and in some cases certain ones have a legacy in an earlier version of one type. This will be noted in the descriptions below.

S.1.1 AIDA (Aerosol Interaction and Dynamics in the Atmosphere) cloud simulation chamber

The Aerosol Interaction and Dynamics in the Atmosphere (AIDA) cloud simulation chamber, which consists of an 84 m^3 isothermal aluminum vessel, is a comprehensive experimental facility that can be used for recreating supercooled clouds in the vessel (Möhler et al., 2003). More specifically, the chamber conditions are precisely controlled by mechanically pumping air in the vessel, inducing concurrent and homogeneous reduction of both gas temperature and pressure. The resulting so-called expansion cooling provides a wide range of simulated atmospheric in-cloud conditions, such as temperature (60 to -90°C with an uncertainty ± 0.3°C), pressure (~1000 to below 1 hPa) and relative humidity (from ~0% to above water saturation). In such cloud simulation experiments, spontaneous droplet activation and ice crystal formation occur in simulated supercooled clouds at or above saturation with respect to water and ice (e.g., Möhler et al., 2005; Niemand et al., 2012). Further, AIDA is unique since its cloud experiments are systematically performed with atmospherically relevant droplet sizes (i.e., a few to tens of micrometer diameter at the largest) as well as under atmospherically relevant cooling rate; i.e., an average cooling rate of 1.7 ± 0.1 (standard error) °C min^{-1}.

Besides its central function as a cloud emulator, the AIDA chamber can be also utilized as a platform for multiple instruments to investigate aerosol-cloud interactions and cloud microphysics in ice nucleation experiments (*DeMott et al.*, 2011). During FIN-02, similar to previous AIDA studies (e.g., Wagner et al., 2011; Hiranuma et al., 2014a and 2014b), a combination of 6 online instruments, including (1) a condensation particle counter (CPC, TSI, Model 3076), (2) a scanning mobility particle sizer (SMPS, TSI, Model 3080 DMA and Model 3010 CPC), (3) an aerosol particle sizer (APS, TSI, Model 3321), (4) the white light aerosol spectrometer optical particle counters (Welas-OPCs, Palas, Sensor series 2300 and 2500; Benz et al., 2005), (5) a tunable diode laser (TDL) water vapor absorption spectroscopy (Fahey et al., 2014) and (6) a home-built device for scattering intensity measurement for the optical detection of ice (hereafter SIMONE - German abbreviation for Streulicht-Intensitätsmessungen zum optischen Nachweis von Eispartikeln; Schnaiter et al., 2012), used to characterize the physical properties of aerosol and hydrometeors (droplets and ice crystals) formed during the AIDA expansion experiments with a detection limit for number concentration of 0.1 cm^{-3}. It is noteworthy that, in dense supercooled liquid clouds, the AIDA-TDL data is offset by +5% in order to match the liquid-phase saturation (Murphy and Koop, 2005) conditions expected for the immersion freezing event. The reason for this systematic deviation of the TDL measurement from the expected saturation is unclear. More technical details on individual instruments and their applications at the AIDA facility are given in above listed publications.

S.1.2 CFDC-CSU (Continuous Flow Diffusion Chamber - Colorado State University)

The Colorado State University (CSU) Continuous Flow Diffusion Chamber (CFDC) operating principles are described in the earlier works of Rogers (1988), Rogers et al. (2001) and Eidhammer et al. (2010). The current versions of the CFDC-CSU used in ground based (CFDC-1F) and aircraft studies (CFDC-1H) are geometrically identical and composed of cylindrical walls that are coated with ice via flooding and expelling water from the chamber when the walls are set at a controlled temperature of ~-27°C before each experimental period. The plate separation is 1.12 cm prior to ice application, which has a typical thickness of 0.015 cm. The chamber is divided into two sections vertically, separated by a Delrin collar. A temperature gradient between the colder (inner) and warmer (outer) ice walls in the upper 50 cm "growth" section creates an ice supersaturated field into which an aerosol lamina is directed. Vapor pressure relations used within the analytical equations given in Rogers et al. (2001) are taken from Murphy and Koop (2005). The Delrin inlet manifold has a stainless-steel knife-edge ring threaded into it, so that aerosol flow is directed centrally between two sheath flows of clean and dry air. The ratio of aerosol and sheath flows can be varied, but typically the aerosol lamina represents 15% of the 10 L min^{-1} total flow. Ice crystals forming on INPs in the growth region of the chamber enter the lower 30 cm "evaporation" section of the chamber where the two walls are held equivalently to the cold (inner) wall temperature. As shown by DeMott et al. (2015), residence time in the growth region is approximately 5 s under conditions used in the present study, although residence at prescribed steady state conditions is probably on the order of 3s, followed by 2 s in the evaporation regime. When the temperature gradient in the growth section is adjusted for water supersaturated conditions that activate cloud droplets in the aerosol lamina, these will evaporate to haze sizes in the evaporation section, at least up to some water relative humidity (RH_w) where they survive, referred to by many as the droplet breakthrough RH_w. Until that high RH_w, only ice crystals and haze particles will exit the CFDC. Ice crystals and aerosols exiting the CFDC at sizes above approximately 500 nm are counted with an optical particle counter (OPC), where the two populations are distinguished in different size modes. For the data collected in this work, we count all particles in size bins above 3 μm as ice particles when not encountering droplet breakthrough. The cut-channel used for analysis of activated ice crystals at a calibrated 3 μm size was channel 50 for FIN-02. In usual operation, aerosol particles larger than 2.4 μm are removed by a set of inertial impactors prior to the chamber inlet to eliminate misidentification as ice crystals, but the impactors were removed for all data reported in this paper. Data archive files indicate times when impactors were used in selected experiments. Some experiments with the impactors in place will be reported in the paper summarizing blind inter-comparisons.

CFDC-1F measurements for FIN-02 were ideally made via slowly scanning RH_w (~1% min^{-1}) at single temperatures, including below and above water saturation to identify the maximum freezing activity prior to the point that water droplets "breakthrough" the lower evaporation section. The RH_w of droplet breakthrough was also identified whenever possible, but this higher RH_w was not always achieved. Figure S1 shows an example for which dRH_w/dt was kept to close to 0.5 % min^{-1}.

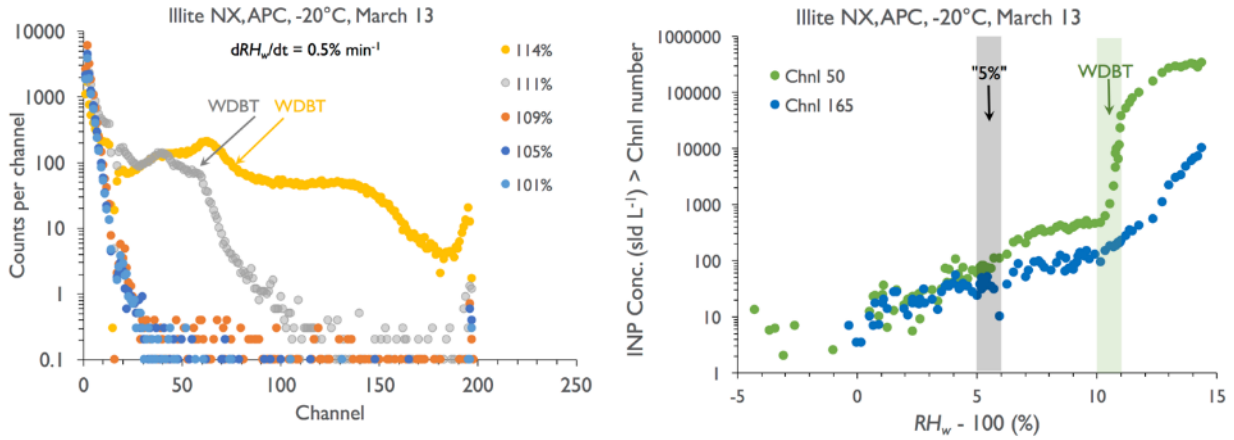

Fig. S.1. Example of data from a slow RH_w scan (~0.5% min^{-1}) with the CFDC-CSU instrument while sampling illite NX and processing it at a temperature of -20°C on March 13, 2015. Each OPC channel size spectra (at the RH_w values in the legend) in the left panel or single point in the right panel represents a 10 s interval. In the left panel, the spectra indicating water droplet breakthrough (WDBT) are indicated by the progressive appearance of a high concentration mode of particles becoming more prominent as RH_w is further increase from 111 to 114%. This point is clear also in the cumulative apparent INP concentration at sizes larger than the standard cut-point for ice at 3 μm (Chnl 50). INP concentrations are referenced for this study primarily at 105% RH_w, which is computed as an average over the range 105 to 106%. As previously reported (DeMott et al., 2015), the maximum INP concentration prior to WDBT is a factor three to four larger than values referenced to 105% RH_w in this case. The comparability of Chnl 50 and Chnl 165 data at RH_w up to 105% makes it clear that most of the first ice crystals nucleated grow to large sizes. This is the basis for using Chnl 165 in cases where aerosol particles were present already at sizes >3 μm before the start of an RH_w scan.

Higher ice cut-point sizes were applied in cases where sufficient large aerosol particles were present initially to "pollute" standard ice size channels. This was a peculiarity of the laboratory study that is not encountered in atmospheric sampling. A higher cut-size for ice was selected to derive INP concentrations from these data because it was expected that large aerosols might retain some water after liquid particle activation and thereby show up even at sizes between channel 50 and some larger channel in the OPC at the exit of the CFDC. The appropriateness of this procedure is demonstrated for a typical experiment Fig. S1. In all cases, the larger cut-size selected and reported is listed as channel 165 in the CFDC-CSU archive files. The cut size employed in each experiment is also noted in Table S1. Note that the channel size is not linearly related to particle size, but typically follows a square relationship to channel, and hence, channel 165 is likely in the range of 5 μm. This was not calibrated. An example of correction for aerosols polluting typical ice cut-size channels by using Chnl 165 for ice definition is shown in Fig. S2.

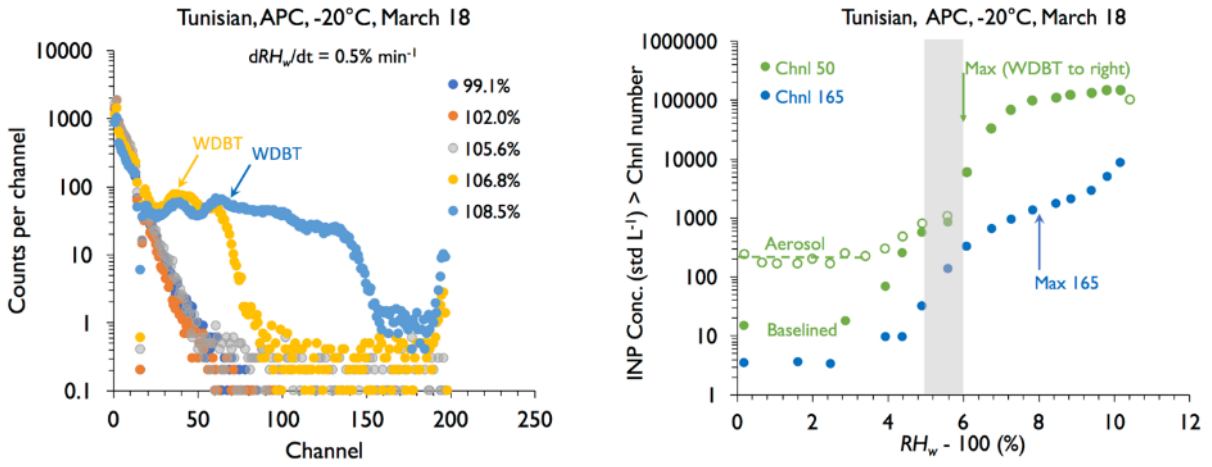

Fig. S2. As in Fig. S1, but for the Tunisian dust experiment on March 18 (Fig. 5) in which aerosols were already present at "ice" channel sizes in the APC when the RH_w scan was initiated in the CFD-CSU instrument (without the upstream impactor in place to remove >2.5 µm particles). In this case, WDBT occurs sooner, despite the slow dRH_w/dt scan. After subtracting the aerosol background, the Chnl 50 data (standard "ice" channel) resemble the Chnl 165 data. Nevertheless, to be conservative, the Chnl 165 data is used to define ice in these cases. It can be seen that the Chnl 165 data also allows definition of a maximum INP concentration in this case.

It was noted in a few experiments, most notably for K-feldspar, that what appeared similar to droplet breakthrough even in the absence of aerosol "pollution", occurred at low water supersaturations. We hypothesize this to be due to small ice crystal formation occurring for evaporating droplets in the lowered temperature region of the evaporation section of the CFDC-CSU instrument, a consequence of both exceeding desired dRH_w/dt rates and the steep activation function of K-feldspar versus temperature. This is demonstrated in Fig. S3, where OPC data from contrasting AIDA chamber sampling experiments on March 20 and March 23, the two days plotted in Fig. 11 of the manuscript, are shown. The discontinuous and strong rise in ice activation at moderate supersaturation, especially noted on March 23 when dRH_w/dt exceeded twice the desired rate for scanning, had not been seen in previous studies (DeMott et al., 2015), just as it is not evident in Fig. S1 or S2. That is, normally, INP freezing in the growth region of the instrument will grow to larger sizes, and not be present frozen at near to the size of activated cloud droplets in the CFDC growth section. While Fig. S3 shows that use of Chnl 165 may derive the most appropriate INP concentrations for relating to the CFDC processing temperature in these cases, Chnl 50 data is plotted in Fig. 11 to emphasize this discovered CFDC sampling issue for K-feldspar in the temperature region near -20°C. RH_w scan rates exceeded 1% min^{-1} in two other K-Feldspar experiments on March 18, one in the APC and one in the AIDA chamber, so these data are not included in Fig. 6 and Fig. 11. Although this situation is considered unusual, as scanning RH_w is not a practice that is often operationally practiced in the field (i.e., constant values or steps of RHw are used), these findings may motivate testing reconfiguration of the CFDC-CSU instrument so that the evaporation section presents warming instead of cooling. This could be accommodated simply by configuring the inner cylindrical wall to be the warmest wall instead of the coldest wall.

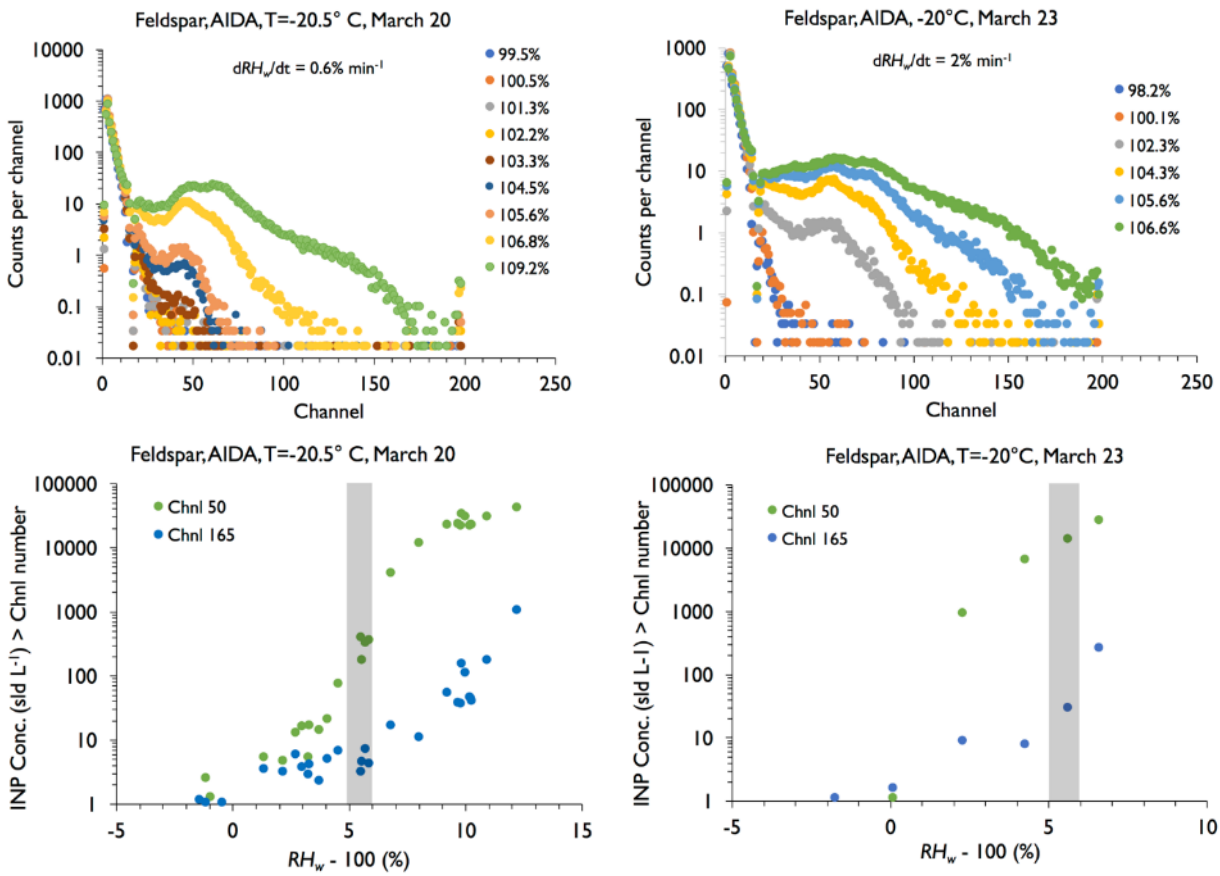

Fig. S3. Spectral and cumulative INP > specific channel plots as in Fig. S2, but for the K-feldspar experiments used to define the low (left panels, March 20, 2015) and high (right panels, March 23, 2015) CFDC-CSU INP concentration data points in Fig. 11 of the manuscript. The occurrence in these cases of "small ice" by 5% water supersaturation is distinct from Fig. S1 despite the absence of aerosol "pollution" of the initial spectra and similar dRH_w/dt rates. The unexpected population of small ice crystals are believed to result from "late" freezing as liquid particles cool before completely evaporating upon entering the evaporation section of this instrument. In the experiment on March 23, dRH_w/dt was three times faster, far above the desirable rates. Less steady control of RH_w led to even stronger growth of the small ice crystal mode and likely overestimation of INP (via the standard Chnl 50 ice point definition) attributable to the processing temperature of -20°C.

Interval periods occurred during RH_w scanning in which the aerosol sample was filtered in order to determine background frost influences on ice particle counts in the OPC, as described in prior publications (e.g., DeMott et al., 2015; Schill et al., 2016). Following Schill et al. (2016), sample period concentrations are those with the interpolated background concentrations of adjacent filter periods subtracted. The standard deviation derived from Poisson counting statistics from both the sample and the interpolated background concentrations were added in quadrature to obtain the INP concentration error. Concentrations are considered significant if they are 1.64 times larger than the INP concentration error, which corresponds to the Z statistic at 95% confidence for a one-tailed distribution.

Particle losses in the aerosol impactor and the inlet manifold of the CFDC have been previously estimated as 30% of total condensation nuclei when sampling ambient air (Rogers et al., 2001), but only 10% for aerosols in the 100 to 800 nm size range based on laboratory tests (Prenni et al., 2009). We apply the 10% correction to all CFDC data herein. Temperature uncertainty is ± 0.5°C at the reported CFDC lamina processing temperature (Hiranuma et al., 2015). RH_w uncertainty depends inversely on temperature, and has been estimated as ± 1.6, 2 and 2.4 % at -20, -25, and -30°C, respectively (Hiranuma et al., 2015).

S.1.3 CFDC-TAMU (Continuous Flow Diffusion Chamber - Texas A&M University)

The Texas A&M Continuous Flow Diffusion Chamber (CFDC-TAMU), including a Cloud Aerosol Spectrometer with Polarization (CASPOL) is an apparatus designed to measure the concentration, backscatter, and depolarization ratio of ice crystals nucleated under controlled conditions. The CFDC, built at Texas A&M University, measures the nucleation and growth of ice crystals under well-controlled temperature and supersaturation conditions (Rogers et al., 2001; Glen and Brooks, 2014; McFarquhar et al., 2011; Zenker et al., 2017). Leaving the CFDC, samples enter the CASPOL (Droplet Measurement Technologies, Inc.) which counts the ice crystals activated on INIPs and determines the optical properties of individual ice crystals at 680 nm (Glen and Brooks, 2014). An inlet at the top of the CFDC allows for an aerosol stream to enter into an annular chamber. Here, the sample air passes between two laminar flows of dry filtered air. The walls of the chamber are coated with ice and held at different temperatures in order to create a controlled supersaturation field between the walls. The aerosol sample has the potential to nucleate and form ice crystals as it travels through this controlled supersaturation region.

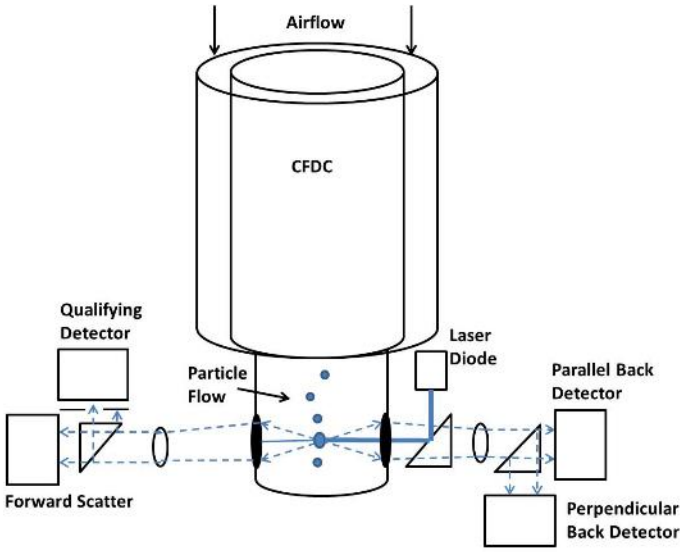

Figure S4: Schematic of the CFDC-TAMU with CASPOL illustrating how the particles are analyzed by the CASPOL after exiting the CFDC.

After nucleation and growth of ice crystals have occurred in the CFDC, the ice crystals are counted by the CASPOL based on size discrimination. The CASPOL employs 3 detectors which measure light scattered in the forward (4°-12°) and backward (168°-176°) directions. The concentration and size of IN are determined by the forward

scattering detector. Backscatter light is split between two detectors, which measure the parallel and perpendicularly polarized light, respectively. The back detectors are used to determine the backscattering intensity and the depolarization ratio of individual ice crystals (Fig. S4).

During FIN-02, TAMU CFDC experimental uncertainty in concentration was +/- 39% based on instrument uncertainties in sheath and total flow rates, particle losses within the CFDC and in the transition zone between the CFDC and CASPOL, background corrections, icing thickness, and CASPOL uncertainties (choice of bin size, coincidence of multiple particles). In FIN-02, uncertainty in supersaturation arose mainly from the possible separation of the hydrophobic material on the lower section of the warm (inner) wall (used to induce evaporation) by as much as 2 mm. Assuming laminar flow considerations and that the hydrodynamic flow is fully developed, this causes an uncertainty in SS_w of +/- 1.75%. The use of spheres to calibrate the CASPOL may lead to uncertainties in particle sizing for aspherical particles. In an earlier version of the CFDC-TAMU, sample air flowing from the CFDC to the CASPOL was observed to warm, causing an estimated ice loss corresponding to a small decrease in radius of less than 1% below ~ -50°C and unquantified changes in the associated optical properties (Glen and Brooks, 2014). Prior to FIN0-2, the connection between the CFDC and CASPOL has been modified to eliminate this warming.

S.1.4 INKA (Ice Nucleation Instrument of the Karlsruhe Institute of Technology)

The new INKA (Ice Nucleation Instrument of the Karlsruhe Institute of Technology) is a continuous flow diffusion chamber that is based on the design of Rogers (1988) and was built in cooperation with Colorado State University. The INKA instrument is most specifically modeled after the Colorado State University "laboratory" CFDC (Archuleta et al., 2005) and is described in detail in Schiebel (2017). INKA is a longer column version of the CSU CFDC-1H, but with cooling baths for temperature control. INKA's ice nucleation chamber consists of concentrically aligned copper tubes that have been ebonized for wetting purpose and are individually cooled via external chillers to temperatures as low as -60°C. During operation, the side walls of the 1 cm annular gap between the copper tubes are coated with a 0.4 mm ice layer. A total flow of 12.5 L min^{-1}l passes through the chamber. This flow consists of 5% to 10% of sample flow encased in 90% to 95% of particle free sheath air. The sample to sheath flow ratio was adapted during the FIN-02 measurements according to available aerosol concentration and fresh synthetic air was used as for sheath flow.

The total length of the INKA chamber is 150 cm, with the upper 2/3 acting as so called "nucleation and growth section". Here, the sample is exposed to defined water vapor levels above ice saturation by setting both walls to different temperatures. Following Rogers (1988), the temperature and relative humidity in the sample lamina is calculated for the measured wall temperatures, flow velocity and sample to sheath ratio. Depending on the chosen conditions, deposition and/or immersion freezing mode nucleation can be studied. During FIN-02, we stepwise increased the relative humidity at the sample location while keeping the laminar mean temperature constant. For most samples, we studied a range from 90% to 110% RH_w with respect to liquid water. INP concentrations close to 105% RH_w were used for intercomparison with other immersion freezing methods. In between the investigated RH_w-plateaus, the chamber background was measured by effective filtering of aerosols from the sample flow.

The lower 1/3 of the outer wall can be cooled separately from the upper section. Here, a Delrin spacer inhibits thermal contact between the outer wall copper pieces. For the FIN-02 measurements, we chose to couple the cooling of the inner wall and the outer lower wall, thus setting those to equal temperatures (colder than the upper outer wall). With entry into this so called "droplet evaporation section", the ice particles, any existent droplets and interstitial aerosol particles quickly adapt to the abruptly lowered vapor pressure. As the sample is still held at ice saturation, the formed ice crystals are able to grow further while droplets will shrink due to evaporation, thus enabling the identification and counting of ice particles by an optical particle counter (Climet CI-3100) at the chamber outlet.

Although the air samples taken from AIDA or the APC were rather dry, we used silica gel equipped diffusion dryers to ensure consistent conditioning. To prevent the erroneous classification of large inactivated aerosol particles as ice particles by OPC counting, an impactor with a well-defined flow dependent cut-off size of about 2 µm was used in some experiments. To account for particle loss in the impactor, the particle number concentrations were measured with and without the impactor in place, at a position before the chamber inlet, using a condensation particle counter (TSI model 3772). Particle losses in the sampling line were found to be negligible.

A detailed description of the INKA instrument will be given in Schiebel (2017). This paper will also include a thorough analysis of measurement uncertainties. For the FIN-02 campaign we estimate an uncertainty in temperature of 1 K and an uncertainty in particle number concentrations of 20%.

S.1.5 PINC (Portable Ice Nucleation Chamber – ETH Zurich)

The Portable Ice Nucleation Chamber (PINC, Chou et al., 2011) is a parallel-plate vertical continuous flow diffusion chamber and the portable version of the Zurich Ice Nucleation Chamber (ZINC, Stetzer et al., 2008). The general operational principle follows that of Rogers (1988) as described in the previous sections. Prior to the ice nucleation experiments, an ice layer is applied to the chamber walls (568 x 300 mm) which have a distance of 1cm between them. A temperature gradient is set between the chamber walls that generates a parabolic supersaturation profile with a peak saturation close to the center plane. The sample aerosol is introduced with a flow rate of 1 $lmin^{-1}$ and layered between two particle-free sheath air flows of 4.5 $lmin^{-1}$ ensuring a narrow, centered sample lamina. Aerosol particles are introduced into the chamber and may nucleate and grow to ice crystals during a residence time of 4-5 s in the ice nucleation and growth section before entering the evaporation section, where both walls are isothermally set to the warm wall temperature. This creates a subsaturated environment with respect to water in which any formed droplets evaporate while ice crystals are maintained at the ice saturated conditions. Exiting aerosol particles and ice crystals are detected at the bottom of the chamber by an optical particle counter (Lighthouse R5104). In this study, particles larger than a set size threshold of 3 µm are counted as ice crystals and no impactor was used upstream of the chamber to limit larger aerosol particles from being sampled. Measurements were performed as RH_w scans (<2 % RH min^{-1}) at prescribed temperatures from ice saturation to above water saturation up to an RH_w at which ice crystals cannot be distinguished from droplets based on their size (droplet breakthrough). Above water saturation conditions condensation freezing and immersion freezing cannot be distinguished in this setup. Before and after each scan, background concentrations of ice crystals in the chamber are obtained by sampling filtered air. The background counts are linearly interpolated between two filter periods and subtracted from the sample signal and the INP concentration

is determined. The INP active fraction is calculated as the ratio of ice crystals detected with the OPC to the number of total aerosol particles measured with a CPC on the aerosol chambers (AIDA or APC).

The accuracy of the temperature sensors is ±0.1°C and the variation of the temperature across the theoretically defined sample lamina is ±0.4°C, which corresponds to an uncertainty in RH_w of ±2 % (Chou et al., 2011). The uncertainty in INP concentration is 10 % due to counting by the OPC and uncertainty in active fraction is 14% including an additional uncertainty of 10 % for the measurement of the total aerosol particle concentration. Chamber characterization experiments with PINC revealed particle losses below 5 % without the use of an impactor upstream of PINC (Boose et al., 2016).

S.1.6 PIMCA-PINC (Portable Immersion Mode Cooling Chamber - ETH Zurich)

PIMCA is a vertical extension of the PINC instrument and used to investigate the ice nucleating ability of aerosol particles explicitly in the immersion mode (Kohn et al., 2016). After entering PIMCA aerosol particles are activated to cloud droplets at 40°C in supersaturated conditions with respect to water (RH_w>115 %) by applying a temperature gradient of ΔT = 25°C between two chamber walls with constantly wetted filter paper. The droplets with single-immersed aerosol particles are then supercooled to the desired ice nucleation temperature prior to entering PINC, which is held at water saturation conditions. Typical flow rates in the PIMCA-PINC setup are 0.6 L min^{-1} sample flow and 2.2 L min^{-1} particle-free sheath air on either side of the aerosol lamina. A frozen fraction of entering cloud droplets is calculated by the ratio of ice crystals to the number of total particles (cloud droplets and ice crystals) in the sample volume using the Ice Optical DEpolarization detector (IODE, Nicolet et al., 2010), which is attached to PINC. Measurements with PIMCA-PINC are performed by scanning the temperature from homogeneous freezing conditions (e.g., T<233 K) until the detected frozen fraction is not distinguishable from the experimental background at water saturation conditions in the entire sample lamina.

Each reported data point consists of about 2-5 individual measurements at one temperature, which corresponds to more than 3000 measured single particle intensity peaks. The sample concentration is diluted upstream of the chamber to avoid coincidence errors for appropriate peak detection and the frozen fraction is the primary data set. For calculation of the INP concentration, the frozen fraction is multiplied by the total aerosol particle concentration in the aerosol chambers measured in parallel.

Temperature and RH uncertainties are equivalent to those for PINC. The uncertainties in frozen fraction are based on the uncertainty from the potential false classification of ice crystals as cloud droplets and vice-versa. Measurements with PIMCA-PINC were conducted on the same sample line as has been used for PccINC and are discussed at the end of section 2.4.

S.1.7 CIC-PNNL (Compact Ice Chamber – Pacific Northwest National Laboratory)

The Pacific Northwest National Laboratory (PNNL) Cloud Ice Chamber (CIC) has been previously described by Friedman et al. (2011) and Kulkarni et al. (2016). This device is modeled after the ice nucleation chamber described by Stetzer et al. (2008), and is the predecessor design on which the SPectrometer for Ice Nucleation (see later sections) was modeled. The chamber consists of two parallel plates through which flow is directed in a downward, vertical

direction, with an evaporation section attached at the bottom of the chamber to remove water droplets (Stetzer et al., 2008). The chamber plates are coated with an ice layer ~0.5 mm thick and independently temperature controlled using two external cooling baths (Lauda Binkmann Inc.). Temperature data are logged using a National Instrument CompactRIO programmable automation controller at 1 Hz sampling rate. Cooling baths were operated such that a linear temperature gradient was developed across the chamber plates. The gradient was adjusted to produce the desired ice-supersaturated conditions inside the chamber, and relative humidity with respect to ice (RH_i) and liquid water was calculated using the Murphy and Koop (2005) vapor pressure formulations. The chamber design ensures that aerosol particles are placed between the layers of two sheath flows. The sheath and sample flows were 6 and 1 L min^{-1}, respectively, which resulted in a particle residence time of the sample stream to ~12 s within the chamber. For FIN-02, the CIC-PNNL instrument was operated for at least part of the time in scanning RH_w mode, wherein the thermal gradient between the chamber walls was slowly increased in a manner that also held the average temperature of the aerosol stream constant. Temperature and RH_i uncertainty limits are ±1.0°C and ±3%, respectively. Ice crystals that grew to sizes greater than ~1.5 μm were detected with an optical particle counter (OPC, CLiMET, Model CI-3100). Background INP counts were calculated by sampling only filtered dry air for at least 15 min at the beginning, middle, and at the end of the experiment. Background INP counts were subtracted from the measured INP counts in each experiment. INP concentrations reported are interquartile means.

S.1.8 SPIN-MIT (Spectrometer for Ice Nuclei – Massachusetts Institute of Technology)

The MIT SPectrometer for Ice Nuclei (SPIN) is a commercially-available ice nuclei counter manufactured by Droplet Measurement Technologies in Boulder, CO, technically described by Garimella et al. (2016). SPIN is a continuous flow diffusion chamber with parallel plate geometry similar to the Zurich Ice Nucleation Chamber (ZINC) (Stetzer et al., 2008) and the Portable Ice Nucleation Chamber (PINC) (Chou et al., 2011). Ice supersaturation conditions are created by coating two parallel plates with ice, holding them at different temperatures (both below 0°C), and owing an aerosol lamina in the center of a sheath flow between the walls. After flowing through the main chamber, the air stream enters an isothermal evaporation section to evaporate liquid droplets. It then passes through a linear depolarization optical particle counter (OPC) for particle, droplet, and ice counting. The instrument can be operated at aerosol temperatures as low as -55°C and ice supersaturations exceeding 60%.

SPIN was operated for FIN-02 in both a “static" mode, where the wall temperatures were controlled to provide constant aerosol temperature and supersaturation conditions, and in a “ramp" mode, also referred to as RH_w scan mode in this paper, where the wall temperatures were set to diverge from a starting temperature, resulting in increasing supersaturation at a relatively constant temperature. Ramps were generally performed such that dT/dt for each wall was 0.5°C min^{-1}. In all cases, the evaporation section is isothermal and held at the desired aerosol temperature.

The aerosol temperature and supersaturation in the lamina are calculated using the method in Rogers (1988). Uncertainties in the temperatures and supersaturations experienced by the aerosol arise from inhomogeneity in wall temperatures, uncertainties in flows, differences in conditions across the width of the aerosol lamina, and deviations from the analytical calculations in Rogers (1988). Below water saturation, aerosol particles and ice crystals are distinguishable by optical size and light depolarization. At certain conditions above water saturation, dependent on

temperature, droplets do not evaporate fully in the evaporation section and can enter the OPC. Size and depolarization signals are used to distinguish particles, droplets, and ice (Garimella et al., 2016).

S.1.9 SPIN-TROPOS (Spectrometer for Ice Nuclei – Leibniz Institute for Tropospheric Research)

The SPIN-TROPOS is nearly identical in configuration, operation, and uncertainties to the SPIN-MIT. A description of the chambers design and functionality can be found in Garimella et al. (2016). During an experiment, a continuous flow of aerosol particles is exposed for 10-12 s to controlled ice supersaturated conditions and temperatures, allowing ice nucleation to occur on the aerosol under investigation. Ice crystals grow subsequently on the fraction of particles acting as ice nuclei. The number of ice crystals formed at a specific condition is detected optically by an OPC measuring the intensity of light scattered by individual particles. The OPC signal of ice crystals is distinguished from the signal of aerosol particles by a higher intensity, caused by the larger size of ice crystals. Sequences of increasing ice saturation ramps up to above water saturation, at several constant temperatures were run during FIN-02. Experimental uncertainties in temperature and saturation, derived from the wall temperature inhomogeneity during each measurement are typically below +/-1K and +/-5%, respectively.

S.2 Instrument systems for post-processing of bulk particle collections

All of these instrument systems employ cooled surfaces or wells holding particles exposed to water vapor, or water droplets/water volumes. Each are unique, and many are documented already in the literature, as noted herein.

S.2.1 NCSU-CS (North Carolina State University Cold Stage)

The design of the NC State cold stage-supported droplet freezing assay and data reduction methods are described in Wright and Petters (2013), Hader et al. (2014) and Hiranuma et al. (2015). For the experiments reported here, aqueous suspensions from impinger collections were distributed on the cold stage as follows. Approximately 64 drops of V = 1 μL, measured with an electronic micropipette, were placed directly on a hydrophobic glass slide. These drops are in contact with a gas-phase composed of dry nitrogen. Squalene oil to immerse the droplets, which was used in previous studies of the NC State CS was not applied. A constant cooling rate of 2°C min^{-1} was applied and the fraction of unfrozen drops was recorded using a microscope camera at incremental ΔT = 0.17°C resolution. Droplet frozen fractions versus temperature data were inverted to first determine the concentration of INPs using the method of Vali (1971):

$$c_{IN}(T) = -\frac{\ln\left(f_{unfrozen}(T)\right)}{V_{drop}} \quad \text{(S1)}$$

where $c_{IN(T)}$ is the concentration of INPs per unit volume of water (m^{-3}), $f_{unfrozen}$ is the fraction of unfrozen drops at T, and V_{drop} is the population-median drop volume.

Volumetric INP concentrations in air ($C_{INP(T)}$) were calculated via,

$$c_{INP}(T) = \frac{c_{IN}(T)\cdot f\cdot V_{imp}}{V_a} \quad \text{(S2)}$$

where V_{imp} is the total impinger water volume collected for distribution to other investigators, f accounts for the dilution of the impinger water (f = 1 for undiluted), and V_a is the air volume collected into liquid.

Samples were stored frozen at inside a -80°C freezer in Raleigh before the experiments, which were performed between April and September 2015. For each dilution, the experiment was repeated three times. In addition, experiments with diluted impinger water and on sample blanks for quality control were performed. This resulted in sample data from 4 to 9 individual experiments for a given collection. Results from these experiments were binned into 1°C temperature intervals; 95% confidence intervals for c_{INP} are reported for the binned data.

S.2.2 CMU-CS (Carnegie Mellon University Cold Stage)

The Carnegie Mellon University Cold Stage (CMU-CS) is composed of an air-cooled cascade 3-stage thermoelectric chiller (TEC) unit (TECA, AHP-1200CAS), topped with a custom-built aluminum stage described further by Polen et al. (2016) and Beydoun et al. (2017). The stage houses an external single-stage thermoelectric element (TE Technology Inc., VT-127-1.4-1.5-72P) and an associated thermistor (TE Technology Inc., MP-3176) placed beneath a removable aluminum sample dish. The thermistor provides temperature measurement for all experiments and is calibrated as described below. Droplet samples are placed on hydrophobically-coated coverslips (Hampton Research, HR3-231) in an inert squalene oil (VWR, H0097, ≥98.0% purity) environment to prevent contamination and droplet interaction. The chiller's plastic lid encloses the entire aluminum chamber that is placed on the cascade TEC to insulate it from ambient conditions. Dry air is flowed over the top of the plastic lid to prevent fogging, and a beaker of desiccant is used to dry the air inside the enclosure. The cooling ramp cycle is controlled by the TE Tech software. The single-stage element is held at 10°C until the experiment begins; it then begins to ramp to 0°C for 1 min. After this 1 min, the temperature is set to ramp down at 5°C intervals every 5 min to -40°C, producing a 1°C min^{-1} cooling rate. The cascade chiller that acts as the heat sink for the single-stage TEC is set to -45°C throughout the experiment.

Temperature calibration of the system was performed by attaching a thermistor to a hydrophobic coverslip, placing it into the sample dish, and covering it in oil. The temperature was ramped down at 1°C min^{-1} using the same program as a typical freezing experiment. The thermistor temperature was recorded at 1 Hz frequency. This was repeated multiple times to insure similar temperature ramp rates for all experiments. Following these ramps, a plot of the thermistor temperature measurement and the system measurement (using the same model thermistor, placed in its usual location in the aluminum stage under the sample dish) is generated. The linear relationship between the system temperature and the cover slip temperature is used to correct the measured system temperature to that of the cover slip during normal droplet freezing assays. Occasional tests of the cover slip temperature during a normal cooling cycle were performed to confirm that the relationship remained the same.

FIN-02 samples were kept frozen at ~ -10°C in their original containers until the droplet freezing experiment was run. Samples were thawed until no ice remained in the sample, but not completely to room temperature. A small volume of the stock sample was then poured into a sterile, unused secondary plastic vial to avoid contamination of the original sample. The original sample was then returned to the freezer. The secondary volume was used for that day's experiments exclusively and then disposed of. The secondary volume was not re-frozen between experiments to avoid repeated freezing and thawing of the sample. The secondary sample was hand shaken briefly to re-suspend any particles that may have settled out.

For Snomax® (FIN02-15-J) dilution experiments, the stock sample was poured into a second vial and returned to the freezer. From the second vial, 100 µL was pipetted into a third vial, which was immediately stored in the freezer until the experiment was performed. Shortly before the cooling experiment, the 100 µL sample was thawed completely and diluted to 50 mL (500X dilution) to examine the colder freezing temperature ice nucleants. The diluted sample was hand-mixed briefly, immediately generated into droplets, and the cooling cycle was started.

The secondary volumes of solutions were used exclusively for droplet generation to avoid contamination of the stock sample. A p2 variable electronic pipette (SEOH, 3824-1LC) was used to create 0.1 µL droplets in squalene oil on top of a hydrophobic glass coverslip. New sterile pipette tips were used between different droplet arrays to avoid contamination. Each droplet was placed on top of the oil and allowed to sink to the bottom to rest on the coverslip. Each array contained 40-60 droplets.

Pure water samples were from an in-house Milli-Q system (18.2 MΩ·cm) which is run for at least 5 min before obtaining a sample. Fourteen independent pure water arrays containing more than 600 droplets total were subjected to the standard droplet generation and temperature program. 10% of droplets had frozen by -25°C and 50% were frozen at ~ -30°C.

For uncertainty analysis, 2-3 replicate droplet arrays were measured for each sample, and their freezing temperature spectra were averaged to produce the averaged droplet freezing spectrum determined from Eqs. (S1) and (S2). A new droplet array was generated from the same secondary volume for each replicate run. The error bars are the 95% confidence intervals determined from the replicate runs for each sample. The Snomax® sample was separated into two different average spectra, due to differences observed between the replicates. The first freezing cycle, performed as soon as droplets were generated immediately after the sample had thawed, was separated from the second and third freezing cycles on new droplet arrays generated from the same secondary volume. The average spectrum from the diluted Snomax® sample was combined with the average of the 2^{nd} & 3^{rd} runs to produce the complete Snomax® spectrum. An additional first freezing cycle was also performed on a later day, by re-thawing out the Snomax® stock sample.

S.2.3 IS (Colorado State University Ice Spectrometer)

The Colorado State University Ice Spectrometer (IS) emanates from the developments of Hill et al. (2014; 2016) and is described in the approximate form used in this study by Hiranuma et al. (2015). Immersion freezing temperature spectra are obtained in the IS following dispensing 24 or 32 aliquots of 50 or 60 µL of suspensions of aerosols into sterile, 96-well PCR trays (Life Science Products Inc.) in a laminar flow cabinet. The IS is constructed using two 96-well aluminum incubation blocks (VWR), designed for cooling or heating PCR plates, placed end-to-end and encased on their sides and base by cold plates (Lytron). A ULT-80 low temperature bath (Thermo Neslab) circulating SYLTHERM XLT heat transfer fluid (Dow Corning Corporation) is used for cooling. Loaded PCR plates were placed in the blocks, the device covered with a plexiglass window and the headspace purged with 0.5-1.5 L min^{-1} of filtered (HEPA-CAP, Whatman) nitrogen. Temperature was lowered at 0.33°C min^{-1}, measured using a thermistor verification probe (Bio-Rad, Hercules, CA, VPT-0300) inserted into a side well. Frozen wells were counted at 0.2-1°C degree intervals to a limit of -27°C, and cumulative numbers of INPs mL^{-1} of suspension were estimated using Eq. (S1). INPs

per volume of air processed were calculated with Eq. (S2), where V_{imp} in this case was either of the impinger sample or of the filter suspension sample. For filter samples, filter blanks were processed in a similar manner as aerosol samples to obtain a mean background INP spectrum. Binomial sampling confidence intervals (95%) were derived using the formula recommended by Agresti and Coull (1998):

$$\mathrm{CI}_{95\%} = \left(\hat{p} + \frac{1.96^2}{2n} \pm 1.96\sqrt{\left[\hat{p}(1-\hat{p}) + {1.96^2}/{4n}\right]/n}\right) / \left(1 + {1.96^2}/{n}\right) \quad \text{(S3)}$$

where $\hat{p}$ is the proportion of droplets frozen and n is the total number of droplets. Using this formula, for a single well frozen out of 32 aliquots the $\mathrm{CI}_{95\%}$ ranges from 18% to 540% of the estimated INP concentration, while for 16/32 wells frozen it is 68-132% of the INP concentration.

Most results reported in this paper were from filter samples, rather than the shared impinger samples. APC air was typically filtered for 120-130 min at 15 L min^{-1} through a 47-mm diameter in-line aluminum filter holder (Pall) fitted with a 0.2 μm diameter pore Nuclepore polycarbonate membrane (Whatman). These were collected at the same position as impinger samples, and the collection times typically aligned. Dis-assembled filter holders were cleaned by soaking in 10% H_2O_2 for 60 min followed by rinses in deionized water (18 MΩ-cm and 0.2 μm diameter-pore filtered) and removal of excess water with a gas duster before drying. Filters were prepared in a laminar flow cabinet (<0.01 particles cc^{-1}) by soaking them in 10% H_2O_2 for 10 min followed by three rinses in deionized water, the last of which had been filtered through a 0.02 μm pore diameter filter (Anotop 25 mm syringe filter, Whatman) and drying on foil.

After particle collection, filters were transferred using clean, plastic forceps to a sterile, 60 mm petri dish (CELLTREAT) and stored frozen at -20°C. For re-suspension of particles, filters were placed in sterile 50 mL Falcon polypropylene tubes (Corning Life Sciences), 6-10 mL of suspension solution added and particles re-suspended by tumbling end-over-end on a Roto-Torque (Cole-Palmer) at 60 cycles min^{-1} for 20 min. The re-suspension solution was 2 mM KCl (to prevent any influence on the ice nucleation activity of K-Feldspar) filtered through a 0.02 μm pore diameter filter (which contained, on average, 1.6 INPs mL^{-1} at -25°C). A series of up to five 20-fold dilutions in 2 mM KCl were used to cover the full temperature range.

For the Snomax® comparison, the IS processed samples from the impingers. A sub-sample of the NCSU impinger water was melted and tested neat and after dilution in 20-fold steps in 0.02 μm pore filter deionized water.

S.2.4 μL-NIPI (Leeds Microliter Nucleation by Immersed Particles Instrument)

This instrument has been previously described in detail by Whale et al. (2015). Briefly, approximately 40 droplets of 1 μL volume are pipetted onto a hydrophobic glass slide (Hampton Research HR3-23) using an electronic pipette (Picus Biohit). The glass slide is placed onto an Asymptote EF600 Stirling cryocooler, which is used to control the temperature of the slide. The slide is enclosed within a Perspex chamber and a gentle flow of dry nitrogen is used to prevent water condensation during cooling. Freezing of droplets is monitored using a digital camera, allowing the fraction of droplets frozen at a given temperature to be determined. Samples were used for freezing experiments immediately following collection at the AIDA facility. All experiments presented here were conducted at a cooling rate of 1°C min^{-1}. Temperature error was calculated by taking the random error of the thermocouple used to measure cold stage temperature, propagated with the melting point range observed for water, resulting in a maximum error of

less than ± 0.4°C. Due to the ice nucleation induced by the slide and other sources of contamination there is a lower limit to the temperature at which this instrument can be used. In order to account for this effect a background freezing curve has been produced, which is subtracted from the cumulative nucleus spectrum for individual experiments. In this way freezing events which are not unambiguously caused by the heterogeneous nucleator under investigation are eliminated from the dataset. This process is described in O'Sullivan et al. (2015). Uncertainties in INP concentration for the binned data shown in this paper were derived from the experiment-to-experiment variability.

S.2.5 BINARY (Bielefeld Ice Nucleation ARraY)

A detailed description of the BINARY setup is given by Budke and Koop (2015). Briefly, the setup as it is used in this study consists of a compartment array for 36 droplets (V_{drop} = 0.6 µL) positioned on a Peltier cooling stage (Linkam LTS120). Each compartment is composed of a lower hydrophobic glass slide with contact to the drop, a polydimethylsiloxane (PDMS) spacer at the sides, and an upper acrylic glass. The drops are cooled down at a constant rate of 1 K min^{-1}. Freezing temperatures are determined optically based on the change in brightness when the transparent liquid drops become opaque during freezing. The temperature uncertainty is ±0.3 K.

The suspension droplets were positioned onto the hydrophobic glass slide using an electronic pipette (Brand Transferpette®, accuracy ≤ ±1.0%). To minimize sedimentation the drops were pipetted in rows of 3 x 12 drops and the suspension was stirred with a vortex mixer (VWR) at 1000 rpm in advance of each row placement.

Due to contact with the lower glass slide and dust contaminations the apparatus has an applicable temperature range from 273 K down to about 245 K (25th percentile freezing temperature of "pure" water). Based on the background freezing temperatures experiments with significant overlap were excluded from further analysis. Additionally, single data points were excluded if they did not satisfy the following rules: 1.) number of INPs per litre of examined suspension (diluted) $[L^{-1}] > 10^{(51.24 - 0.186 \cdot (T\,[K]-1))}$, 2.) number of INPs per litre of examined suspension (diluted) $[L^{-1}] > 10^5$.

Data subsampling was done by temperature binning into 1 K intervals giving the midpoint of each bin. INP concentrations c_{IN} for each bin are shown in terms of median (50th percentile) values. Error bars indicate the 5th and 95th percentile, respectively. Please note that especially for samples as Snomax® where INP concentrations increase strongly with decreasing temperature the large error bars do not stem from a significant spread of the data but rather from the steep increase in c_{IN} within a 1 K temperature bin.

S.2.6 M-AL (Mainz Acoustic Levitator)

For a detailed description of the Mainz Acoustic Levitator see Diehl et al. (2014). The M-AL consists of an ultrasonic trap (APOS BA 10, tec5 AG, Germany) in which single water droplets of 2 mm in diameter were levitated; the imaging digital video camera which served for determining the drop size; and an infrared thermometer (KT 19.82 II from Heitronics) which measured the drop surface temperature (ΔT (2σ) = 0.5 K) continuously. The M-AL was placed in the walk-in cold chamber of the Mainz vertical wind tunnel laboratory in which the air temperature was cooled down to –26±2°C, and monitored by a platinum resistance (Pt-100) thermometer. For each measurement, a single drop was generated using a medical syringe and injected into the M-AL. Prior to injection the sample was hand

shaken briefly in order to avoid any sedimentation. When injecting, the drop temperature was approximately +10°C which decayed continuously adapting to the ambient temperature. The onset of drop freezing in the M-AL is characterized by a rapid increase of the drop surface temperature ensuing from the latent heat release as the phase change is initiated. Thus, the freezing temperature could be determined in the experiments from the lowest surface temperature recorded by the infrared thermometer. For each collected impinger sample, 22 to 60 individual drops were measured without diluting the delivered FIN-02 suspensions, and the fraction of frozen drops, f_{ice}, was calculated. The only exception was the mystery sample M2-D used for blind studies, which was diluted to 1:9 (i.e., 10%). Since the Snomax samples were also measured undiluted, i.e., the INPs were in high concentration, they initiated freezing at high temperatures (just below zero °C). It resulted in a very limited number of observed freezing events, and large freezing temperature uncertainties. Because of these insufficient statistics, the Snomax results from M-AL are not presented here.

FIN-02 samples were kept frozen inside a refrigerator until the freezing experiment was carried out. Samples were thawed at room temperature until no ice remained in the sample. The whole sample volume in the sample tube was used for that day's experiments exclusively.

The frozen fractions were binned into 1 °C temperature intervals giving the midpoint of each bin, and the concentration of active sites per liter water was calculated using Eq. (S1). The error of c_{IN}(T) was derived from,

$$\Delta c_{IN} = \sqrt{\left(\frac{3\cdot\ln(1-f_{ice})}{\frac{\pi}{6}d_t^4}\Delta d_t\right)^2 + \left(\frac{1}{1-f_{ice}}\cdot\frac{1}{\frac{\pi}{6}d_t^3}\Delta f_{ice}\right)^2} \quad \text{(S4)}$$

where Δf_{ice} represents the error originating from the temperature uncertainty (the error due to the drop volume uncertainty on Δf_{ice} was neglected), and was calculated from the number of drops frozen within a temperature interval of 0.5 ΔT (the factor 0.5 comes from the fact that the drops were continuously cooled down, thus, only one direction of temperature uncertainty was taken into account). Δd_t is the uncertainty of the drop size which was determined from the individual drop images, and represents a 2σ error.

The INP per liter air was calculated from Eq. (S3). Since no errors are assumed in the values of the V_{imp} or V_a, the error of INP (per liter) in air was derived from,

$$\Delta INP = \frac{\Delta c_{IN}\cdot V_{imp}}{V_a} \quad \text{(S5)}$$

where only the uncertainty from Δc_{IN} was taken into account.

S.2.7 KIT-CS (Karlsruhe Institute of Technology Cold Stage)

The central part of the experimental setup of the KIT-CS includes a Cold Stage (Linkham, Model MDBCS-196), which was used to carry out temperature ramp experiments with defined cooling rates. Cooling is achieved by pumping liquid nitrogen from a reservoir to the sample holder.

A silicon substrate (Plano GmbH, 10x10mm) for supporting droplets was first cleaned with high grade acetone (p.a.), then rinsed several times with NanoPure® water. Finally, the silicon wafer was purged with nitrogen to remove residual water. The cleaned silicon wafer was mounted into a copper basin on top of the sample holder.

A piezo injector (GeSIM, Model A010-006 SPIP) was filled with aqueous suspensions. Before printing, the substrate was cooled to the ambient dew point to reduce the evaporation of droplets. Up to one thousand identical suspension droplets (0.5 nL) were printed onto the silicon wafer, resulting in 100µm drops in spherical cap geometry. After printing, the droplets were covered with silicone oil (VWR, Rhodorsil® 47 V 1000,) to prevent any interaction between supercooled and frozen droplets. Typical ramp experiments started from 0°C to -40°C with the cooling rate of -1K min^{-1} and followed by heating the sample up to +1°C.

To accurately determine the temperature of the droplets a calibrated thin film platinum resistance sensor (Pt-100) was directly fixed on the surface of silicon substrate by applying the small amount of heat conducting paste. The Pt-100 was calibrated in the temperature range from -40°C to +30°C prior to the experiment.

A charge-coupled device (CCD)-camera (EO® progressive) with a wide field objective (DiCon fiberoptics Inc.) was used to visualize the droplets. The substrate was illuminated by a circular light emitting array installed around the objective lens. Two polarizers (one in front of the light emitting diode and one in front of the objective) were used to detect the frozen droplets. A video (AVI) and temperature file were recorded, allowing for identification of individual freezing events with 0.125s temporal resolution and 0.1K temperature accuracy. Subsequent data processing with a LabView® routine allowed for calculation of a fraction frozen curve.

For data processing, the number of INP per liter water was calculated according to Eq. (S1). The initial concentration of impurities was obtained from experiments with NanoPure® water. To estimate the background prior to homogenous freeing limit a 3rd degree polynomial was applied to pure water data. Equation (S2) was used to calculate the number of IN per liter air. The scaling factors were calculated by dividing the volumes of the impingers and the added water during operation through the sample volume. For the impingers, a sampling efficiency of 100% was assumed.

S.2.8 VODCA (Vienna Optical Droplet Crystallization Analyzer)

The Vienna Optical Droplet Crystallization Analyzer (VODCA) device has at its core a cryo-microscope cell that consists of a single-stage Peltier element (Quick-cool QC-31-1.4-3.7M) mounted on a copper cooling block on ice water sewage, placed in an airtight cell, that can be flushed with dry nitrogen between measurements (Pummer et al., 2012). A glass window in the cover of the cell allows observation of the sample via a light microscope (Olympus BX51M) and an attached camera (Hengtech MDC320), linked to a computer. The temperature measurement has a standard deviation of 0.5 K. Samples were measured as emulsion with 90 wt% paraffin and 10 wt% lanolin (water-free grade) as oil phase. The emulsion was created directly on a thin glass slide with the help of a pipette tip. We use slightly more oil than liquid phase. Droplets diameters ranged from 20-41 µm. Prepared samples were placed on a glass slide and set onto the Peltier stage, where they were chilled with a cooling rate of approx. 10 K min^{-1}. Each slide was measured at four different positions with all measured droplets being summed up to one freezing curve. This was done twice for each sample. Droplet sizes were divided in three groups regarding their diameter to minimize the error of their non-uniformity (20-26 µm, 26-35 µm, 35-41 µm). Calculations of INP concentrations in air were made following the procedures used by other investigators.

S.2.9 WISDOM

The **We**I**z**mann **S**upercooled **D**roplets **O**bservation on **M**icroarray (**WISDOM**) is an instrument designed to study immersion freezing down to the homogeneous freezing temperature region, which combines a cryo-optic-stage with microfluidics techniques for fast generation of static picoliter to nanoliter droplet arrays (Reicher et al., 2018). The droplets are generated in a flow-focusing junction, and trapped in chamber arrays following their generation. In this study, the microfluidic device was based on a design by Schmitz et al. (2009). Each experiment contained about 500 droplets with diameter of 30-40µm, suspended in an oil phase, and a cooling rate of 1 K min^{-1} was applied. Temperature uncertainty of ±0.3 K was estimated. The suspension was sonicated for 5 min prior to droplet generation process. After droplet production, the microfluidic device, which contained the droplets, was placed in a cooling stage (Linkam, THMS 600), and the experiments were monitored using an optical microscope (Olympus, BX-51, transmitted mode) and a CCD camera. Freezing events were determined automatically based on the optical difference of frozen and unfrozen droplets. The microfluidic devices were fabricated in our laboratory using polydimethylsiloxane (PDMS) and a 1-mm thick microscope slide. For each material processed, same microfluidic device was recycled, each time with a new freshly prepared array.

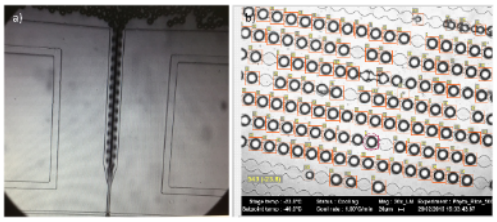

Figure S5. a) Generation process of monodispersed droplets by the microfluidic device. b) Example of an array filled with ~40 µm diameter droplets, which are trapped inside the microfluidic device chambers, before cooling applied. The orange squares present the automatic online identification of the droplets.

S.2.10 FRIDGE (FRankfurt Ice nucleation Deposition freezinG Experiment)

The FRIDGE methods address either,

a) deposition/condensation freezing INP or

b) immersion freezing INP number concentration

Both approaches work offline: aerosol particles are first collected on substrates, and the samples are then processed in the FRIDGE INP counter (Klein et al., 2010; Schrod et al., 2016). The ice nucleus counter FRIDGE itself is a 500 ml thermostated vessel with a cold table inside that carries the sample. A CCD camera records images of the sample through a window on top of the chamber.

a) Deposition/Condensation mode operation (standard mode: FRIDGE-STD)

For this measurement aerosol is collected from the atmosphere by electrostatic precipitation of the particles onto the surface of a silicon wafer of 45mm diameter Klein et al., 2010). For sampling of aerosol particles air is pumped through the central tube of a cylindrical sampler that carries 12 electrodes of gold wire. The electrodes are arranged concentrically around the inlet, and are at 12 kV voltage against the grounded substrate at the bottom of the sampler. Aerosol particles are charged by emitted electrons and are deposited downstream on the substrate. Usually 30-100 L

of air sample volume are collected. In an effort to limit the depletion of water vapor during analysis by the presence of too many particles (volume effect) the sample volume was adjusted according to the estimated particle number concentration.

After collection, the substrates are stored in at room temperature in petri dishes until analysis. During FIN-02 samples were stored at room temperature. Most samples were analyzed on-site within a couple of days. For some cases the storage ranged between 10 to 47 days. For analysis, a wafer is placed on the cold table inside the FRIDGE INP counter. The chamber is evacuated, and the temperature of the cold table is adjusted to the desired temperature. Operational temperatures may range between 0 and -35°C. For practical reasons (sample volume, detection limit, occurrence of blank counts) samples are routinely analyzed at -20°C, -25°C and -30°C, and at up to 1% water supersaturation. When the chamber is inflated with water vapor ice grows on the activated INPs to become macroscopic crystals. The vapor pressure is regulated to the desired value. The water vapor saturation is calculated from the pressure inside the chamber and from the temperature of the substrate. The substrate is photographed by a CCD camera. During the first 100 seconds of crystal growth one image is stored every 10 seconds. The image at 100 seconds is usually taken as the final image for counting. The ice crystals are counted automatically. It is assumed that one crystal represents one INP. Only bright objects (i.e., ice crystals) that grow during the 100 seconds to sizes larger than 30 Pixels (*~600µm) are counted. The operating parameters of the chamber, as well as the image processing and the counting of crystals, are controlled by LabView software.

After analysis, the sampling cell is evacuated, the temperature and vapor pressure may be set to new conditions, and the sample may be processed again. The substrates carry a coordinate system (3 laser-marked crosses) that allows to identify from the images the positions of the ice crystals on the substrate. Using this information, the morphology and composition of individual particles at the sites of crystal growth (i.e., the INPs) can be analyzed subsequently by electron microscopical analysis (with EDX) of the substrate.

b) immersion freezing mode operation (FRIDGE-IMM)

The measurement of immersion freezing INPs combines membrane filter sampling of aerosol particles with analysis of droplet freezing temperatures of aqueous filter extracts on the cold stage of FRIDGE. Aerosol is sampled on Teflon membrane filters (Fluoropore PTFE, 47 mm, 0.2µm, Merck Millipore Ltd.). Air sample volumes range between a few to 200 liters, the maximum during FIN-02. The particles are extracted into 5 or 10 ml of DIW by agitating. Around 150 drops of 0.5 µl each are taken with a pipette from the washing solution and placed randomly on a silicon plate on the cold stage of FRIDGE. With the chamber almost closed, but at ambient atmospheric pressure the temperature of the cold stage is lowered by 1°C min^{-1}. The number of drops that freeze as function of temperature is recorded by the CCD camera and is counted. This process is repeated several times with fresh droplets. A total number of 1000 droplets at minimum is exposed. The INP number concentration is derived following Eqs. (S1) and (S2).

The uncertainty in the measurement is ± 0.2°C for T, and is estimated at around 40% for INP number concentrations at -20°C for Illite NX, but may become lower with decreasing temperature.

S.2.11 DFPC-ISAC (Dynamic Filter Processing Chamber – Institute of Atmospheric Sciences and Climate (CNR Bologna))

The Dynamic Filter Processing Chamber (DFPC) (Santachiara et al., 2010; Belosi et al., 2014) is a replica of the Langer dynamic developing chamber (Langer and Rogers, 1975). Concentrations of INPs are detected by the membrane filter technique. Aerosol particles are sampled onto nitrocellulose black gridded membrane filters (0.45 μm porosity Millipore). At the FIN-02 workshop sampling flow rate was 2 L min^{-1} and the volume sampled was about 20 L. After collection, the filters are stored in Petri dishes. Before being processed the sampled filter is inserted onto a metal plate, previously covered with a smooth surface of paraffin, in order to assure good thermal contact of the filter with the supporting substrate. Subsequently the paraffin is slightly heated and rapidly cooled in order to fill the filter pores.

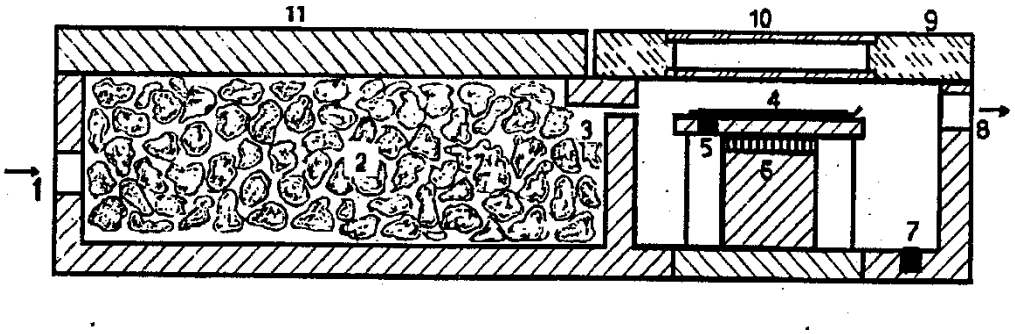

Figure S6. 1: air inlet; 2: minced ice; 3: slit and air temperature thermocouple; 4: filter; 5: filter temperature thermocouple; 6: Peltier cooling device; 7: thermocouple; 8: air outlet; 9: plexiglass cover; 10: observation slit; 11: aluminium plate.

Figure S6 shows the schematic of the chamber, which is housed in a refrigerator. Filtered air is forced by a pump to flow through the chamber in a closed loop. Air enters the chamber through a perforated plate (1), spreads into the ice bed (2) and becomes saturated with respect to ice, which is cooled by the base plate. The temperature of the air is measured just in front of the nozzle (3) aiming the air at the metal plate supporting the sampled filter (4), placed on a top of the Peltier cooled surface (6). The temperatures of the air and of the Peltier device (7) are measured with resistance temperature sensors (PT 100). By controlling the temperatures of the filter and of the air, saturated with respect to finely minced ice and flowing continuously grazing the filter, it is possible to obtain different supersaturations with respect to ice and water, SS_{ice} and SS_w, respectively. Therefore, deposition and condensation freezing ice nucleation modes can be investigated. Measurement uncertainties in consideration of T and SS_w uncertainties are estimated as 30% in all cases. Limit of detection is estimated as 0.025 L^{-1} on the basis of contaminant background of 0.5 per filter (Belosi et al., 2014) and the sample volumes used in this study.

Supersaturations are calculated theoretically from vapour pressures of ice and water (Buck, 1981) at the considered temperatures. The exposure time of the filter is 20 min, long enough to grow sizeable ice crystals on INPs at the considered relative humidity and temperature. Use of the dynamic chamber circumvents some of the problems arising with the static chamber, e.g. that the moisture supply under static conditions may be rather inadequate at the filter

surface, both in overcoming the effect of hygroscopic particles and in activating all potential INPs. Fig. S7 shows a picture of the DFPC with the top cover removed (minced ice is visible) and a filter with ice crystals.

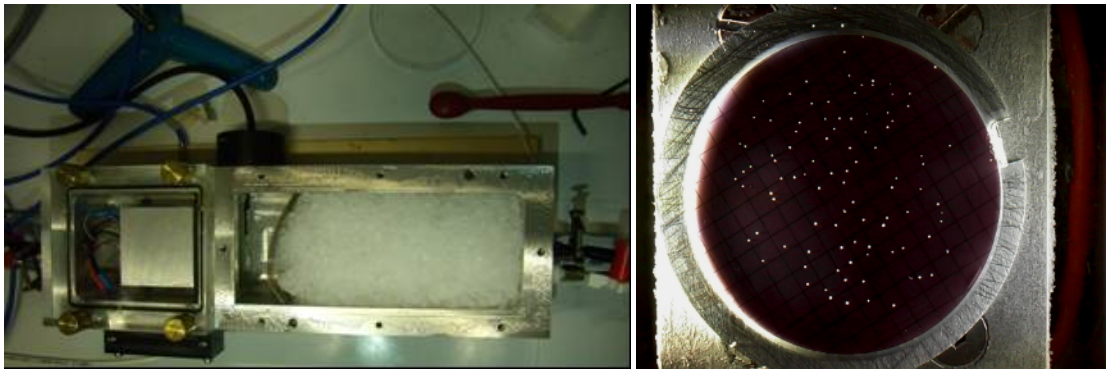

Figure S7. DFPC housed in a refrigerator (on the left). Ice crystal growth (on the right).

S3. References

Agresti, A. and Coull, B. A.: Approximate is better than "exact" for interval estimation of binomial proportions, The American Statistician, 52, 119-126, doi:10.1080/00031305.1998.10480550, 1998.

Archuleta, C. M., DeMott, P. J., and Kreidenweis, S. M.: Ice nucleation by surrogates for atmospheric mineral dust and mineral dust/sulfate particles at cirrus temperatures, Atmos. Chem. Phys., 5, 2617–2634, doi:10.5194/acp-5-2617-2005, 2005.

Belosi, F., Santachiara, G., and Prodi, F.: Ice-forming nuclei in Antarctica: New and past measurements, Atmospheric Research 145–146, 105–11, doi: 10.1016/j.atmosres.2014.03.030, 2014.

Benz, S., Megahed, K., Möhler, O., Saathoff, H., Wagner, R., and Schurath, U.: T-dependent rate measurements of homogeneous ice nucleation in cloud droplets using a large atmospheric simulation chamber, J. Photochem. Photobiol. A, 176, 208–217, doi:10.1016/j.jphotochem.2005.08.026, 2005.

Beydoun, H., Polen, M. and Sullivan, R. C.: A new multicomponent heterogeneous ice nucleation model and its application to Snomax bacterial particles and a Snomax–illite mineral particle mixture, Atmos. Chem. Phys., 17(22), 13545–13557, doi:10.5194/acp-17-13545-2017, 2017.

Boose, Y., Kanji, Z. A., Kohn, M., Sierau, B., Zipori, A., Crawford, I., Lloyd, G., Bukowiecki, N, Herrmann, E., Kupiszewski, P., Steinbacher, M. and U. Lohmann: Ice Nucleating Particle Measurements at 241K during Winter Months at 3580m MSL in the Swiss Alps, J. Atmos. Sci., 73, 2203-2228, 2016.

Buck, A.L.: New equations for computing vapour pressure and enhancement factor. J. Appl. Meteorol., 20, 1527–1532, doi:10.1175/1520-0450(1981)020<1527:NEFCVP>2.0.CO;2, 1981.

Budke, C. and Koop, T.: BINARY: an optical freezing array for assessing temperature and time dependence of heterogeneous ice nucleation, Atmos. Meas. Tech., 8, 689–703, doi:10.5194/amt-8-689-2015, 2015.

Chou, C., Stetzer, O., Weingartner, E., Juranyi, Z., Kanji, Z. A. and Lohmann, U.: Ice nuclei properties within a Saharan dust event at the Jungfraujoch in the Swiss Alps, Atmos. Chem. Phys., 11(10), 4725-4738, doi:10.5194/acp-11-4725-2011, 2011.

DeMott, P. J., Möhler, O., Stetzer, O., Vali, G., Levin, Z., Petters, M. D., Murakami, M., Leisner, T., Bundke, U., Klein, H., Kanji, Z., Cotton, R., Jones, H., Petters, M., Prenni, A., Benz, S., Brinkmann, M., Rzesanke, D., Saathoff, H., Nicolet, M., Gallavardin, S., Saito, A., Nillius, B., Bingemer, H., Abbatt, J., Ardon, K., Ganor, E., Georgakopoulos, D. G., and Saunders, C.: Resurgence in ice nucleation research. Bull. Amer. Meteor. Soc., 92, 1623-1635, doi:10.1175/2011BAMS3119.12011, 2011.

DeMott, P. J., Prenni, A. J., McMeeking, G. R., Tobo, Y., Sullivan, R. C., Petters, M. D., Niemand, M., Möhler, O., and Kreidenweis, S. M.: Integrating laboratory and field data to quantify the immersion freezing ice nucleation activity of mineral dust particles, Atmos. Chem. Phys., 15, 393–409, doi:10.5194/acp-15-393-2015, 2015.

Diehl, K., Debertshäuser, M., Eppers, O., Schmithüsen, H., Mitra, S. K., and Borrmann, S.: Particle surface area dependence of mineral dust in immersion freezing mode: investigations with freely suspended drops in an acoustic levitator and a vertical wind tunnel, Atmos. Chem. Phys., 14, 12343-12355, doi:10.5194/acp-14-12343-2014, 2014.

Eidhammer, T., DeMott, P. J., Prenni, A. J., Petters, M. D., Twohy, C. H., Rogers, D. C., Stith, J., Heymsfield, A., Wang, Z., Haimov, S., French, J., Pratt, K., Prather, K., Murphy, S., Seinfeld, J., Subramanian, R., and Kreidenweis, S. M.: Ice initiation by aerosol particles: Measured and predicted ice nuclei concentrations versus measured ice crystal concentrations in an orographic wave cloud, J. Atmos. Sci., 67, 2417–2436, doi:10.1175/2010JAS3266.1, 2010.

Fahey, D. W., Gao, R.-S., Möhler, O., Saathoff, H., Schiller, C., Ebert, V., Krämer, M., Peter, T., Amarouche, N., Avallone, L. M., Bauer, R., Bozóki, Z., Christensen, L. E., Davis, S. M., Durry, G., Dyroff, C., Herman, R. L., Hunsmann, S., Khaykin, S. M., Mackrodt, P., Meyer, J., Smith, J. B., Spelten, N., Troy, R. F., Vömel, H., Wagner, S., and Wienhold, F. G.: The AquaVIT-1 intercomparison of atmospheric water vapor measurement techniques, Atmos. Meas. Tech., 7, 3177-3213, doi:10.5194/amt-7-3177-2014, 2014.

Friedman, B., Kulkarni, G., Beránek, J., A. Zelenyuk, A., Thornton, J. A., and D. J. Cziczo, D. J.: Ice nucleation and droplet formation by bare and coated soot particles, J. Geophys. Res., 116, D17203, doi:10.1029/2011JD015999, 2011.

Garimella, S., Kristensen, T. B., Ignatius, K., Welti, A., Voigtländer, J., Kulkarni, G. R., Sagan, F., Kok, G. L., Dorsey, J., Nichman, L., Rothenberg, D. A., Rösch, M., Kirchgäßner, A. C. R., Ladkin, R., Wex, H., Wilson, T. W., Ladino, L. A., Abbatt, J. P. D., Stetzer, O., Lohmann, U., Stratmann, F., and Cziczo, D. J.: The SPectrometer for Ice Nuclei (SPIN): an instrument to investigate ice nucleation, Atmos. Meas. Tech., 9, 2781-2795, doi:10.5194/amt-9-2781-2016, 2016.

Glen, A. and Brooks, S. D.: Single particle measurements of the optical properties of small ice crystals and heterogeneous ice nuclei, AS&T, 48:1, 1123-1132, doi:10.1080/02786826.2014.963023, 2014.

Hader, J. D., Wright, T. P., and Petters, M. D.: Contribution of pollen to atmospheric ice nuclei concentrations, Atmos. Chem. Phys., 14, 5433–5449, doi:10.5194/acp-14-5433-2014, 2014.

Hill, T. C. J., Moffett, B. F., DeMott, P. J., Georgakopoulos, D. G., Stump, W. L., and Franc, G. D.: Measurement of ice nucleation-active bacteria on plants and in precipitation by quantitative PCR. Appl. Environ. Microbiol. 80(4):1256-1267, doi:10.1128/AEM.02967-13, 2014.

Hill, T. C. J., DeMott, P. J., Tobo, Y., Fröhlich-Nowoisky, J., Moffett, B. F., Franc, G. D., and Kreidenweis, S. M.: Sources of organic ice nucleating particles in soils, Atmos. Chem. Phys., 16, 7195–7211, doi:10.5194/acp-2016-1, 2016

Hiranuma, N., Paukert, M., Steinke, I., Zhang, K., Kulkarni, G., Hoose, C., Schnaiter, M., Saathoff, H., and Möhler, O.: A comprehensive parameterization of heterogeneous ice nucleation of dust surrogate: laboratory study with hematite particles and its application to atmospheric models, Atmos. Chem. Phys., 14, 13145–13158, doi:10.5194/acp-14-13145-2014, 2014a.

Hiranuma, N., Hoffmann, N., Kiselev, A., Dreyer, A., Zhang, K., Kulkarni, G., Koop, T., and Möhler, O.: Influence of surface morphology on the immersion mode ice nucleation efficiency of hematite particles, Atmos. Chem. Phys., 14, 2315–2324, doi:10.5194/acp-14-2315-2014, 2014b.

Hiranuma, N., Augustin-Bauditz, S., Bingemer, H., Budke, C., Curtius, J., Danielczok, A., Diehl, K., Dreischmeier, K., Ebert, M., Frank, F., Ho mann, N., Kandler, K., Kiselev, A., Koop, T., Leisner, T., Möhler, O., Nillius, B., Peckhaus, A., Rose, D., Weinbruch, S., Wex, H., Boose, Y., DeMott, P. J., Hader, J. D., Hill, T. C. J., Kanji, Z. A., Kulkarni, G., Levin, E. J. T., McCluskey, C. S., Murakami, M., Murray, B. J., Niedermeier, D., Petters, M. D., O'Sullivan, D., Saito, A., Schill, G. P., Tajiri, T., Tolbert, M. A., Welti, A., Whale, T. F., Wright, T. P., and Yamashita, K.: A comprehensive laboratory study on the immersion freezing behavior of illite NX particles: a comparison of 17 ice nucleation measurement techniques, Atmos. Chem. Phys., 15, 2489–2518, doi:10.5194/acp-15-2489-2015, 2015.

Klein, H., Haunold, W., Bundke, U., Nillius, B., Wetter, T., Schallenberg, S., Bingemer, H.: A new method for sampling of atmospheric ice nuclei with subsequent analysis in a static diffusion chamber, Atmospheric Research, 96, 218-224, doi:10.1016/j.atmosres.2009.08.002, 2010.

Kohn, M., Lohmann, U., Welti, A., and Kanji, Z. A.: Immersion mode ice nucleation measurements with the new Portable Immersion Mode Cooling chAmber (PIMCA), J. Geophys. Res. Atmos., 121, 4713–4733, doi:10.1002/2016JD024761, 2016.

Langer, G. and Rogers, J.: An Experimental Study of the Detection of Ice Nuclei on Membrane Filters and Other Substrata, J. Appl. Meteor., 14, 560-570, doi:10.1175/1520-0450(1975)014<0560:AESOTD>2.0.CO;2, 1975

McFarquhar, G. M., Ghan, S., Verlinde, J., Korolev, A., Strapp, J. W., Schmid, B., Tomlinson, J. M., Wolde, M., Brooks, S. D., Cziczo, D., Dubey, M. K., Fan, J., Flynn, C., Gultepe, I., Hubbe, J., Gilles, M. K., Laskin, A., Lawson, P., Leaitch, W. R., Liu, P., Liu, X., Lubin, D., Mazzoleni, C., Macdonald, A.-M., Moffet, R. C., Morrison, H., Ovchinnikov, M., Shupe, M. D., Turner, D. D., Xie, S., Zelenyuk, A., Bae, K., Freer, M., and Glen, A.: Indirect and Semi-direct Aerosol Campaign, Bulletin of the American Meteorological Society, 92, 183-201, 10.1175/2010bams2935.1, 2011.

Möhler, O., Stetzer, O., Schaefers, S., Linke, C., Schnaiter, M., Tiede, R., Saathoff, H., Krämer, M., Mangold, A., Budz, P., Zink, P., Schreiner, J., Mauersberger, K., Haag, W., Kärcher, B., and Schurath, U.: Experimental

investigation of homogeneous freezing of sulphuric acid particles in the aerosol chamber AIDA, Atmos. Chem. Phys., 3, 211–223, doi:10.5194/acp-3-211-2003, 2003.

Möhler, O., Büttner, S., Linke, C., Schnaiter, M., Saathoff, H., Stetzer, O., Wagner, R., Krämer, M., Mangold, A., Ebert, V., and Schurath, U.: Effect of sulphuric acid coating on heterogeneous ice nucleation by soot aerosol particles, J. Geophys. Res., 110, D11 210, doi:10.1029/2004JD005 169, 2005

Murphy, D. M. and Koop, T.: Review of the vapour pressures of ice and supercooled water for atmospheric applications, Q. J. Roy. Meteor. Soc., 131, 1539–1565, doi/10.1256/qj.04.942005.

Nicolet, M., Stetzer, O., Lüond, F., Möhler, O., and Lohmann, U.: Single ice crystal measurements during nucleation experiments with the depolarization detector IODE, Atmos. Chem. Phys., 10, 313–325, 2010.

Niemand, M., Möhler, O., Vogel, B., Vogel, H., Hoose, C., Connolly, P., Klein, H., Bingemer, H., DeMott, P., and Skrotzki, J.: A particle-surface-area-based parameterization of immersion freezing on desert dust particles, J. Atmos. Sci., 69, 3077–3092, doi:10.1175/Jas-D-11-0249.1, 2012.

O′Sullivan, D., Murray, B. J., Ross, J. F., Whale, T. F., Price, H. C., Atkinson, J. D., Umo, N. S., and Webb, M. E.: The relevance of nanoscale biological fragments for ice nucleation in clouds, Sci. Rep., 5, 8082, doi: 10.1038/srep08082, 2015.

Polen, M., Lawlis, E. and Sullivan, R. C.: The unstable ice nucleation properties of Snomax® bacterial particles, J. Geophys. Res. Atmos., 121(19), 11,666-11,678, doi:10.1002/2016JD025251, 2016.

Prenni, A. J., DeMott, P. J., Rogers, D. C., Kreidenweis, S. M., McFarquhar, G. M., Zhang, G., and Poellot, M. R.: Ice nuclei characteristics from M-PACE and their relation to ice formation in clouds, Tellus B, 61, 436–448, https://doi.org/10.1111/j.1600-45 0889.2009.00415.x, 2009.

Pummer, B. G., Bauer, H., Bernardi, J., Bleicher, S., and Grothe, H.: Suspendable macromolecules are responsible for ice nucleation activity of birch and conifer pollen, Atmos. Chem. Phys., 12, 2541-2550, doi:10.5194/acp-12-2541-2012, 2012.

Reicher, N., Segev, L., and Rudich, Y., The WeIzmann Supercooled Droplets Observation on a Microarray (WISDOM), Atmospheric Measurement Techniques, 11, 233–248, 2018.

Rogers, D. C.: Development of a continuous flow thermal gradient diffusion chamber for ice nucleation studies, Atmospheric Research, *22*(2), 149-181, doi:10.1016/0169-8095(88)90005-1, 1988.

Rogers, D. C., DeMott, P. J., Kreidenweis S. M., and Chen, Y., A continuous flow diffusion chamber for airborne measurements of ice nuclei, J. Atmos. Oceanic Technol., 18, 725-741, doi:10.1175/1520-0426(2001)018<0725:ACFDCF>2.0.CO;2, 2001.

Santachiara, G., Di Matteo, L., Prodi, F., Belosi, F.: Atmospheric particles acting as Ice Forming Nuclei in different size ranges, Atmos. Res. 96, 266-272, 2010.

Schiebel, T.: Ice Nucleation Activity of Soil Dust Aerosols, Ph. D. Dissertation, Institute for Meteorology and Climate Research - Atmospheric Aerosol Research (IMK-AAF), 131 pp., DOI: 10.5445 /IR/1000076327, 2017.

Schill, G. P., Jathar, S. H., Kodros, J. K., Levin, E. J. T., Galang, A. M., Friedman, B., Link, M. F., Farmer, D. K., Pierce, J. R., Kreidenweis, S. M. and DeMott, P. J.: Ice-nucleating particle emissions from photochemically-aged diesel and biodiesel exhaust, Geophys. Res. Lett., 43, 5524–5531, doi:10.1002/2016GL069529, 2016.

Schmitz, C. H. J., Rowat, A. C., Koster, S. and Weitz, D. A.: Dropspots: a picoliter array in a microfluidic device, Lab on a Chip, 9, 44–49, doi:10.1039/B809670H, 2009.

Schnaiter, M., Büttner, S., Möhler, O., Skrotzki, J., Vragel, M., and Wagner, R.: Influence of particle size and shape on the backscattering linear depolarisation ratio of small ice crystals – cloud chamber measurements in the context of contrail and cirrus microphysics, Atmos. Chem. Phys., 12, 10465-10484, doi:10.5194/acp-12-10465-2012, 2012.

Schrod, J., Danielczok, A., Weber, D., Ebert, M., Thomson, E. S., and Bingemer, H. G.: Re-evaluating the Frankfurt isothermal static diffusion chamber for ice nucleation, Atmos. Meas. Tech., 9, 1313-1324, doi:10.5194/amt-9-1313-2016, 2016.

Stetzer, O., Baschek, B., Löünd, F., and Lohmann, U.: The Zurich Ice Nucleation Chamber (ZINC)—A new instrument to investigate atmospheric ice formation, Aerosol Sci. Technol., 42(1), 64–74, doi:10.1080/02786820701787944, 2008.

Vali, G.: Quantitative evaluation of experimental results on the heterogeneous freezing nucleation of supercooled liquids. J. Atmos. Sci., 28, 402–409, doi:10.1175/1520-0469(1971)028<0402:QEOERA>2.0.CO;2, 1971.

Wagner, R., Möhler, O., Saathoff, H., Schnaiter, M., and Leisner, T.: New cloud chamber experiments on the heterogeneous ice nucleation ability of oxalic acid in the immersion mode, Atmos. Chem. Phys., 11, 2083–2110, doi:10.5194/acp-11-2083-2011, 2011.

Whale, T. F., Murray, B. J., O'Sullivan, D., Wilson, T. W., Umo, N. S., Baustian, K. J., Atkinson, J. D., Workneh, D. A., and Morris, G. J.: A technique for quantifying heterogeneous ice nucleation in microlitre supercooled water droplets, Atmos. Meas. Tech., 8, 2437-2447, 2015

Wright, T. P. and Petters, M. D.: The role of time in heterogeneous freezing nucleation, J. Geophys. Res. Atmos., 118, 3731–3743, doi:10.1002/jgrd.50365, 2013.

Zenker, J., Collier, K. N., Xu, G., Yang, P., Levin, E. J. T., Suski, K. J., DeMott, P. J., and Brooks, S. D., Using depolarization to quantify ice nucleating particle concentrations: a new method, Atmos. Meas. Tech., 10, 4639–4657, https://doi.org/10.5194/amt-10-4639-0, 2017.

Table S1. Direct processing (online) instrument data used in the manuscript figures. Listed are the date, experiment identifier, aerosol particle sample type, sample number if applicable, instrument, relative humidity, temperature, correction factor (*: see footnote), INP concentration in air (#: see footnote), positive INP concentration uncertainty defined by confidence interval, negative INP uncertainty, total particle number of reference to INP concentration, surface area concentration, INP active fraction, positive uncertainty in active fraction defined by confidence interval, negative uncertainty in active fraction, active site density, positive uncertainty in active site density, negative uncertainty in active site density, threshold size or optical particle counter channel for defining ice crystals versus aerosol particles ("depol" refers to depolarization detection of ice), and evaporation section temperature (&: see footnote).

Date	Expt	Aerosol	Instrument	Sample	RHw	Temp	Corr fact*	INP Conc.#	ci INP+	ci INP-	total particles	Sfc area	frac	frac_ci+	frac_ci-	$n_{s,geo}$	$n_{s,geo}$ ci+	$n_{s,geo}$ ci-	Ice threshold	Evap T&
					%	°C		m^{-3}	m^{-3}	m^{-3}	cm^{-3}	$\mu m^2 cm^{-3}$				m^{-2}	m^{-2}	m^{-2}		
11-Mar-15	APC-01	IS03	SPIN-TROPOS		101.3	-34.4	1.0	9750000.0	390000.0	390000.0	390.0	230.0	2.50E-02	1.00E-03	1.00E-03	4.24E+10	1.07E+10	1.07E+10	3 μm	lamina T
13-Mar-15	APC-03	IS03	CFDC-CSU		105.5	-20.9	1.0	70900.0	10500.0	10500.0	2000.0	430.0	3.55E-05	5.25E-06	5.25E-06	1.74E+08	8.58E+07	8.58E+07	3 μm	cold wall
13-Mar-15			INKA		105.5	-20.3	1.0	75753.7	15150.7	15150.7	1800.0	414.0	4.21E-05	8.42E-06	8.42E-06	3.08E+09	7.80E+08	3.29E+09	>4 μm	cold wall
16-Mar-15	APC-08	IS03	CFDC-CSU		105.5	-30.3	4.0	18107847.8	680412.3	171600.0	18636.0	5569.0	9.72E-04	3.65E-05	3.65E-05	3.08E+09	7.80E+08	3.29E+09	Chnl 165	cold wall
					105.4	-25.0	12.2	234774.7	148406.8	12227.0	18636.0	5569.0	1.26E-05	7.96E-06	7.96E-06	4.00E+07	2.72E+07	8.37E+08	Chnl 165	cold wall
					105.5	-20.0	10.8	79853.2	93881.4	7392.0	18636.0	5569.0	4.28E-06	5.04E-06	5.04E-06	1.36E+07	1.64E+07	1.86E+08	Chnl 165	cold wall
		IS03	SPIN-TROPOS		103.7	-34.4	1.8	181542633.7	2648820.8	2648820.8	18636.0	5569.0	1.04E-01	1.51E-03	1.51E-03	4.51E+11	6.58E+09	6.58E+09	3 μm	lamina T
					103.6	-27.0	3.3	4853838.9	616796.0	616796.0	18636.0	5569.0	4.26E-03	5.41E-04	5.41E-04	1.85E+10	2.35E+09	2.35E+09	3 μm	lamina T
		IS03	INKA		105.1	-25.0	5.0	196000.0	39200.0	39200.0	18636.0	5569.0	1.06E-05	2.12E-06	2.12E-06	4.41E+07	8.83E+06	8.83E+06	>4 μm	cold wall
					104.7	-30.1	12.1	20449000.0	4089800.0	4089800.0	18636.0	5569.0	7.35E-04	1.47E-04	1.47E-04	3.19E+09	6.39E+08	6.39E+08	>4 μm	cold wall
16-Mar-15	AIDA-04	IS03	AIDA		101.7	-30.6	1.0	1569810.0	1883770.0	1255850.0	484.0	86.0	4.18E-03	5.02E-03	3.35E-03	2.35E+10	2.84E+10	1.90E+10	N/A	N/A
					101.3	-31.1	1.0	3459500.0	4151400.0	2767600.0	484.0	86.0	9.34E-03	1.12E-02	7.47E-03	5.26E+10	6.33E+10	4.24E+10	N/A	N/A
					101.1	-31.6	1.0	6587250.0	7904700.0	5269800.0	484.0	86.0	1.81E-02	2.17E-02	1.45E-02	1.02E+11	1.23E+11	8.21E+10	N/A	N/A
			CFDC-CSU		105.5	-25.0	1.0	68778.0	16326.0	16326.0	394.0	93.0	1.75E-04	4.14E-05	4.14E-05	7.40E+08	1.90E+08	1.90E+08	3 μm	cold wall
					105.6	-30.2	1.0	584341.0	68601.0	68601.0	421.0	97.2	1.39E-03	1.63E-04	1.63E-04	6.01E+09	9.27E+08	9.27E+08	3 μm	cold wall
					109.4	-25.3	1.0	828162.0	59964.0	59964.0	394.0	93.0	2.10E-03	1.52E-04	1.52E-04	8.90E+09	1.10E+09	1.10E+09	3 μm	cold wall
					111.5	-30.0	1.0	8946137.0	193338.0	193338.0	421.0	97.2	2.12E-02	4.59E-04	4.59E-04	9.20E+10	9.42E+09	9.42E+09	3 μm	cold wall
			CIC-PNNL		106.0	-30.0	1.0	17160000.0	-	-	550.0	99.0	1.50E-02	-	-	8.33E+10	2.08E+10	2.08E+10	3 μm	lamina T
19-Mar-15	AIDA-10	IS03	AIDA		101.1	-26.3	1.0	192448.0	230938.0	153958.0	400.0	132.0	6.17E-04	7.40E-04	4.93E-04	1.87E+09	2.25E+09	1.51E+09	N/A	N/A
					101.2	-26.5	1.0	543041.0	651649.0	434433.0	400.0	132.0	1.76E-03	2.12E-03	1.41E-03	5.34E+09	6.44E+09	4.31E+09	N/A	N/A
					102.5	-26.7	1.0	732475.0	878970.0	585980.0	400.0	132.0	2.41E-03	2.89E-03	1.93E-03	7.30E+09	8.79E+09	5.89E+09	N/A	N/A
					102.2	-26.9	1.0	823390.0	988068.0	658712.0	400.0	132.0	2.74E-03	3.29E-03	2.19E-03	8.31E+09	1.00E+10	6.70E+09	N/A	N/A
					100.8	-27.0	1.0	1162000.0	1394400.0	929600.0	400.0	132.0	3.92E-03	4.70E-03	3.13E-03	1.19E+10	1.43E+10	9.57E+09	N/A	N/A
			CFDC-CSU		105.5	-30.6	1.0	2413879.0	120848.0	120848.0	378.0	134.0	6.39E-03	3.20E-04	3.20E-04	1.80E+10	2.01E+09	2.01E+09	3 μm	cold wall
			PIMCA-PINC		N/A	-38.5	1.0	299061333.2	33953807.2	38404474.0	400.0	134.0	7.48E-01	8.49E-02	9.60E-02	2.23E+12	6.13E+11	1.72E+11	depol	N/A
					N/A	-38.2	1.0	276145333.2	36848323.2	34481656.8	400.0	134.0	6.90E-01	9.21E-02	8.62E-02	2.06E+12	5.84E+11	1.63E+11	depol	N/A
					N/A	-37.8	1.0	212377000.0	48921000.0	38201000.0	400.0	134.0	5.31E-01	1.22E-01	9.55E-02	1.58E+12	5.39E+11	1.66E+11	depol	N/A
					N/A	-36.5	1.0	134644000.0	68755168.4	47004502.0	400.0	134.0	3.37E-01	1.72E-01	1.18E-01	1.00E+12	5.71E+11	2.45E+11	depol	N/A
					N/A	-36.4	1.0	120190000.0	62093168.8	40477168.8	400.0	134.0	3.00E-01	1.55E-01	1.01E-01	8.97E+11	5.15E+11	2.16E+11	depol	N/A
					N/A	-36.3	1.0	97368000.0	54838768.0	36028768.0	400.0	134.0	2.43E-01	1.37E-01	9.01E-02	7.27E+11	4.48E+11	2.00E+11	depol	N/A
					N/A	-34.0	1.0	83825333.2	67323007.2	37000340.8	400.0	134.0	2.10E-01	1.68E-01	9.25E-02	6.26E+11	5.26E+11	2.67E+11	depol	N/A
26-Mar-15	AIDA-22	IS03	CFDC-TAMU		103.0	-25.5	1.0	171540.1129	148194.826	148194.826	1850.0	890.0	9.27E-05	8.01E-05	8.01E-05	1.93E+08	1.67E+08	1.67E+08	2 μm	~lamina T@
					101.7	-26.5	1.0	1865311.781	287731.3033	287731.3033	1600.0	870.0	1.17E-03	1.80E-04	1.80E-04	2.14E+09	3.31E+08	3.31E+08	2 μm	~lamina T@
					104.0	-30.4	1.0	1302200.052	287731.3033	287731.3033	1507.0	802.0	8.64E-04	1.91E-04	1.91E-04	1.62E+09	3.59E+08	3.59E+08	2 μm	~lamina T@
			PINC		112.4	-30.5	1.0	521000.0	50000.0	50000	1500.0	901.0	3.47E-04	3.33E-05	3.33E-05	7.32E+08	1.96E+08	1.96E+08	3 μm	warm wall
					109.8	-25.5	1.0	17700.0	10000.0	10000	1500.0	892.0	1.18E-05	6.67E-06	6.67E-06	2.23E+07	1.38E+07	1.38E+07	3 μm	warm wall
27-Mar-15	AIDA-25	IS03	PINC		101.9	-35.5	1.0	7500000.0	200000.0	200000.0	973.0	303.0	3.75E-02	1.00E-03	1.00E-03	1.20E+11	3.03E+10	3.03E+10	3 μm	warm wall

18-Mar-15	AIDA-08	FS02	CFDC-CSU		105.5	-30.0	1.0	175974148.0	1175834.0	1175834.0	380.0	155.0	4.78E-01	3.19E-03	3.19E-03	1.17E+12	2.93E+11	2.93E+11	3 μm	cold wall
			PIMCA-PINC		N/A	-34.8	1.0	358134800.0	9184517.9	11168117.9	380.0	155.0	9.42E-01	2.42E-02	2.94E-02	2.31E+12	5.81E+11	1.46E+11	depol	N/A
					N/A	-31.4	1.0	365743666.5	4440032.5	4448899.4	380.0	155.0	9.62E-01	1.17E-02	1.17E-02	2.36E+12	5.91E+11	1.48E+11	depol	N/A
					N/A	-29.0	1.0	361282466.5	7665231.2	7829898.1	380.0	155.0	9.51E-01	2.02E-02	2.06E-02	2.33E+12	5.85E+11	1.47E+11	depol	N/A
					N/A	-27.0	1.0	288390866.5	23884327.0	20018460.4	380.0	155.0	7.59E-01	6.29E-02	5.27E-02	1.86E+12	4.90E+11	1.27E+11	depol	N/A
					N/A	-25.9	1.0	193612533.5	32959764.4	24299564.4	380.0	155.0	5.10E-01	8.67E-02	6.39E-02	1.25E+12	3.78E+11	1.06E+11	depol	N/A
					N/A	-25.0	1.0	92454000.0	46089619.0	30184085.5	380.0	155.0	2.43E-01	1.21E-01	7.94E-02	5.96E+11	3.33E+11	1.37E+11	depol	N/A
					N/A	-24.0	1.0	52326000.0	47028852.4	26026252.4	380.0	155.0	1.38E-01	1.24E-01	6.85E-02	3.38E+11	3.15E+11	1.75E+11	depol	N/A
					N/A	-23.2	1.0	34250666.5	39367891.7	19691491.7	380.0	155.0	9.01E-02	1.04E-01	5.18E-02	2.21E+11	2.60E+11	1.63E+11	depol	N/A
19-Mar-15	APC-14	FS02	CFDC-CSU		105.0	-25.0	15.1	1927241005.9	7604512.7	7604512.7	7750.2	3703.1	2.49E-01	9.81E-04	5.80E-04	5.20E+11	1.30E+11	1.30E+11	3 μm	cold wall
			INKA		104.1	-20.0	4.1	5378173.7	114153.8	114153.8	7750.2	3703.1	6.94E-04	1.47E-05	1.47E-05	1.45E+09	3.64E+08	3.64E+08	>4 μm	cold wall
					104.7	-25.0	5.7	903242700.7	2460189.4	2460189.4	7750.2	3703.1	1.17E-01	3.17E-04	3.17E-04	2.44E+11	6.10E+10	6.10E+10	>4 μm	cold wall
					104.7	-30.1	8.6	2670340000.0	18051988.9	18051988.9	7750.2	3703.1	3.45E-01	2.33E-03	2.33E-03	7.21E+11	1.80E+11	1.80E+11	>4 μm	cold wall
			PIMCA-PINC		N/A	-32.9	1.0	7575532413.6	48408615.5	78324372.0	7750.2	3703.1	9.77E-01	6.25E-03	1.01E-02	2.05E+12	5.12E+11	5.12E+11	depol	N/A
					N/A	-29.4	1.0	7558494901.9	44331121.1	86995950.1	7750.2	3703.1	9.75E-01	5.72E-03	1.12E-02	2.04E+12	5.10E+11	5.11E+11	depol	N/A
					N/A	-28.4	1.0	7299031259.4	135528351.7	202877555.0	7750.2	3703.1	9.42E-01	1.75E-02	2.62E-02	1.97E+12	4.94E+11	4.96E+11	depol	N/A
					N/A	-28.1	1.0	7097371159.5	219962614.0	194154461.4	7750.2	3703.1	9.16E-01	2.84E-02	2.51E-02	1.92E+12	4.83E+11	4.82E+11	depol	N/A
					N/A	-27.4	1.0	6882354883.3	244974891.3	305633094.6	7750.2	3703.1	8.88E-01	3.16E-02	3.94E-02	1.86E+12	4.69E+11	4.72E+11	depol	N/A
					N/A	-27.1	1.0	6434755232.9	380252656.0	427838859.4	7750.2	3703.1	8.30E-01	4.91E-02	5.52E-02	1.74E+12	4.46E+11	4.50E+11	depol	N/A
					N/A	-26.1	1.0	5234714884.3	554639769.7	479643711.5	7750.2	3703.1	6.75E-01	7.16E-02	6.19E-02	1.41E+12	3.84E+11	3.76E+11	depol	N/A
					N/A	-25.5	1.0	3817694879.0	599085113.2	434806789.4	7750.2	3703.1	4.93E-01	7.73E-02	5.61E-02	1.03E+12	3.04E+11	2.83E+11	depol	N/A
			SPIN-TROPOS		105.7	-36.5	6.6	3013418082.5	17131132.6	17131132.6	7750.2	3703.1	3.89E-01	2.21E-03	1.43E-03	8.14E+11	2.03E+11	2.03E+11	3 μm	lamina T
					105.1	-31.7	8.0	3235505258.5	19002992.0	19002992.0	7750.2	3703.1	4.17E-01	2.45E-03	1.59E-03	8.74E+11	2.18E+11	2.18E+11	3 μm	lamina T
					103.9	-27.2	7.5	1965720157.0	16199258.7	16199258.7	7750.2	3703.1	2.54E-01	2.09E-03	1.94E-03	5.31E+11	1.33E+11	1.33E+11	3 μm	lamina T
					102.8	-22.9	9.5	147317204.7	5739492.3	5739492.3	7750.2	3703.1	1.90E-02	7.41E-04	7.55E-04	3.98E+10	1.01E+10	1.01E+10	3 μm	lamina T
			SPIN-MIT		105.0	-30.8	4.8	331363861.3	-	-	7750.2	3703.1	4.28E-02	-	-	8.95E+10	2.24E+10	2.24E+10	depol	lamina T[%]
					105.0	-21.3	6.2	217900313.9	-	-	7750.2	3703.1	2.81E-02	-	-	5.88E+10	1.47E+10	1.47E+10	depol	lamina T[%]
20-Mar-15	AIDA-11	FS02	CFDC-CSU		105.7	-20.1	1.0	67556.0	7422.0	7422.0	389.0	151.0	1.80E-04	9.00E-05	9.00E-05	4.64E+08	3.43E+09	3.43E+09	3 μm	cold wall
			CIC-PNNL		106.0	-30.0	1.0	171000000.0	-	-	380.0	151.0	4.50E-01	-	-	1.13E+12	2.83E+11	2.83E+11	3 μm	lamina T
			SPIN-MIT		103.0	-31.1	1.0	80000.0	79.0	79.0	405.0	252.0	1.98E-01	9.88E-04	9.88E-04	3.17E+11	7.94E+10	7.94E+10	depol	lamina T[%]
					106.0	-21.7	1.0	15000.0	6.8	6.8	382.0	151.0	3.93E-02	4.53E-04	4.53E-04	9.93E+10	2.49E+10	2.49E+10	depol	lamina T[%]
			SPIN-TROPOS		104.1	-27.2	1.0	120590.0	448.7	448.7	389.0	151.0	3.10E-01	3.72E-03	3.72E-03	7.99E+11	2.00E+11	2.00E+11	3 μm	lamina T
					103.3	-24.4	1.0	37500.0	94.8	94.8	375.0	145.0	1.00E-01	2.53E-03	2.53E-03	2.59E+11	6.50E+10	6.50E+10	3 μm	lamina T
23-Mar-15	AIDA-14	FS02	AIDA		101.6	-20.3	1.0	1332420.0	1598900.0	1065940.0	300.0	114.0	5.03E-03	6.04E-03	4.03E-03	1.32E+10	1.60E+10	1.07E+10	N/A	N/A
					100.8	-20.9	1.0	6922620.0	8307140.0	5538100.0	300.0	114.0	2.66E-02	3.19E-02	2.13E-02	7.00E+10	8.43E+10	5.64E+10	N/A	N/A
			CFDC-CSU		105.6	-20.2	1.0	9917338.0	150739.0	150739.0	300.0	114.0	3.41E-02	5.19E-04	5.19E-04	8.98E+10	2.40E+10	2.40E+10	3 μm	cold wall
					105.5	-25.6	1.0	105206098.0	751115.0	751115.0	268.0	102.0	3.69E-01	2.63E-03	2.63E-03	9.69E+11	2.42E+11	2.42E+11	3 μm	cold wall
					105.5	-30.2	1.0	121683497.0	1277222.0	1277222.0	270.0	107.0	4.51E-01	4.73E-03	4.73E-03	1.14E+12	2.84E+11	2.84E+11	3 μm	cold wall
			INKA		104.0	-20.0	1.0	139424.0	27884.9	27884.9	290.0	115.0	4.81E-04	9.62E-05	9.62E-05	1.21E+09	3.88E+08	3.88E+08	>4 μm	cold wall
					103.3	-30.0	1.0	70256300.0	14051300.0	14051300.0	290.0	102.0	2.42E-01	4.85E-02	4.85E-02	6.89E+11	2.21E+11	2.21E+11	>4 μm	cold wall
			PINC		110.9	-30.5	1.0	98000.0	700.0	700.0	300.0	114.0	3.92E-01	2.80E-03	2.80E-03	1.03E+12	2.58E+11	2.58E+11	3 μm	warm wall
					104.7	-25.3	1.0	2840.0	140.0	140.0	268.0	102.0	1.14E-02	5.60E-04	5.60E-04	2.98E+10	7.61E+09	7.61E+09	3 μm	warm wall
					106.6	-20.3	1.0	14.7	20.0	20.0	270.0	107.0	5.88E-05	8.00E-05	8.00E-05	1.48E+08	2.05E+08	2.05E+08	3 μm	warm wall
17-Mar-15	APC-16	SM04	CFDC-CSU		105.2	-9.3	12.9	169686600.0	3096.0	3096.0	27802.0	4028.0	6.10E-03	1.11E-04	1.11E-04	4.21E+10	1.06E+10	1.06E+10	2 μm	cold wall
					101.8	-19.9	5.0	186550000.0	2205.0	2205.0	27802.0	4028.0	6.71E-03	7.93E-05	7.93E-05	4.63E+10	1.16E+10	1.16E+10	3 μm	cold wall
			CFDC-TAMU		109.3	-33.0	2.8	242718750.0	94660312.0	94660312.0	27802.0	4028.0	8.73E-03	3.40E-03	3.40E-03	6.03E+10	2.79E+10	2.79E+10	2 μm	~lamina T[@]
					101.0	-21.0	5.3	847058824.0	330352941.0	330352941.0	27802.0	4028.0	3.05E-02	1.19E-02	1.19E-02	2.10E+11	9.74E+10	9.74E+10	2 μm	~lamina T[@]

			INKA		104.3	-10.1	3.8	151875000.0	30375000.0	30375000.0	27802.0	4028.0	4.98E-03	1.13E-03	1.13E-03	3.44E+10	1.16E+10	1.16E+10	>4 μm	cold wall
					104.4	-10.1	4.0	156246400.0	31249320.0	31249320.0	27802.0	4028.0	3.16E-03	1.14E-04	1.14E-04	2.18E+10	5.51E+09	5.51E+09	>4 μm	cold wall
					104.9	-15.0	5.7	149797834.4	29959509.6	29959509.6	27802.0	4028.0	5.39E-03	1.08E-03	1.11E-04	3.72E+10	1.19E+10	9.33E+09	>4 μm	cold wall
					109.8	-15.0	5.9	530290657.9	106057894.7	106057894.7	27802.0	4028.0	1.91E-02	3.81E-03	1.11E-04	1.32E+11	4.21E+10	3.29E+10	>4 μm	cold wall
					104.2	-20.1	8.5	175567924.5	35113584.9	35113584.9	27802.0	4028.0	6.31E-03	1.26E-03	1.11E-04	4.36E+10	1.40E+10	1.09E+10	>4 μm	cold wall
					104.2	-20.1	8.6	171373714.3	34274742.9	34274742.9	27802.0	4028.0	6.16E-03	1.23E-03	1.11E-04	4.25E+10	1.36E+10	1.07E+10	>4 μm	cold wall
					110.2	-20.0	10.5	202632907.0	40526476.7	40526476.7	27802.0	4028.0	7.29E-03	1.46E-03	1.11E-04	5.03E+10	1.61E+10	1.26E+10	>4 μm	cold wall
			SPIN-MIT		105.0	-20.0	3.4	82127547.2	-	-	27802.0	4028.0	2.95E-03	-	-	2.04E+10	5.10E+09	5.10E+09	depol	lamina T[%]
					105.0	-15.0	4.1	180294545.5	-	-	27802.0	4028.0	6.48E-03	-	-	4.48E+10	1.12E+10	1.12E+10	depol	lamina T[%]
			SPIN-TROPOS		101.3	-18.6	3.5	138461538.5	31475769.2	31475769.2	27802.0	4028.0	4.98E-03	1.13E-03	1.13E-03	3.44E+10	1.16E+10	1.16E+10	3 μm	lamina T
					100.9	-14.0	4.4	87804878.0	3165365.9	3165365.9	27802.0	4028.0	3.16E-03	1.14E-04	1.14E-04	2.18E+10	5.51E+09	5.51E+09	3 μm	lamina T
17-Mar-15	AIDA-06	SM04	AIDA		101.6	-24.2	1.0	2505730.0	3006880.0	2004580.0	241.0	23.3	1.11E-02	1.33E-02	8.85E-03	1.14E+11	1.38E+11	9.23E+10	N/A	N/A
					101.6	-24.6	1.0	2316010.0	2779210.0	1852810.0	241.0	23.3	1.04E-02	1.24E-02	8.30E-03	1.07E+11	1.29E+11	8.65E+10	N/A	N/A
					101.8	-25.2	1.0	4938950.0	5926740.0	3951160.0	241.0	23.3	2.26E-02	2.71E-02	1.80E-02	2.33E+11	2.81E+11	1.88E+11	N/A	N/A
			CFDC-CSU		105.5	-10.0	1.0	552972.0	59028.0	59028.0	259.0	24.0	2.14E-03	2.28E-04	2.28E-04	2.30E+10	3.37E+09	3.37E+09	3 μm	cold wall
					105.5	-15.0	1.0	799823.0	73751.0	73751.0	241.0	23.0	3.24E-03	2.99E-04	2.99E-04	3.48E+10	4.73E+09	4.73E+09	3 μm	cold wall
					108.4	-9.9	1.0	733245.0	32036.0	32036.0	259.0	24.0	2.83E-03	1.24E-04	1.24E-04	3.06E+10	3.33E+09	3.33E+09	3 μm	cold wall
					124.4	-15.4	1.0	1140013.0	115665.0	115665.0	241.0	23.0	4.62E-03	4.68E-04	4.68E-04	4.96E+10	7.06E+09	7.06E+09	3 μm	cold wall
			SPIN-TROPOS		102.0	-18.3	1.0	1912.5	215.0	215.0	255.0	26.0	7.50E-03	8.43E-04	8.43E-04	7.36E+10	2.02E+10	2.02E+10	3 μm	lamina T
					101.2	-13.8	1.0	725.2	139.1	139.1	259.0	24.0	2.80E-03	5.37E-04	5.37E-04	3.02E+10	9.52E+09	9.52E+09	3 μm	lamina T
21-Mar-15	AIDA-13	SM04	AIDA		101.1	-9.1	1.0	2215550.0	2658660.0	1772440.0	229.0	23.0	9.81E-03	1.18E-02	7.85E-03	1.18E+11	7.88E+10	7.88E+10	N/A	N/A
			CFDC-CSU		105.5	-9.5	1.0	1135824.0	44125.0	44125.0	229.0	23.0	4.53E-03	1.76E-04	1.76E-04	4.94E+10	5.30E+09	5.30E+09	3 μm	cold wall
					105.5	-14.9	1.0	1128809.0	73599.0	73599.0	229.0	23.0	4.50E-03	2.93E-04	2.93E-04	4.91E+10	5.86E+09	5.86E+09	3 μm	cold wall
					106.0	-9.6	1.0	733245.0	32036.0	32036.0	229.0	23.0	4.57E-03	1.73E-04	1.73E-04	4.99E+10	5.34E+09	5.34E+09	3 μm	cold wall
					109.4	-14.5	1.0	1148100.0	43328.0	115665.0	229.0	23.0	4.82E-03	3.11E-04	3.11E-04	5.26E+10	6.26E+09	6.26E+09	3 μm	cold wall
			CFDC-TAMU		102.4	-15.0	1.0	984751.9	406643.9	406643.9	75.0	8.0	4.10E-03	1.69E-03	1.69E-03	3.85E+10	1.86E+10	1.86E+10	2 μm	~lamina T[@]
					101.2	-20.0	1.0	839963.3	685955.4	685955.4	230.0	23.0	3.50E-03	2.86E-03	2.86E-03	3.50E+10	2.99E+10	2.99E+10	2 μm	~lamina T[@]
			INKA		104.6	-10.0	1.0	1210537.0	77950.0	216243.0	279.0	24.9	4.51E-03	9.01E-04	9.01E-04	5.05E+10	1.62E+10	1.62E+10	>4 μm	cold wall
					104.6	-15.0	1.0	866660.0	173332.0	173332.0	250.0	23.0	3.61E-03	7.22E-04	7.22E-04	3.93E+10	1.26E+10	1.26E+10	>4 μm	cold wall
27-Mar-15	AIDA-27	SM04	AIDA		99.5	-12.6	1.0	1953930.0	2344720.0	1563140.0	236.0	28.3	9.01E-03	1.08E-02	7.21E-03	9.05E+10	6.06E+10	6.06E+10	N/A	N/A
					101.3	-13.6	1.0	2453210.0	2943850.0	1962570.0	236.0	28.3	1.15E-02	1.38E-02	9.22E-03	1.16E+11	7.75E+10	7.75E+10	N/A	N/A
16-Mar-15	AIDA-05	SDAr01	CFDC-CSU		105.5	-25.0	1.0	4403989.0	215519.0	215519.0	370.0	185.0	1.26E-02	6.15E-04	6.15E-04	2.51E+10	6.36E+09	6.36E+09	3 μm	cold wall
					105.4	-30.1	1.0	9803125.0	135193.0	135193.0	370.0	185.0	2.93E-02	4.04E-04	4.04E-04	5.86E+10	1.47E+10	1.47E+10	3 μm	cold wall
					105.5	-30.3	1.0	21252577.0	448727.0	448727.0	370.0	185.0	6.61E-02	1.40E-03	1.40E-03	1.32E+11	3.31E+10	3.31E+10	3 μm	cold wall
					109.6	-25.2	1.0	14823835.0	366291.0	366291.0	370.0	185.0	4.23E-02	1.04E-03	1.04E-03	8.45E+10	2.11E+10	2.11E+10	3 μm	cold wall
					110.5	-29.0	1.0	35103544.0	542065.0	542065.0	370.0	185.0	1.05E-01	1.61E-03	1.61E-03	2.09E+11	5.24E+10	5.24E+10	3 μm	cold wall
					110.5	-30.5	1.0	48786312.0	599960.0	599960.0	370.0	185.0	1.52E-01	1.87E-03	1.87E-03	3.03E+11	7.59E+10	7.59E+10	3 μm	cold wall
			PIMCA-PINC		N/A	-36.1	1.0	223032300.0	50843550.0	32954050.0	370.0	185.0	6.03E-01	1.37E-01	8.91E-02	1.21E+12	4.08E+11	1.18E+11	depol	N/A
					N/A	-34.9	1.0	174525300.0	73737127.2	44798194.0	370.0	185.0	4.72E-01	1.99E-01	1.21E-01	9.43E+11	4.63E+11	1.66E+11	depol	N/A
					N/A	-33.1	1.0	108551833.2	60830879.0	29242745.4	370.0	185.0	2.93E-01	1.64E-01	7.90E-02	5.87E+11	3.60E+11	1.32E+11	depol	N/A
					N/A	-30.5	1.0	67196933.2	61870305.9	21883172.7	370.0	185.0	1.82E-01	1.67E-01	5.91E-02	3.63E+11	3.47E+11	1.42E+11	depol	N/A
17-Mar-15	APC-10	SDAr01	CFDC-CSU		105.4	-19.9	5.2	151304.3	83478.3	83478.3	3439.0	3038.0	4.40E-05	2.43E-05	2.43E-05	4.98E+07	3.02E+07	3.02E+07	Chnl 165	cold wall
					105.5	-25.0	5.5	12992727.3	681818.2	681818.2	3439.0	3038.0	3.78E-03	1.98E-04	1.98E-04	4.28E+09	1.09E+09	1.09E+09	Chnl 165	cold wall
					105.5	-30.2	6.3	235515789.5	3448421.1	3448421.1	3439.0	3038.0	6.85E-02	1.00E-03	1.00E-03	7.75E+10	1.94E+10	1.94E+10	Chnl 165	cold wall
			INKA		104.2	-20.0	1.9	474285.7	95238.1	95238.1	3439.0	3038.0	1.38E-04	2.77E-05	2.43E-05	1.56E+08	5.01E+07	4.77E+07	>4 μm	cold wall
					104.9	-25.0	3.0	16350000.0	3270000.0	3270000.0	3439.0	3038.0	4.75E-03	9.51E-04	1.98E-04	5.38E+09	1.72E+09	1.36E+09	>4 μm	cold wall
					104.8	-30.0	4.6	156073846.2	31213846.2	31213846.2	3439.0	3038.0	4.54E-02	9.08E-03	1.00E-03	5.14E+10	1.64E+10	1.29E+10	>4 μm	cold wall
			CIC-PNNL		106.0	-25.0	2.4	26860800.0	-	-	3439.0	3038.0	7.81E-03	-	-	8.84E+09	2.21E+09	2.21E+09	3 μm	lamina T

					106.0	-30.0	3.4	328097142.9	-	-	3439.0	3038.0	9.54E-02	-	-	1.08E+11	2.70E+10	2.70E+10	3 μm	lamina T
			SPIN-TROPOS		106.2	-36.5	3.5	402185792.3	5434754.1	5434754.1	3439.0	3038.0	1.17E-01	1.58E-03	2.43E-05	1.32E+11	3.31E+10	3.31E+10	3 μm	lamina T
					105.6	-31.7	4.3	209066666.7	4462933.3	4462933.3	3439.0	3038.0	6.08E-02	1.30E-03	2.43E-05	6.88E+10	1.73E+10	1.72E+10	3 μm	lamina T
					104.3	-27.2	5.3	53333333.3	2602666.7	2602666.7	3439.0	3038.0	1.55E-02	7.57E-04	2.43E-05	1.76E+10	4.47E+09	4.39E+09	3 μm	lamina T
					102.9	-23.0	5.6	5861052.6	887017.5	887017.5	3439.0	3038.0	1.70E-03	2.58E-04	2.43E-05	1.93E+09	5.64E+08	4.83E+08	3 μm	lamina T
			PIMCA-PINC		N/A	-37.4	1.0	2866688000.0	137243683.2	136539683.2	3439.0	3038.0	8.34E-01	3.99E-02	3.97E-02	9.44E+11	2.40E+11	2.40E+11	depol	N/A
					N/A	-36.4	1.0	2634869334.4	243020144.0	213569475.2	3439.0	3038.0	7.66E-01	7.07E-02	6.21E-02	8.67E+11	2.31E+11	2.28E+11	depol	N/A
					N/A	-35.5	1.0	2523424000.0	278050764.8	253282764.8	3439.0	3038.0	7.34E-01	8.08E-02	7.36E-02	8.31E+11	2.27E+11	2.24E+11	depol	N/A
					N/A	-33.9	1.0	2056736000.0	407975027.2	304839027.2	3439.0	3038.0	5.98E-01	1.19E-01	8.86E-02	6.77E+11	2.16E+11	1.97E+11	depol	N/A
					N/A	-32.2	1.0	1574480000.0	456975712.0	305167712.0	3439.0	3038.0	4.58E-01	1.33E-01	8.87E-02	5.18E+11	1.99E+11	1.64E+11	depol	N/A
					N/A	-31.2	1.0	1151029334.4	537707110.4	306197776.0	3439.0	3038.0	3.35E-01	1.56E-01	8.90E-02	3.79E+11	2.01E+11	1.38E+11	depol	N/A
					N/A	-29.3	1.0	775477334.4	513819776.0	226929107.2	3439.0	3038.0	2.25E-01	1.49E-01	6.60E-02	2.55E+11	1.81E+11	9.82E+10	depol	N/A
19-Mar-15	AIDA-09	SDAr01	AIDA		101.4	-24.1	1.0	609000.0	731000.0	487000.0	310.0	172.0	2.12E-03	1.70E-03	2.54E-03	3.82E+09	4.60E+09	3.08E+09	N/A	N/A
					101.1	-24.8	1.0	1730000.0	2070000.0	1380000.0	310.0	172.0	6.10E-03	4.88E-03	7.32E-03	1.10E+10	1.32E+10	8.86E+09	N/A	N/A
					100.9	-25.3	1.0	5180000.0	6210000.0	4140000.0	310.0	172.0	1.86E-02	1.49E-02	2.23E-02	3.36E+10	4.04E+10	2.71E+10	N/A	N/A
			SPIN-MIT		108.0	-30.0	1.0	4840000.0	96234.2	96234.2	310.0	172.0	1.53E-02	3.10E-04	3.10E-04	2.79E+10	7.00E+09	7.00E+09	depol	lamina T[%]
					104.0	-25.0	1.0	5500000.0	108825.5	108825.5	310.0	172.0	1.84E-02	3.51E-04	3.51E-04	3.21E+10	8.05E+09	8.05E+09	depol	lamina T[%]
			SPIN-TROPOS		104.4	-27.3	1.0	10850000.0	500000.4	500.4	310.0	172.0	3.50E-02	1.63E-03	1.63E-03	6.31E+10	1.60E+10	1.60E+10	3 μm	warm wall
26-Mar-15	AIDA-24	SDAr01	PINC		105.1	-30.5	1.0	2040000.0	101957.0	101957.0	177.0	105.0	8.33E-03	5.76E-04	1.00E-06	1.40E+10	3.51E+09	3.51E+09	3 μm	warm wall
18-Mar-15	APC-12	SDT01	CFDC-CSU		105.3	-19.9	6.0	980255.2	214538.4	214538.4	3001.0	2010.0	3.27E-04	7.15E-05	7.15E-05	4.88E+08	1.62E+08	1.62E+08	Chnl 165	cold wall
					105.6	-30.6	2.8	107772733.3	621116.7	621116.7	3001.0	2010.0	3.59E-02	2.07E-04	2.07E-04	5.36E+10	1.34E+10	1.34E+10	Chnl 165	cold wall
			INKA		103.8	-20.0	2.2	307368.5	61517.6	61517.6	3001.0	2010.0	1.02E-04	2.05E-05	2.05E-05	1.53E+08	4.90E+07	4.90E+07	>4 μm	cold wall
					104.8	-25.0	3.5	7555123.3	1511372.1	1511372.1	3001.0	2010.0	2.52E-03	5.04E-04	5.04E-04	3.76E+09	1.20E+09	1.20E+09	>4 μm	cold wall
					104.8	-30.0	5.0	52200360.0	10438080.0	10438080.0	3001.0	2010.0	1.74E-02	3.48E-03	3.48E-03	2.60E+10	8.31E+09	8.31E+09	>4 μm	cold wall
			CIC-PNNL		106.0	-25.0	2.4	54370689.7	-	-	3001.0	2010.0	1.81E-02	0.00E+00	-	-	6.76E+09	6.76E+09	3 μm	lamina T
					106.0	-30.0	5.6	137950400.0	-	-	3001.0	2010.0	4.60E-02	0.00E+00	-	-	1.72E+10	1.72E+10	3 μm	lamina T
			SPIN-TROPOS		105.0	-36.4	2.6	407329565.2	4763478.3	4763478.3	3001.0	2010.0	1.36E-01	1.59E-03	1.59E-03	2.03E+11	5.07E+10	5.07E+10	3 μm	lamina T
					105.0	-31.7	3.5	157894736.8	3600000.0	3600000.0	3001.0	2010.0	5.26E-02	1.20E-03	1.20E-03	7.86E+10	1.97E+10	1.97E+10	3 μm	lamina T
					103.1	-26.7	4.4	35912408.8	1927007.3	1927007.3	3001.0	2010.0	1.20E-02	6.42E-04	6.42E-04	1.79E+10	4.57E+09	4.57E+09	3 μm	lamina T
			PIMCA-PINC		N/A	-36.2	1.0	2380899999.0	177632439.0	181722438.0	3001.0	2010.0	7.93E-01	5.92E-02	6.06E-02	1.51E-02	3.95E-03	3.96E-03	depol	N/A
					N/A	-35.2	1.0	1967649999.0	232633491.0	195113490.0	3001.0	2010.0	6.56E-01	6.76E-02	6.50E-02	1.63E-02	4.40E-03	4.37E-03	depol	N/A
					N/A	-33.7	1.0	1732509999.0	306133458.0	262643457.0	3001.0	2010.0	5.77E-01	8.90E-02	8.75E-02	2.19E-02	6.43E-03	6.40E-03	depol	N/A
					N/A	-32.4	1.0	1299159999.0	236006148.0	165046149.0	3001.0	2010.0	4.33E-01	6.86E-02	5.50E-02	1.37E-02	4.07E-03	3.86E-03	depol	N/A
					N/A	-28.9	1.0	803850000.0	244168851.0	152658852.0	3001.0	2010.0	2.68E-01	7.10E-02	5.09E-02	1.27E-02	4.63E-03	3.99E-03	depol	N/A
18-Mar-15	AIDA-07	SDT01	AIDA		102.3	-23.8	1.0	259237.0	311084.0	207390.0	270.0	131.0	1.08E-03	8.62E-04	1.29E-03	2.22E+09	2.67E+09	1.79E+09	N/A	N/A
					102.3	-24.5	1.0	537809.0	645371.0	430247.0	270.0	131.0	2.27E-03	1.82E-03	2.73E-03	4.68E+09	5.64E+09	3.78E+09	N/A	N/A
					102.2	-25.0	1.0	1093630.0	1312360.0	874904.0	270.0	131.0	4.69E-03	3.75E-03	5.62E-03	9.66E+09	1.16E+10	7.79E+09	N/A	N/A
					101.6	-25.4	1.0	1567560.0	1881070.0	1254050.0	270.0	131.0	6.81E-03	5.44E-03	8.17E-03	1.40E+10	1.69E+10	1.13E+10	N/A	N/A
					100.7	-25.7	1.0	2011470.0	2413760.0	1609180.0	270.0	131.0	8.85E-03	7.08E-03	1.06E-02	1.82E+10	2.20E+10	1.47E+10	N/A	N/A
			CFDC-CSU		105.5	-25.6	1.0	923063.0	33533.0	33533.0	270.0	131.0	3.76E-03	1.37E-04	1.37E-04	7.76E+09	7.74E+09	1.94E+09	3 μm	cold wall
					105.6	-30.3	1.0	5842154.0	203342.0	203342.0	270.0	131.0	2.43E-02	8.47E-04	8.47E-04	5.08E+10	5.01E+10	1.25E+10	3 μm	cold wall
					112.0	-25.2	1.0	5273442.0	113137.0	113137.0	270.0	131.0	2.16E-02	4.64E-04	4.64E-04	4.50E+10	4.46E+10	1.13E+10	3 μm	cold wall
					106.5	-30.3	1.0	6523451.0	234653.0	234653.0	270.0	131.0	2.72E-02	9.78E-04	9.78E-04	5.68E+10	5.60E+10	1.40E+10	3 μm	cold wall
			SPIN-TROPOS		104.1	-27.1	1.0	1781000.0	194000.0	194000.0	270.0	131.0	6.50E-03	7.98E-04	7.98E-04	1.36E+10	3.79E+09	3.79E+09	3 μm	lamina T
20-Mar-15	AIDA-12	SDT01	CFDC-CSU		105.6	-20.6	1.0	4400.0	4575.0	4399.0	285.0	118.0	1.69E-05	1.76E-05	1.68E-05	4.09E+07	1.02E+07	1.02E+07	3 μm	cold wall
					110.8	-20.4	1.0	22400.0	18153.0	18153.0	285.0	118.0	8.60E-05	6.97E-05	6.97E-05	2.08E+08	5.19E+07	5.19E+07	3 μm	cold wall
			SPIN-TROPOS		105.8	-36.3	1.0	7275000.0	401209.0	401209.0	291.0	120.0	2.50E-02	1.48E-03	1.48E-03	6.06E+10	1.56E+10	1.56E+10	3 μm	lamina T
			PIMCA-PINC		N/A	-33.5	1.0	59357899.9	37332147.2	18606697.0	285.0	118.0	2.08E-01	1.31E-01	6.53E-02	5.03E+11	3.40E+11	1.37E+11	depol	N/A

					N/A	-31.3	1.0	45349200.0	44806043.0	18488193.1	285.0	118.0	1.59E-01	1.57E-01	6.49E-02	3.84E+11	3.92E+11	1.87E+11	depol	N/A
					N/A	-28.2	1.0	37908799.9	47585575.1	18572575.1	285.0	118.0	1.33E-01	1.67E-01	6.52E-02	3.21E+11	4.11E+11	2.26E+11	depol	N/A

*: correction factor refers to the particle number concentration ratio in Eq. (3) of the manuscript, the ratio between the integrated average particle concentration during offline sampling to the total particle concentration at the time of online sampling.

#: INP concentration is the actual INP concentration at the time of sampling when the correction factor is 1, but is equal to $n_{INP,online,corr}$ (sample time) when the correction factor exceeds 1.

&: evaporation section temperature refers to the temperature of the online flow chamber walls within the evaporation region of the instruments. Cold wall means that the ice surfaces on both walls are adjusted to the cold wall temperature to induce evaporation. Warm wall is just the opposite. Lamina T means that the walls are adjusted to the aerosol lamina temperature to induce evaporation without a change in temperature.

@: For the CFDC-TAMU, wall temperatures are maintained in the evaporation section, but the warm wall is covered by a hydrophobic material to actively stimulate evaporation, rather than wall temperature control alone. It is not known the extent to which this limits heat transfer from the warm wall, and thereby leads to cooling in the evaporation region.

%: The SPIN-MIT evaporation region temperature was 0 to 5°C warmer than the lamina temperature.

Table S2. Post-processed (offline) instrument data used in the manuscript figures. Listed are the date, experiment identifier, aerosol particle sample type, instrument, sample identifier (shared, or separate filter and number if applicable), temperature, INP concentration in air, positive INP concentration uncertainty defined by confidence interval, negative INP uncertainty, total particle number of reference to INP concentration, surface area concentration, INP active fraction, positive uncertainty in active fraction defined by confidence interval, negative uncertainty in active fraction, active site density, positive uncertainty in active site density, negative uncertainty in active site density, droplet or aliquot volumes used, and notes regarding the data point ("binned" if multiple experiments are combined, and "selected points" if not all temperature points are shown.

Date	Expt	aerosol	Instrument	Sample	Temp	INP Conc	ci INP+	ci INP-	total particles	Sfc area	frac	frac_ci+	frac_ci-	ns,geo	ns,geo ci+	ns,geo ci-	Drop/aliquot volume	Notes
					°C	m^{-3}	m^{-3}	m^{-3}	cm^{-3}	$\mu m^2 cm^{-3}$				m^{-2}	m^{-2}	m^{-2}	µL	
16-Mar-15	APC-07	IS03	BINARY	Shared impinger	-21.0	1630.0	0.0	0.0	18636.2	5568.6	8.75E-08	0.00E+00	0.00E+00	2.93E+05	7.32E+04	7.32E+04	0.6	binned data
					-22.0	4710.0	17400.0	2500.0	18636.2	5568.6	2.53E-07	9.34E-07	1.34E-07	8.46E+05	3.13E+06	4.96E+05	0.6	binned data
					-23.0	19900.0	48600.0	12300.0	18636.2	5568.6	1.07E-06	2.61E-06	6.60E-07	3.57E+06	8.77E+06	2.38E+06	0.6	binned data
					-24.0	84000.0	205000.0	53300.0	18636.2	5568.6	4.51E-06	1.10E-05	2.86E-06	1.51E+07	3.70E+07	1.03E+07	0.6	binned data
					-25.0	260000.0	350000.0	119000.0	18636.2	5568.6	1.40E-05	1.88E-05	6.39E-06	4.67E+07	6.39E+07	2.44E+07	0.6	binned data
					-26.0	542000.0	416000.0	336000.0	18636.2	5568.6	2.91E-05	2.23E-05	1.80E-05	9.73E+07	7.86E+07	6.51E+07	0.6	binned data
					-27.0	1520000.0	1080000.0	1050000.0	18636.2	5568.6	8.16E-05	5.80E-05	5.63E-05	2.73E+08	2.06E+08	2.01E+08	0.6	binned data
					-28.0	3510000.0	3170000.0	1290000.0	18636.2	5568.6	1.88E-04	1.70E-04	6.92E-05	6.30E+08	5.91E+08	2.80E+08	0.6	binned data
					-29.0	6070000.0	650000.0	650000.0	18636.2	5568.6	3.26E-04	3.49E-05	3.49E-05	1.09E+09	2.96E+08	2.96E+08	0.6	binned data
			IS	Filter	-8.9	2.8	12.1	2.3	18636.2	5568.6	1.48E-10	6.49E-10	1.23E-10	4.95E+02	2.18E+03	4.27E+02	50	selected points
					-9.0	5.6	13.9	4.1	18636.2	5568.6	3.01E-10	7.46E-10	2.20E-10	1.01E+03	2.51E+03	7.76E+02	50	selected points
					-9.5	5.6	13.9	4.1	18636.2	5568.6	3.01E-10	7.46E-10	2.20E-10	1.01E+03	2.51E+03	7.76E+02	50	selected points
					-10.0	18.0	19.8	9.9	18636.2	5568.6	9.67E-10	1.06E-09	5.31E-10	3.24E+03	3.64E+03	1.96E+03	50	selected points
					-11.0	18.0	19.8	9.9	18636.2	5568.6	9.67E-10	1.06E-09	5.31E-10	3.24E+03	3.64E+03	1.96E+03	50	selected points
					-12.0	36.6	26.6	16.7	18636.2	5568.6	1.96E-09	1.43E-09	8.96E-10	6.57E+03	5.05E+03	3.43E+03	50	selected points
					-13.3	45.3	29.5	19.7	18636.2	5568.6	2.43E-09	1.58E-09	1.06E-09	8.13E+03	5.68E+03	4.08E+03	50	selected points
					14.0	45.3	29.5	19.7	18636.2	5568.6	2.43E-09	1.58E-09	1.06E-09	8.13E+03	5.68E+03	4.08E+03	50	selected points
					-15.0	85.1	42.7	32.8	18636.2	5568.6	4.57E-09	2.29E-09	1.76E-09	1.53E+04	8.57E+03	7.03E+03	50	selected points
					-16.0	170.9	310.5	113.7	18636.2	5568.6	9.17E-09	1.67E-08	6.10E-09	3.07E+04	5.63E+04	2.18E+04	50	selected points
					-17.0	295.0	368.3	171.5	18636.2	5568.6	1.58E-08	1.98E-08	9.20E-09	5.30E+04	6.75E+04	3.35E+04	50	selected points
					-18.0	499.4	449.5	252.6	18636.2	5568.6	2.68E-08	2.41E-08	1.36E-08	8.97E+04	8.38E+04	5.06E+04	50	selected points
					-19.0	816.0	560.5	363.7	18636.2	5568.6	4.38E-08	3.01E-08	1.95E-08	1.47E+05	1.07E+05	7.49E+04	50	selected points
					-20.0	1853.9	905.0	708.2	18636.2	5568.6	9.95E-08	4.86E-08	3.80E-08	3.33E+05	1.83E+05	1.52E+05	50	selected points
					-20.5	4109.6	1844.5	1647.7	18636.2	5568.6	2.21E-07	9.90E-08	8.84E-08	7.38E+05	3.79E+05	3.49E+05	50	selected points
					-21.0	5899.3	7366.7	3430.1	18636.2	5568.6	3.17E-07	3.95E-07	1.84E-07	1.06E+06	1.35E+06	6.70E+05	50	selected points
					-21.5	11466.7	9529.0	5592.4	18636.2	5568.6	6.15E-07	5.11E-07	3.00E-07	2.06E+06	1.79E+06	1.13E+06	50	selected points
					-22.0	28704.1	15292.0	11355.4	18636.2	5568.6	1.54E-06	8.21E-07	6.09E-07	5.15E+06	3.03E+06	2.41E+06	50	selected points
					-22.5	64454.8	28560.3	24623.7	18636.2	5568.6	3.46E-06	1.53E-06	1.32E-06	1.16E+07	5.89E+06	5.28E+06	50	selected points
					-23.0	171430.6	169050.9	90319.4	18636.2	5568.6	9.20E-06	9.07E-06	4.85E-06	3.08E+07	3.13E+07	1.80E+07	50	selected points
					-23.5	229334.5	190579.1	111847.6	18636.2	5568.6	1.23E-05	1.02E-05	6.00E-06	4.12E+07	3.57E+07	2.26E+07	50	selected points
					-24.0	292509.4	212709.8	133978.3	18636.2	5568.6	1.57E-05	1.14E-05	7.19E-06	5.25E+07	4.04E+07	2.74E+07	50	selected points
					-24.5	526170.6	290088.8	211357.3	18636.2	5568.6	2.82E-05	1.56E-05	1.13E-05	9.45E+07	5.72E+07	4.47E+07	50	selected points
					-25.0	574082.3	305839.2	227107.8	18636.2	5568.6	3.08E-05	1.64E-05	1.22E-05	1.03E+08	6.07E+07	4.82E+07	50	selected points
					-25.5	719508.3	360434.7	279306.3	18636.2	5568.6	3.86E-05	1.93E-05	1.50E-05	1.29E+08	7.23E+07	5.97E+07	50	selected points
					-26.0	1094122.5	515677.1	429288.1	18636.2	5568.6	5.87E-05	2.77E-05	2.30E-05	1.96E+08	1.05E+08	9.14E+07	50	selected points
					-26.6	1444056.6	733940.5	630831.2	18636.2	5568.6	7.75E-05	3.94E-05	3.38E-05	2.59E+08	1.47E+08	1.31E+08	50	selected points
			KIT-CS	Shared impinger	-26.8	938469.4	0.0	0.0	18636.2	5568.6	5.04E-05	0.00E+00	0.00E+00	1.69E+08	4.21E+07	4.21E+07	4.2	
					-27.7	2303457.9	2039358.3	2039358.3	18636.2	5568.6	1.24E-04	1.09E-04	1.09E-04	4.14E+08	3.81E+08	3.81E+08	4.2	

					-28.7	7287660.4	4318310.9	4318310.9	18636.2	5568.6	3.91E-04	2.32E-04	2.32E-04	1.31E+09	8.42E+08	8.42E+08	4.2	
					-29.7	16616677.8	7473340.4	7473340.4	18636.2	5568.6	8.92E-04	4.01E-04	4.01E-04	2.98E+09	1.54E+09	1.54E+09	4.2	
					-30.6	32222547.3	10854765.2	10854765.2	18636.2	5568.6	1.73E-03	5.82E-04	5.82E-04	5.79E+09	2.43E+09	2.43E+09	4.2	
					-31.6	55556777.0	11227616.0	11227616.0	18636.2	5568.6	2.98E-03	6.02E-04	6.02E-04	9.98E+09	3.21E+09	3.21E+09	4.2	
					-32.7	90103941.6	5543139.6	5543139.6	18636.2	5568.6	4.83E-03	2.97E-04	2.97E-04	1.62E+10	4.17E+09	4.17E+09	4.2	
			M-AL	Shared impinger	-22.0	1124.2	346.7	346.7	18636.2	5568.6	6.03E-08	1.86E-08	1.86E-08	2.02E+05	8.01E+04	8.01E+04	4.2	
					-21.0	860.8	262.0	262.0	18636.2	5568.6	4.62E-08	1.41E-08	1.41E-08	1.55E+05	6.09E+04	6.09E+04	4.2	
					-20.0	737.8	227.5	227.5	18636.2	5568.6	3.96E-08	1.22E-08	1.22E-08	1.32E+05	5.26E+04	5.26E+04	4.2	
					-19.0	562.7	179.2	179.2	18636.2	5568.6	3.02E-08	9.62E-09	9.62E-09	1.01E+05	4.09E+04	4.09E+04	4.2	
					-18.0	344.9	111.4	111.4	18636.2	5568.6	1.85E-08	5.98E-09	5.98E-09	6.19E+04	2.53E+04	2.53E+04	4.2	
					-17.0	191.9	63.1	63.1	18636.2	5568.6	1.03E-08	3.39E-09	3.39E-09	3.45E+04	1.42E+04	1.42E+04	4.2	
					-16.0	94.3	28.5	28.5	18636.2	5568.6	5.06E-09	1.53E-09	1.53E-09	1.69E+04	6.64E+03	6.64E+03	4.2	
					-15.0	94.3	28.5	28.5	18636.2	5568.6	5.06E-09	1.53E-09	1.53E-09	1.69E+04	6.64E+03	6.64E+03	4.2	
					-14.0	94.3	37.3	37.3	18636.2	5568.6	5.06E-09	2.00E-09	2.00E-09	1.69E+04	7.92E+03	7.92E+03	4.2	
			NCSU-CS	Shared impinger	-17.0	233.5	0.0	0.0	18636.2	5568.6	1.25E-08	0.00E+00	0.00E+00	4.19E+04	1.05E+04	1.05E+04	1	binned data
					-18.0	297.1	0.0	0.0	18636.2	5568.6	1.59E-08	0.00E+00	0.00E+00	5.34E+04	1.33E+04	1.33E+04	1	binned data
					-19.0	360.8	0.0	0.0	18636.2	5568.6	1.94E-08	0.00E+00	0.00E+00	6.48E+04	1.62E+04	1.62E+04	1	binned data
					-20.0	439.3	0.0	0.0	18636.2	5568.6	2.36E-08	0.00E+00	0.00E+00	7.89E+04	1.97E+04	1.97E+04	1	binned data
					-21.0	49167.9	95188.9	49167.0	18636.2	5568.6	2.64E-06	5.11E-06	2.64E-06	8.83E+06	1.72E+07	9.10E+06	1	binned data
					-22.0	83620.9	97537.7	83620.0	18636.2	5568.6	4.49E-06	5.23E-06	4.49E-06	1.50E+07	1.79E+07	1.55E+07	1	binned data
					-23.0	232405.8	229532.0	229532.0	18636.2	5568.6	1.25E-05	1.23E-05	1.23E-05	4.17E+07	4.25E+07	4.25E+07	1	binned data
					-24.0	525003.8	501473.1	501473.1	18636.2	5568.6	2.82E-05	2.69E-05	2.69E-05	9.43E+07	9.31E+07	9.31E+07	1	binned data
					-25.0	1315450.4	1284452.0	1284452.0	18636.2	5568.6	7.06E-05	6.89E-05	6.89E-05	2.36E+08	2.38E+08	2.38E+08	1	binned data
			NIPI	Shared impinger	-24.0	35300.0	47900.0	20400.0	18636.2	5568.6	1.89E-06	2.57E-06	1.09E-06	6.34E+06	8.75E+06	3.99E+06	1	binned data
					-23.0	15400.0	33700.0	10580.0	18636.2	5568.6	8.26E-07	1.81E-06	5.68E-07	2.77E+06	6.09E+06	2.02E+06	1	binned data
					-22.0	5600.0	15000.0	4080.0	18636.2	5568.6	3.00E-07	8.05E-07	2.19E-07	1.01E+06	2.71E+06	7.75E+05	1	binned data
					-21.0	2100.0	8000.0	1665.0	18636.2	5568.6	1.13E-07	4.29E-07	8.93E-08	3.77E+05	1.44E+06	3.14E+05	1	binned data
					-20.0	701.0	3979.0	596.0	18636.2	5568.6	3.76E-08	2.14E-07	3.20E-08	1.26E+05	7.15E+05	1.12E+05	1	binned data
					-19.0	342.0	838.0	242.6	18636.2	5568.6	1.84E-08	4.50E-08	1.30E-08	6.14E+04	1.51E+05	4.62E+04	1	binned data
					-18.0	119.0	393.0	91.5	18636.2	5568.6	6.39E-09	2.11E-08	4.91E-09	2.14E+04	7.08E+04	1.73E+04	1	binned data
					-17.0	89.4	89.6	44.7	18636.2	5568.6	4.80E-09	4.81E-09	2.40E-09	1.61E+04	1.66E+04	8.97E+03	1	binned data
					-12.0	205.0	205.0	103.0	18636.2	5568.6	1.10E-08	1.10E-08	5.53E-09	3.68E+04	3.79E+04	2.07E+04	1	binned data
			VODCA	Shared impinger	-34.0	410000000.0	39513400.3	39513400.3	18636.2	5568.6	2.20E-02	2.12E-03	2.12E-03	7.36E+10	1.97E+10	1.97E+10	0.000004 - 0.000036	selected points
					-33.0	205000000.0	144781645.5	144781645.5	18636.2	5568.6	1.10E-02	7.77E-03	7.77E-03	3.68E+10	2.76E+10	2.76E+10	0.000004 - 0.000036	selected points
					-32.0	110000000.0	45533430.3	45533430.3	18636.2	5568.6	5.90E-03	2.44E-03	2.44E-03	1.98E+10	9.55E+09	9.55E+09	0.000004 - 0.000036	selected points
					-31.0	48000000.0	5213291.1	5213291.1	18636.2	5568.6	2.58E-03	2.80E-04	2.80E-04	8.62E+09	2.35E+09	2.35E+09	0.000004 - 0.000036	selected points
26-Mar-15	AIDA-22		FRIDGE-IMM	Filter 17	-13.2	1090.0	1700.0	793.0	1688	892	6.46E-07	1.01E-06	4.70E-07	1.22E+06	1.93E+06	9.40E+05	0.5	selected points
					-14.1	1910.0	2030.0	1141.0	1688	892	1.13E-06	1.20E-06	6.76E-07	2.14E+06	2.34E+06	1.39E+06	0.5	selected points
					-16.0	3010.0	2380.0	1510.0	1688	892	1.78E-06	1.41E-06	8.95E-07	3.37E+06	2.80E+06	1.89E+06	0.5	selected points
					-18.0	5780.0	3050.0	2200.0	1688	892	3.42E-06	1.81E-06	1.30E-06	6.48E+06	3.78E+06	2.95E+06	0.5	selected points
					-20.0	14000.0	4400.0	3600.0	1688	892	8.29E-06	2.61E-06	2.13E-06	1.57E+07	6.30E+06	5.63E+06	0.5	selected points
					-22.0	38500.0	7200.0	6300.0	1688	892	2.28E-05	4.27E-06	3.73E-06	4.32E+07	1.35E+07	1.29E+07	0.5	selected points
					-24.0	149000.0	15000.0	14000.0	1688	892	8.83E-05	8.89E-06	8.29E-06	1.67E+08	4.50E+07	4.46E+07	0.5	selected points
					-26.0	826000.0	80000.0	74000.0	1688	892	6.99E-04	9.48E-05	8.89E-05	1.32E+09	3.76E+08	3.71E+08	0.5	selected points
					-27.4	1600000.0	430000.0	300000.0	1688	892	9.48E-04	2.55E-04	1.78E-04	1.79E+09	6.58E+08	5.61E+08	0.5	selected points
			FRIDGE-STD	73	-20	4390	3740	3740	1500	852	2.93E-06	2.49E-06	2.49E-06	5.15E+06	4.39E+06	4.39E+06	N/A	N/A
					-25	14800	12600	12600	1500	852	9.87E-06	8.40E-06	8.40E-06	1.74E+07	1.48E+07	1.48E+07	N/A	N/A
					-30	159000	136000	136000	1500	852	1.06E-04	9.07E-05	9.07E-05	1.87E+08	1.60E+08	1.60E+08	N/A	N/A
			FRIDGE-STD	74	-20	1100	936	936	1500	852	7.33E-07	6.24E-07	6.24E-07	1.39E+06	1.23E+06	1.23E+06	N/A	N/A

					-25	82300	70200	70200	1500	852	5.49E-05	4.68E-05	4.68E-05	1.04E+08	9.23E+07	9.23E+07	N/A	N/A
					-30	777000	663000	663000	1500	852	5.18E-04	4.42E-04	4.42E-04	9.80E+08	8.72E+08	8.72E+08	N/A	N/A
			DFPC-ISAC		-20.2	600	180	180	1600	850	4.00E-07	1.20E-07	1.20E-07	7.53E+05	2.94E+05	2.94E+05	N/A	N/A
17-Mar-15	APC-09	SDAr01	BINARY	Shared impinger	-10.2	1720.0	0.0	0.0	3439.3	3038.1	5.00E-07	0.00E+00	0.00E+00	5.66E+05	1.42E+05	1.42E+05	0.6	binned data
					-11.2	1720.0	0.0	0.0	3439.3	3038.1	5.00E-07	0.00E+00	0.00E+00	5.66E+05	1.42E+05	1.42E+05	0.6	binned data
					-12.2	2330.0	0.0	0.0	3439.3	3038.1	6.77E-07	0.00E+00	0.00E+00	7.67E+05	1.92E+05	1.92E+05	0.6	binned data
					-13.2	2330.0	630.0	610.0	3439.3	3038.1	6.77E-07	1.83E-07	1.77E-07	7.67E+05	2.82E+05	2.78E+05	0.6	binned data
					-14.2	2960.0	650.0	0.0	3439.3	3038.1	8.61E-07	1.89E-07	0.00E+00	9.74E+05	3.24E+05	2.44E+05	0.6	binned data
					-15.2	4280.0	700.0	670.0	3439.3	3038.1	1.24E-06	2.04E-07	1.95E-07	1.41E+06	4.21E+05	4.16E+05	0.6	binned data
					-16.2	4980.0	720.0	700.0	3439.3	3038.1	1.45E-06	2.09E-07	2.04E-07	1.64E+06	4.73E+05	4.70E+05	0.6	binned data
					-17.2	7220.0	9980.0	1520.0	3439.3	3038.1	2.10E-06	2.90E-06	4.42E-07	2.38E+06	3.34E+06	7.77E+05	0.6	binned data
					-18.2	12200.0	5150.0	4120.0	3439.3	3038.1	3.55E-06	1.50E-06	1.20E-06	4.02E+06	1.97E+06	1.69E+06	0.6	binned data
					-19.2	29800.0	27400.0	14900.0	3439.3	3038.1	8.66E-06	7.97E-06	4.33E-06	9.81E+06	9.35E+06	5.48E+06	0.6	binned data
					-20.2	107000.0	95000.0	64200.0	3439.3	3038.1	3.11E-05	2.76E-05	1.87E-05	3.52E+07	3.25E+07	2.29E+07	0.6	binned data
					-21.2	298000.0	412000.0	137000.0	3439.3	3038.1	8.66E-05	1.20E-04	3.98E-05	9.81E+07	1.38E+08	5.13E+07	0.6	binned data
					-22.2	931000.0	1400000.0	503000.0	3439.3	3038.1	2.71E-04	4.07E-04	1.46E-04	3.06E+08	4.67E+08	1.82E+08	0.6	binned data
					-23.2	2750000.0	3690000.0	1260000.0	3439.3	3038.1	8.00E-04	1.07E-03	3.66E-04	9.05E+08	1.24E+09	4.72E+08	0.6	binned data
					-24.2	7220000.0	6480000.0	3670000.0	3439.3	3038.1	2.10E-03	1.88E-03	1.07E-03	2.38E+09	2.21E+09	1.35E+09	0.6	binned data
					-25.2	21800000.0	28000000.0	10200000.0	3439.3	3038.1	6.34E-03	8.14E-03	2.97E-03	7.18E+09	9.39E+09	3.81E+09	0.6	binned data
					-26.2	43500000.0	63500000.0	20000000.0	3439.3	3038.1	1.26E-02	1.85E-02	5.82E-03	1.43E+10	2.12E+10	7.49E+09	0.6	binned data
					-27.2	80300000.0	68700000.0	31100000.0	3439.3	3038.1	2.33E-02	2.00E-02	9.04E-03	2.64E+10	2.36E+10	1.22E+10	0.6	binned data
					-28.2	173000000.0	102000000.0	102000000.0	3439.3	3038.1	5.03E-02	2.97E-02	2.97E-02	5.69E+10	3.65E+10	3.65E+10	0.6	binned data
					-29.2	254000000.0	137000000.0	105000000.0	3439.3	3038.1	7.39E-02	3.98E-02	3.05E-02	8.36E+10	4.97E+10	4.04E+10	0.6	binned data
					-30.2	355000000.0	137000000.0	137000000.0	3439.3	3038.1	1.03E-01	3.98E-02	3.98E-02	1.17E+11	5.37E+10	5.37E+10	0.6	binned data
					-31.2	572000000.0	0.0	137000000.0	3439.3	3038.1	1.66E-01	0.00E+00	3.98E-02	1.88E+11	4.71E+10	6.52E+10	0.6	binned data
					-32.2	641000000.0	69000000.0	149000000.0	3439.3	3038.1	1.86E-01	2.01E-02	4.33E-02	2.11E+11	5.74E+10	7.20E+10	0.6	binned data
			CMU-CS	Shared impinger	-20.0	288560.0	32308.6	32308.6	3439.3	3038.1	8.39E-05	9.39E-06	9.39E-06	9.50E+07	2.60E+07	2.60E+07	0.1	binned data
					-6.0	717.4	1406.1	717.3	3439.3	3038.1	2.09E-07	4.09E-07	2.09E-07	2.36E+05	4.67E+05	2.36E+05	0.1	binned data
					-7.0	1330.0	1410.8	1329.0	3439.3	3038.1	3.87E-07	4.10E-07	3.86E-07	4.38E+05	4.77E+05	4.38E+05	0.1	binned data
					-8.0	2382.1	571.2	571.2	3439.3	3038.1	6.93E-07	1.66E-07	1.66E-07	7.84E+05	2.72E+05	2.72E+05	0.1	binned data
					-9.0	2875.7	756.7	756.7	3439.3	3038.1	8.36E-07	2.20E-07	2.20E-07	9.47E+05	3.44E+05	3.44E+05	0.1	binned data
					-10.0	3358.4	1016.5	1016.5	3439.3	3038.1	9.76E-07	2.96E-07	2.96E-07	1.11E+06	4.34E+05	4.34E+05	0.1	binned data
					-11.0	3843.7	1312.9	1312.9	3439.3	3038.1	1.12E-06	3.82E-07	3.82E-07	1.27E+06	5.36E+05	5.36E+05	0.1	binned data
					-12.0	4783.2	2100.3	2100.3	3439.3	3038.1	1.39E-06	6.11E-07	6.11E-07	1.57E+06	7.96E+05	7.96E+05	0.1	binned data
					-13.0	6232.0	3426.1	3426.1	3439.3	3038.1	1.81E-06	9.96E-07	9.96E-07	2.05E+06	1.24E+06	1.24E+06	0.1	binned data
					-13.2	3010.0	13790.0	2933.8	4747.0	4117.0	6.34E-07	2.90E-06	6.18E-07	7.31E+05	3.35E+06	7.36E+05	0.1	binned data
					-14.0	8142.2	4925.1	4925.1	3439.3	3038.1	2.37E-06	1.43E-06	1.43E-06	2.68E+06	1.75E+06	1.75E+06	0.1	binned data
					-15.0	10344.4	6119.4	6119.4	3439.3	3038.1	3.01E-06	1.78E-06	1.78E-06	3.40E+06	2.19E+06	2.19E+06	0.1	binned data
					-16.0	14318.2	4593.9	4593.9	3439.3	3038.1	4.16E-06	1.34E-06	1.34E-06	4.71E+06	1.92E+06	1.92E+06	0.1	binned data
					-17.0	21726.3	8777.4	8777.4	3439.3	3038.1	6.32E-06	2.55E-06	2.55E-06	7.15E+06	3.40E+06	3.40E+06	0.1	binned data
					-18.0	46312.1	13612.2	13612.2	3439.3	3038.1	1.35E-05	3.96E-06	3.96E-06	1.52E+07	5.88E+06	5.88E+06	0.1	binned data
			FRIDGE-IMM	Filter 3	-19.0	131096.0	51909.2	51909.2	3439.3	3038.1	3.81E-05	1.51E-05	1.51E-05	4.32E+07	2.02E+07	2.02E+07	0.5	selected points
					-14.0	3010.0	13790.0	2933.8	4747.0	4117.0	6.34E-07	2.90E-06	6.18E-07	7.31E+05	3.35E+06	7.36E+05	0.5	selected points
					-15.0	6020.0	15780.0	5291.0	4747.0	4117.0	1.27E-06	3.32E-06	1.11E-06	1.46E+06	3.85E+06	1.34E+06	0.5	selected points
					-16.0	9040.0	17360.0	7180.0	4747.0	4117.0	1.90E-06	3.66E-06	1.51E-06	2.20E+06	4.25E+06	1.83E+06	0.5	selected points
					-17.1	24200.0	23400.0	13800.0	4747.0	4117.0	5.10E-06	4.93E-06	2.91E-06	5.88E+06	5.87E+06	3.66E+06	0.5	selected points
					-18.0	42500.0	28800.0	19300.0	4747.0	4117.0	8.95E-06	6.07E-06	4.07E-06	1.03E+07	7.46E+06	5.35E+06	0.5	selected points
					-19.0	76300.0	36700.0	26900.0	4747.0	4117.0	1.61E-05	7.73E-06	5.67E-06	1.85E+07	1.00E+07	8.01E+06	0.5	selected points
					-20.0	243000.0	61000.0	51000.0	4747.0	4117.0	5.12E-05	1.29E-05	1.07E-05	5.90E+07	2.09E+07	1.93E+07	0.5	selected points

					-21.1	751000.0	108000.0	97000.0	4747.0	4117.0	1.58E-04	2.28E-05	2.04E-05	1.82E+08	5.26E+07	5.13E+07	0.5	selected points
					-22.0	2050000.0	200000.0	190000.0	4747.0	4117.0	4.32E-04	4.21E-05	4.00E-05	4.98E+08	1.34E+08	1.33E+08	0.5	selected points
					-23.0	5170000.0	480000.0	440000.0	4747.0	4117.0	1.09E-03	1.01E-04	9.27E-05	1.26E+09	3.35E+08	3.32E+08	0.5	selected points
					-24.0	15200000.0	5400000.0	3200000.0	4747.0	4117.0	3.20E-03	1.14E-03	6.74E-04	3.69E+09	1.60E+09	1.21E+09	0.5	selected points
			IS	Filter	-6.0	2.8	12.5	2.3	3439.3	3038.1	9.92E-10	8.25E-10	3.63E-09	9.34E+02	4.11E+03	8.06E+02	50	selected points
					-7.0	67.7	37.4	27.2	3439.3	3038.1	2.37E-08	1.97E-08	1.09E-08	2.23E+04	1.35E+04	1.06E+04	50	selected points
					-7.5	247.9	114.8	104.7	3439.3	3038.1	8.66E-08	7.21E-08	3.34E-08	8.16E+04	4.29E+04	4.00E+04	50	selected points
					-8.0	176.0	319.9	117.1	3439.3	3038.1	6.15E-08	5.12E-08	9.30E-08	5.79E+04	1.06E+05	4.12E+04	50	selected points
					-9.1	590.6	490.8	288.0	3439.3	3038.1	2.06E-07	1.72E-07	1.43E-07	1.94E+05	1.69E+05	1.07E+05	50	selected points
					-10.0	1354.9	747.0	544.3	3439.3	3038.1	4.73E-07	3.94E-07	2.17E-07	4.46E+05	2.70E+05	2.11E+05	50	selected points
					-11.0	1478.3	787.6	584.8	3439.3	3038.1	5.16E-07	4.30E-07	2.29E-07	4.87E+05	2.86E+05	2.28E+05	50	selected points
					-12.0	1909.6	932.2	729.5	3439.3	3038.1	6.67E-07	5.55E-07	2.71E-07	6.29E+05	3.45E+05	2.87E+05	50	selected points
					-13.0	2479.1	1135.0	932.3	3439.3	3038.1	8.66E-07	7.21E-07	3.30E-07	8.16E+05	4.26E+05	3.68E+05	50	selected points
					-14.1	3319.6	1470.9	1268.2	3439.3	3038.1	1.16E-06	9.65E-07	4.28E-07	1.09E+06	5.56E+05	4.99E+05	50	selected points
					-15.0	3718.6	1649.3	1446.6	3439.3	3038.1	1.30E-06	1.08E-06	4.80E-07	1.22E+06	6.23E+05	5.66E+05	50	selected points
					-15.0	3520.7	6397.6	2342.7	3439.3	3038.1	1.23E-06	1.02E-06	1.86E-06	1.16E+06	2.13E+06	8.24E+05	50	selected points
					-16.0	7426.3	8151.5	4096.7	3439.3	3038.1	2.59E-06	2.16E-06	2.37E-06	2.44E+06	2.75E+06	1.48E+06	50	selected points
					-17.0	13401.1	10379.0	6324.2	3439.3	3038.1	4.68E-06	3.90E-06	3.02E-06	4.41E+06	3.59E+06	2.36E+06	50	selected points
					-18.0	15064.9	10955.0	6900.2	3439.3	3038.1	5.26E-06	4.38E-06	3.19E-06	4.96E+06	3.81E+06	2.59E+06	50	selected points
					-19.0	27098.9	14940.2	10885.4	3439.3	3038.1	9.47E-06	7.88E-06	4.34E-06	8.92E+06	5.40E+06	4.22E+06	50	selected points
					-20.0	99162.7	45918.1	41863.3	3439.3	3038.1	3.46E-05	2.88E-05	1.34E-05	3.26E+07	1.72E+07	1.60E+07	50	selected points
					-21.0	148526.0	163030.3	81933.5	3439.3	3038.1	5.19E-05	4.32E-05	4.74E-05	4.89E+07	5.50E+07	2.96E+07	50	selected points
					-22.0	388852.3	253009.5	169443.7	3439.3	3038.1	1.36E-04	1.13E-04	7.36E-05	1.28E+08	8.92E+07	6.43E+07	50	selected points
					-22.5	717669.6	369515.7	283325.9	3439.3	3038.1	2.51E-04	2.09E-04	1.07E-04	2.36E+08	1.35E+08	1.10E+08	50	selected points
					-23.0	1441275.4	658624.0	572434.2	3439.3	3038.1	5.03E-04	4.19E-04	1.91E-04	4.74E+08	2.47E+08	2.23E+08	50	selected points
					-23.0	987022.5	2444017.8	720220.5	3439.3	3038.1	3.45E-04	2.87E-04	7.11E-04	3.25E+08	8.09E+08	2.51E+08	50	selected points
					-23.5	3316189.0	3613041.9	1833354.1	3439.3	3038.1	1.16E-03	9.64E-04	1.05E-03	1.09E+09	1.22E+09	6.62E+08	50	selected points
					-24.0	8507970.1	5505748.7	3726060.9	3439.3	3038.1	2.97E-03	2.47E-03	1.60E-03	2.80E+09	1.94E+09	1.41E+09	50	selected points
					-24.5	13868391.4	7352539.1	5572851.3	3439.3	3038.1	4.84E-03	4.03E-03	2.14E-03	4.56E+09	2.68E+09	2.16E+09	50	selected points
					-25.0	31433828.0	15155397.1	13252284.6	3439.3	3038.1	1.10E-02	9.14E-03	4.41E-03	1.03E+10	5.62E+09	5.07E+09	50	selected points
					-25.5	30893909.1	15144476.9	13172991.1	3439.3	3038.1	1.08E-02	8.98E-03	4.40E-03	1.02E+10	5.60E+09	5.03E+09	50	selected points
					-26.0	36694554.5	18333861.4	16362375.7	3439.3	3038.1	1.28E-02	1.07E-02	5.33E-03	1.21E+10	6.75E+09	6.17E+09	50	selected points
			KIT-CS	Shared impinger	-21.7	279.5			3439.3	3038.1	8.13E-05			9.20E+07	2.30E+07	2.30E+07	5.00E-04	
					-22.7	1278.4			3439.3	3038.1	3.72E-04			4.21E+08	1.05E+08	1.05E+08	5.00E-04	
					-23.9	3885.2			3439.3	3038.1	1.13E-03			1.28E+09	3.20E+08	3.20E+08	5.00E-04	
					-24.8	10341.1			3439.3	3038.1	3.01E-03			3.40E+09	8.51E+08	8.51E+08	5.00E-04	
					-25.6	23074.2			3439.3	3038.1	6.71E-03			7.60E+09	1.90E+09	1.90E+09	5.00E-04	
					-26.7	42851.0			3439.3	3038.1	1.25E-02			1.41E+10	3.53E+09	3.53E+09	5.00E-04	
					-27.7	66387.9			3439.3	3038.1	1.93E-02			2.19E+10	5.46E+09	5.46E+09	5.00E-04	
					-28.5	85979.9			3439.3	3038.1	2.50E-02			2.83E+10	7.08E+09	7.08E+09	5.00E-04	
					-29.4	108076.6			3439.3	3038.1	3.14E-02			3.56E+10	8.89E+09	8.89E+09	5.00E-04	
			M-AL	Shared impinger	-7.7	185.0	73.8	73.8	3439.3	3038.1	5.38E-08	2.15E-08	2.15E-08	6.09E+04	2.87E+04	2.87E+04	4.2	
					-8.7	382.5	127.1	127.1	3439.3	3038.1	1.11E-07	3.69E-08	3.69E-08	1.26E+05	5.23E+04	5.23E+04	4.2	
					-9.7	744.6	246.1	246.1	3439.3	3038.1	2.16E-07	7.16E-08	7.16E-08	2.45E+05	1.02E+05	1.02E+05	4.2	
					-10.7	744.6	226.4	226.4	3439.3	3038.1	2.16E-07	6.58E-08	6.58E-08	2.45E+05	9.65E+04	9.65E+04	4.2	
					-11.7	822.7	251.0	251.0	3439.3	3038.1	2.39E-07	7.30E-08	7.30E-08	2.71E+05	1.07E+05	1.07E+05	4.2	
					-12.7	902.9	275.4	275.4	3439.3	3038.1	2.63E-07	8.01E-08	8.01E-08	2.97E+05	1.17E+05	1.17E+05	4.2	
					-13.7	1436.9	460.9	460.9	3439.3	3038.1	4.18E-07	1.34E-07	1.34E-07	4.73E+05	1.92E+05	1.92E+05	4.2	
					-14.7	2090.4	661.6	661.6	3439.3	3038.1	6.08E-07	1.92E-07	1.92E-07	6.88E+05	2.78E+05	2.78E+05	4.2	

					-15.7	2624.4	811.5	811.5	3439.3	3038.1	7.63E-07	2.36E-07	2.36E-07	8.64E+05	3.43E+05	3.43E+05	4.2	
					-16.7	4654.4	1593.7	1593.7	3439.3	3038.1	1.35E-06	4.63E-07	4.63E-07	1.53E+06	6.50E+05	6.50E+05	4.2	
					-17.7	11398.0	7445.7	7445.7	3439.3	3038.1	3.31E-06	2.16E-06	2.16E-06	3.75E+06	2.62E+06	2.62E+06	4.2	
			NCSU-CS	Shared impinger	-9.2	790.8	0.0	0.0	3439.3	3038.1	2.30E-07	0.00E+00	0.00E+00	2.60E+05	6.51E+04	6.51E+04	1	binned
					-10.2	1419.0	0.0	0.0	3439.3	3038.1	4.13E-07	0.00E+00	0.00E+00	4.67E+05	1.17E+05	1.17E+05	1	binned
					-11.2	8420.5	14269.0	8420.5	3439.3	3038.1	2.45E-06	4.15E-06	2.45E-06	2.77E+06	4.75E+06	2.86E+06	1	binned
					-12.2	11034.6	18648.1	11034.0	3439.3	3038.1	3.21E-06	5.42E-06	3.21E-06	3.63E+06	6.20E+06	3.74E+06	1	binned
					-13.2	13600.5	23048.8	13600.4	3439.3	3038.1	3.95E-06	6.70E-06	3.95E-06	4.48E+06	7.67E+06	4.61E+06	1	binned
					-14.2	16098.7	27525.5	16098.0	3439.3	3038.1	4.68E-06	8.00E-06	4.68E-06	5.30E+06	9.16E+06	5.46E+06	1	binned
					-15.2	18907.9	31698.3	18907.0	3439.3	3038.1	5.50E-06	9.22E-06	5.50E-06	6.22E+06	1.05E+07	6.41E+06	1	binned
					-16.2	22044.2	35573.3	22044.0	3439.3	3038.1	6.41E-06	1.03E-05	6.41E-06	7.26E+06	1.18E+07	7.48E+06	1	binned
					-17.2	25962.5	39037.5	25962.4	3439.3	3038.1	7.55E-06	1.14E-05	7.55E-06	8.55E+06	1.30E+07	8.81E+06	1	binned
					-18.2	31815.5	41449.8	31815.5	3439.3	3038.1	9.25E-06	1.21E-05	9.25E-06	1.05E+07	1.39E+07	1.08E+07	1	binned
					-19.2	40835.8	40746.1	89.7	3439.3	3038.1	1.19E-05	1.18E-05	2.61E-08	1.34E+07	1.38E+07	3.36E+06	1	binned
					-20.2	131163.7	84126.8	47036.9	3439.3	3038.1	3.81E-05	2.45E-05	1.37E-05	4.32E+07	2.97E+07	1.89E+07	1	binned
					-21.2	387421.4	145078.4	242343.0	3439.3	3038.1	1.13E-04	4.22E-05	7.05E-05	1.28E+08	5.74E+07	8.59E+07	1	binned
					-22.2	883621.2	111642.9	771978.3	3439.3	3038.1	2.57E-04	3.25E-05	2.24E-04	2.91E+08	8.15E+07	2.64E+08	1	binned
					-23.2	2439642.4	0.0	0.0	3439.3	3038.1	7.09E-04	0.00E+00	0.00E+00	8.03E+08	2.01E+08	2.01E+08	1	binned
			NIPI	Shared impinger	-8.0	243.0	243.0	121.0	3439.3	3038.1	7.07E-08	7.07E-08	3.52E-08	8.00E+04	8.24E+04	4.46E+04	1	binned
					-9.0	464.0	926.0	309.0	3439.3	3038.1	1.35E-07	2.69E-07	8.98E-08	1.53E+05	3.07E+05	1.09E+05	1	binned
					-10.0	1180.0	1830.0	720.0	3439.3	3038.1	3.43E-07	5.32E-07	2.09E-07	3.88E+05	6.10E+05	2.56E+05	1	binned
					-11.0	2040.0	2510.0	1127.0	3439.3	3038.1	5.93E-07	7.30E-07	3.28E-07	6.71E+05	8.43E+05	4.07E+05	1	binned
					-12.0	2300.0	2610.0	1220.0	3439.3	3038.1	6.69E-07	7.59E-07	3.55E-07	7.57E+05	8.80E+05	4.44E+05	1	binned
					-13.0	3110.0	3970.0	1740.0	3439.3	3038.1	9.04E-07	1.15E-06	5.06E-07	1.02E+06	1.33E+06	6.27E+05	1	binned
					-14.0	4320.0	5780.0	2470.0	3439.3	3038.1	1.26E-06	1.68E-06	7.18E-07	1.42E+06	1.94E+06	8.87E+05	1	binned
					-15.0	8040.0	26560.0	6170.0	3439.3	3038.1	2.34E-06	7.72E-06	1.79E-06	2.65E+06	8.77E+06	2.14E+06	1	binned
					-16.0	8040.0	10360.0	4520.0	3439.3	3038.1	2.34E-06	3.01E-06	1.31E-06	2.65E+06	3.47E+06	1.63E+06	1	binned
					-17.0	10600.0	12700.0	5750.0	3439.3	3038.1	3.08E-06	3.69E-06	1.67E-06	3.49E+06	4.27E+06	2.08E+06	1	binned
					-18.0	24900.0	74800.0	18670.0	3439.3	3038.1	7.24E-06	2.17E-05	5.43E-06	8.20E+06	2.47E+07	6.48E+06	1	binned
					-19.0	57700.0	196300.0	44600.0	3439.3	3038.1	1.68E-05	5.71E-05	1.30E-05	1.90E+07	6.48E+07	1.54E+07	1	binned
					-20.0	293000.0	356000.0	160000.0	3439.3	3038.1	8.52E-05	1.04E-04	4.65E-05	9.64E+07	1.20E+08	5.79E+07	1	binned
					-21.0	554000.0	876000.0	339000.0	3439.3	3038.1	1.61E-04	2.55E-04	9.86E-05	1.82E+08	2.92E+08	1.21E+08	1	binned
					-22.0	1550000.0	3150000.0	1036000.0	3439.3	3038.1	4.51E-04	9.16E-04	3.01E-04	5.10E+08	1.04E+09	3.64E+08	1	binned
					-23.0	4560000.0	4550000.0	2280000.0	3439.3	3038.1	1.33E-03	1.32E-03	6.63E-04	1.50E+09	1.54E+09	8.39E+08	1	binned
			VODCA	Shared impinger	-28.2	44256043.6	9052157.0	9052157.0	3439.3	3038.1	1.29E-02	2.63E-03	2.63E-03	1.46E+10	4.71E+09	4.71E+09	0.000004 - 0.000036	selected points
					-29.2	72460652.7	5781348.2	5781348.2	3439.3	3038.1	2.11E-02	1.68E-03	1.68E-03	2.39E+10	6.26E+09	6.26E+09	0.000004 - 0.000036	selected points
					-30.2	85924020.0	5379733.4	5379733.4	3439.3	3038.1	2.50E-02	1.56E-03	1.56E-03	2.83E+10	7.29E+09	7.29E+09	0.000004 - 0.000036	selected points
					-31.2	89119003.3	8459165.1	8459165.1	3439.3	3038.1	2.59E-02	2.46E-03	2.46E-03	2.93E+10	7.84E+09	7.84E+09	0.000004 - 0.000036	selected points
					-32.2	128910268.6	8536962.3	8536962.3	3439.3	3038.1	3.75E-02	2.48E-03	2.48E-03	4.24E+10	1.10E+10	1.10E+10	0.000004 - 0.000036	selected points
					-33.2	166819951.3	8950755.3	8950755.3	3439.3	3038.1	4.85E-02	2.60E-03	2.60E-03	5.49E+10	1.40E+10	1.40E+10	0.000004 - 0.000036	selected points
					-34.2	272951854.4	43641504.0	43641504.0	3439.3	3038.1	7.94E-02	1.27E-02	1.27E-02	8.98E+10	2.67E+10	2.67E+10	0.000004 - 0.000036	selected points
					-35.2	403858245.0	4248181.3	4248181.3	3439.3	3038.1	1.17E-01	1.24E-03	1.24E-03	1.33E+11	3.33E+10	3.33E+10	0.000004 - 0.000036	selected points
			WISDOM	Shared impinger	-23.2	513132.7	1007231.9	513132.7	3439.3	3038.1	1.49E-04	2.93E-04	1.49E-04	1.69E+08	3.34E+08	1.74E+08	0.000014 - 0.000034	binned
					-24.2	2570813.1	4563101.7	2570813.1	3439.3	3038.1	7.47E-04	1.33E-03	7.47E-04	8.46E+08	1.52E+09	8.72E+08	0.000014 - 0.000034	binned
					-25.2	8793855.6	8674513.8	8793855.5	3439.3	3038.1	2.56E-03	2.52E-03	2.56E-03	2.89E+09	2.95E+09	2.98E+09	0.000014 - 0.000034	binned
					-26.2	16680368.7	7099952.2	9089337.5	3439.3	3038.1	4.85E-03	2.06E-03	2.64E-03	5.49E+09	2.71E+09	3.29E+09	0.000014 - 0.000034	binned
					-27.2	27387983.7	5391155.5	6404778.5	3439.3	3038.1	7.96E-03	1.57E-03	1.86E-03	9.01E+09	2.87E+09	3.09E+09	0.000014 - 0.000034	binned
					-28.2	38323923.2	6044116.8	5244841.7	3439.3	3038.1	1.11E-02	1.76E-03	1.52E-03	1.26E+10	3.73E+09	3.60E+09	0.000014 - 0.000034	binned
					-29.2	69071543.3	14032422.5	13277624.1	3439.3	3038.1	2.01E-02	4.08E-03	3.86E-03	2.27E+10	7.32E+09	7.17E+09	0.000014 - 0.000034	binned

					-30.2	98662951.9	33486521.3	31043537.2	3439.3	3038.1	2.87E-02	9.74E-03	9.03E-03	3.25E+10	1.37E+10	1.31E+10	0.000014 - 0.000034	binned
					-31.2	136049870.3	52189404.6	44512630.2	3439.3	3038.1	3.96E-02	1.52E-02	1.29E-02	4.48E+10	2.05E+10	1.84E+10	0.000014 - 0.000034	binned
					-32.2	178552717.2	61531625.3	53190537.8	3439.3	3038.1	5.19E-02	1.79E-02	1.55E-02	5.88E+10	2.50E+10	2.29E+10	0.000014 - 0.000034	binned
					-33.2	228089258.6	64815788.3	55146372.3	3439.3	3038.1	6.63E-02	1.88E-02	1.60E-02	7.51E+10	2.84E+10	2.61E+10	0.000014 - 0.000034	binned
					-34.2	294634848.7	124283866.9	95950524.2	3439.3	3038.1	8.57E-02	3.61E-02	2.79E-02	9.70E+10	4.76E+10	3.98E+10	0.000014 - 0.000034	binned
					-35.2	346348975.4	137283550.9	105460755.9	3439.3	3038.1	1.01E-01	3.99E-02	3.07E-02	1.14E+11	5.34E+10	4.49E+10	0.000014 - 0.000034	binned
					-36.2	403868339.9	165903706.7	123383389.2	3439.3	3038.1	1.17E-01	4.82E-02	3.59E-02	1.33E+11	6.39E+10	5.25E+10	0.000014 - 0.000034	binned
					-37.2	706910603.2	318719021.1	195083065.3	3439.3	3038.1	2.06E-01	9.27E-02	5.67E-02	2.33E+11	1.20E+11	8.66E+10	0.000014 - 0.000034	binned
18-Mar-15	APC-11	SDT01	BINARY	Shared impinger	-15.2	1690.0	0.0	0.0	3000.6	2009.7	5.63E-07	0.00E+00	0.00E+00	8.41E+05	2.10E+05	2.10E+05	0.6	binned
					-16.2	2600.0	310.0	310.0	3000.6	2009.7	8.67E-07	1.03E-07	1.03E-07	1.29E+06	3.58E+05	3.58E+05	0.6	binned
					-17.2	3550.0	0.0	0.0	3000.6	2009.7	1.18E-06	0.00E+00	0.00E+00	1.77E+06	4.42E+05	4.42E+05	0.6	binned
					-18.2	4210.0	12700.0	2520.0	3000.6	2009.7	1.40E-06	4.23E-06	8.40E-07	2.09E+06	6.34E+06	1.36E+06	0.6	binned
					-19.2	19800.0	23000.0	12700.0	3000.6	2009.7	6.60E-06	7.67E-06	4.23E-06	9.85E+06	1.17E+07	6.78E+06	0.6	binned
					-20.2	100000.0	114000.0	65000.0	3000.6	2009.7	3.33E-05	3.80E-05	2.17E-05	4.98E+07	5.81E+07	3.47E+07	0.6	binned
					-21.2	352000.0	358000.0	154000.0	3000.6	2009.7	1.17E-04	1.19E-04	5.13E-05	1.75E+08	1.83E+08	8.83E+07	0.6	binned
					-22.2	790000.0	900000.0	499000.0	3000.6	2009.7	2.63E-04	3.00E-04	1.66E-04	3.93E+08	4.59E+08	2.67E+08	0.6	binned
					-23.2	1580000.0	1610000.0	1020000.0	3000.6	2009.7	5.27E-04	5.37E-04	3.40E-04	7.86E+08	8.25E+08	5.44E+08	0.6	binned
					-24.2	3490000.0	2140000.0	1780000.0	3000.6	2009.7	1.16E-03	7.13E-04	5.93E-04	1.74E+09	1.15E+09	9.87E+08	0.6	binned
					-25.2	6340000.0	4160000.0	2060000.0	3000.6	2009.7	2.11E-03	1.39E-03	6.87E-04	3.16E+09	2.22E+09	1.29E+09	0.6	binned
					-26.2	13500000.0	9600000.0	6400000.0	3000.6	2009.7	4.50E-03	3.20E-03	2.13E-03	6.73E+09	5.07E+09	3.61E+09	0.6	binned
					-27.2	20600000.0	8700000.0	8200000.0	3000.6	2009.7	6.87E-03	2.90E-03	2.73E-03	1.03E+10	5.05E+09	4.83E+09	0.6	binned
					-28.2	33400000.0	15000000.0	6400000.0	3000.6	2009.7	1.11E-02	5.00E-03	2.13E-03	1.67E+10	8.59E+09	5.26E+09	0.6	binned
					-29.2	48400000.0	21400000.0	9900000.0	3000.6	2009.7	1.61E-02	7.13E-03	3.30E-03	2.43E+10	1.23E+10	7.84E+09	0.6	binned
					-30.2	63100000.0	6750000.0	6750000.0	3000.6	2009.7	2.10E-02	2.25E-03	2.25E-03	3.17E+10	8.63E+09	8.63E+09	0.6	binned
			CMU-CS	Shared impinger	-15.0	1292.1	2532.6	1292.0	3000.6	2009.7	4.31E-07	4.31E-07	8.44E-07	6.43E+05	6.63E+05	1.27E+06	0.1	binned
					-16.0	3114.6	3518.7	3114.0	3000.6	2009.7	1.04E-06	1.04E-06	1.17E-06	1.55E+06	1.60E+06	1.79E+06	0.1	binned
					-17.0	6979.7	5726.3	5726.3	3000.6	2009.7	2.33E-06	1.91E-06	1.91E-06	3.47E+06	2.98E+06	2.98E+06	0.1	binned
					-18.0	14464.7	13234.0	13234.0	3000.6	2009.7	4.82E-06	4.41E-06	4.41E-06	7.20E+06	6.83E+06	6.83E+06	0.1	binned
					-19.0	63275.1	60178.8	60178.8	3000.6	2009.7	2.11E-05	2.01E-05	2.01E-05	3.15E+07	3.10E+07	3.10E+07	0.1	binned
					-20.0	278445.0	210245.0	210245.0	3000.6	2009.7	9.28E-05	7.01E-05	7.01E-05	1.39E+08	1.10E+08	1.10E+08	0.1	binned
					-21.0	589866.0	390655.0	390655.0	3000.6	2009.7	1.97E-04	1.30E-04	1.30E-04	2.94E+08	2.08E+08	2.08E+08	0.1	binned
			FRIDGE-IMM	Filter 5	-16.3	1560.0	7140.0	1520.5	2368.0	1884.0	6.59E-07	3.02E-06	6.42E-07	8.28E+05	3.79E+06	8.33E+05	0.5	selected points
					-17.1	4690.0	9010.0	3724.0	2368.0	1884.0	1.98E-06	3.81E-06	1.57E-06	2.49E+06	4.82E+06	2.07E+06	0.5	selected points
					-18.0	15700.0	13100.0	8190.0	2368.0	1884.0	6.63E-06	5.53E-06	3.46E-06	8.33E+06	7.26E+06	4.82E+06	0.5	selected points
					-19.0	157000.0	35000.0	30000.0	2368.0	1884.0	6.63E-05	1.48E-05	1.27E-05	8.33E+07	2.79E+07	2.62E+07	0.5	selected points
					-20.0	357000.0	52000.0	47000.0	2368.0	1884.0	1.51E-04	2.20E-05	1.98E-05	1.89E+08	5.48E+07	5.35E+07	0.5	selected points
					-21.0	787000.0	82000.0	77000.0	2368.0	1884.0	3.32E-04	3.46E-05	3.25E-05	4.18E+08	1.13E+08	1.12E+08	0.5	selected points
					-22.0	1530000.0	130000.0	120000.0	2368.0	1884.0	6.46E-04	5.49E-05	5.07E-05	8.12E+08	2.14E+08	2.13E+08	0.5	selected points
					-23.0	2830000.0	230000.0	210000.0	2368.0	1884.0	1.20E-03	9.71E-05	8.87E-05	1.50E+09	3.95E+08	3.92E+08	0.5	selected points
					-24.0	6180000.0	760000.0	670000.0	2368.0	1884.0	2.61E-03	3.21E-04	2.83E-04	3.28E+09	9.14E+08	8.94E+08	0.5	selected points
				Filter 4	-18.2	3380.0	4510.0	2280.0	3402.0	2509.0	9.93E-07	0.00E+00	1.33E-06	1.35E+06	3.37E+05	1.83E+06	0.5	selected points
					-19.0	10900.0	6800.0	4690.0	3402.0	2509.0	3.20E-06	0.00E+00	2.00E-06	4.34E+06	1.09E+06	2.92E+06	0.5	selected points
					-20.0	77300.0	16100.0	13900.0	3402.0	2509.0	2.27E-05	0.00E+00	4.73E-06	3.08E+07	7.70E+06	1.00E+07	0.5	selected points
					-21.0	357000.0	37000.0	35000.0	3402.0	2509.0	1.05E-04	0.00E+00	1.09E-05	1.42E+08	3.56E+07	3.85E+07	0.5	selected points
					-22.1	998000.0	80000.0	82000.0	3402.0	2509.0	3.00E-04	0.00E+00	2.35E-05	4.07E+08	1.02E+08	1.07E+08	0.5	selected points
					-23.0	2040000.0	210000.0	200000.0	3402.0	2509.0	6.00E-04	0.00E+00	6.17E-05	8.13E+08	2.03E+08	2.20E+08	0.5	selected points
			IS	Filter	-6.2	4.0	10.0	2.9	3000.6	2009.7	1.33E-09	3.32E-09	9.73E-10	1.99E+03	4.98E+03	1.54E+03	50	selected points
					-6.5	6.1	11.1	4.1	3000.6	2009.7	2.03E-09	3.70E-09	1.35E-09	3.04E+03	5.57E+03	2.16E+03	50	selected points
					-7.0	6.1	11.1	4.1	3000.6	2009.7	2.03E-09	3.70E-09	1.35E-09	3.04E+03	5.57E+03	2.16E+03	50	selected points

					-8.0	10.5	13.2	6.1	3000.6	2009.7	3.51E-09	4.38E-09	2.04E-09	5.24E+03	6.68E+03	3.32E+03	50	selected points
					-9.0	15.3	15.1	8.1	3000.6	2009.7	5.10E-09	5.03E-09	2.69E-09	7.62E+03	7.75E+03	4.44E+03	50	selected points
					-10.0	29.1	20.0	13.0	3000.6	2009.7	9.71E-09	6.67E-09	4.33E-09	1.45E+04	1.06E+04	7.41E+03	50	selected points
					-11.0	35.7	22.2	15.2	3000.6	2009.7	1.19E-08	7.40E-09	5.05E-09	1.78E+04	1.19E+04	8.76E+03	50	selected points
					-12.0	43.0	24.6	17.6	3000.6	2009.7	1.43E-08	8.20E-09	5.85E-09	2.14E+04	1.34E+04	1.02E+04	50	selected points
					-13.0	60.8	30.5	23.5	3000.6	2009.7	2.03E-08	1.02E-08	7.82E-09	3.03E+04	1.70E+04	1.39E+04	50	selected points
					-14.2	115.1	51.0	44.0	3000.6	2009.7	3.84E-08	1.70E-08	1.47E-08	5.73E+04	2.91E+04	2.62E+04	50	selected points
					-15.0	356.8	321.1	180.5	3000.6	2009.7	1.19E-07	1.07E-07	6.02E-08	1.78E+05	1.66E+05	1.00E+05	50	selected points
					-16.0	939.8	518.1	377.5	3000.6	2009.7	3.13E-07	1.73E-07	1.26E-07	4.68E+05	2.83E+05	2.21E+05	50	selected points
					-17.0	1719.4	787.2	646.6	3000.6	2009.7	5.73E-07	2.62E-07	2.15E-07	8.56E+05	4.46E+05	3.86E+05	50	selected points
					-18.0	2936.0	1317.8	1177.1	3000.6	2009.7	9.78E-07	4.39E-07	3.92E-07	1.46E+06	7.51E+05	6.90E+05	50	selected points
					-18.0	5150.7	5653.7	2841.4	3000.6	2009.7	1.72E-06	1.88E-06	9.47E-07	2.56E+06	2.89E+06	1.55E+06	50	selected points
					-19.0	20506.8	10924.9	8112.5	3000.6	2009.7	6.83E-06	3.64E-06	2.70E-06	1.02E+07	6.00E+06	4.78E+06	50	selected points
					-20.0	85971.7	42925.6	40113.2	3000.6	2009.7	2.87E-05	1.43E-05	1.34E-05	4.28E+07	2.39E+07	2.26E+07	50	selected points
					-20.0	122473.2	120773.1	64525.9	3000.6	2009.7	4.08E-05	4.03E-05	2.15E-05	6.09E+07	6.20E+07	3.55E+07	50	selected points
					-21.0	486613.0	243961.5	187714.3	3000.6	2009.7	1.62E-04	8.13E-05	6.26E-05	2.42E+08	1.36E+08	1.11E+08	50	selected points
					-22.0	1174386.9	527103.8	470856.5	3000.6	2009.7	3.91E-04	1.76E-04	1.57E-04	5.84E+08	3.00E+08	2.76E+08	50	selected points
					-22.0	1324962.7	1944077.9	819133.2	3000.6	2009.7	4.42E-04	6.48E-04	2.73E-04	6.59E+08	9.81E+08	4.40E+08	50	selected points
					-23.0	3402862.6	2820735.4	1661542.9	3000.6	2009.7	1.13E-03	9.40E-04	5.54E-04	1.69E+09	1.47E+09	9.29E+08	50	selected points
					-23.5	5394013.7	3509653.0	2350460.5	3000.6	2009.7	1.80E-03	1.17E-03	7.83E-04	2.68E+09	1.87E+09	1.35E+09	50	selected points
					-24.0	7887676.3	4340009.2	3180816.7	3000.6	2009.7	2.63E-03	1.45E-03	1.06E-03	3.92E+09	2.37E+09	1.86E+09	50	selected points
					-24.5	11226315.5	5479810.2	4320617.7	3000.6	2009.7	3.74E-03	1.83E-03	1.44E-03	5.59E+09	3.06E+09	2.56E+09	50	selected points
					-25.0	13115096.7	6265112.3	5069518.5	3000.6	2009.7	4.37E-03	2.09E-03	1.69E-03	6.53E+09	3.52E+09	3.00E+09	50	selected points
					-25.5	17778698.6	8141968.8	6946375.0	3000.6	2009.7	5.93E-03	2.71E-03	2.32E-03	8.85E+09	4.62E+09	4.10E+09	50	selected points
					-26.0	33411927.6	17166214.3	15931856.0	3000.6	2009.7	1.11E-02	5.72E-03	5.31E-03	1.66E+10	9.50E+09	8.95E+09	50	selected points
			KIT-CS	Shared impinger	-20.6	142930.1	0.0	0.0	3000.6	2009.7	4.76E-05	0.00E+00	0.00E+00	7.11E+07	1.78E+07	1.78E+07	5.00E-04	
					-21.9	201932.9	0.0	0.0	3000.6	2009.7	6.73E-05	0.00E+00	0.00E+00	1.00E+08	2.51E+07	2.51E+07	5.00E-04	
					-22.7	564378.5	235338.5	235338.5	3000.6	2009.7	1.88E-04	7.84E-05	7.84E-05	2.81E+08	1.37E+08	1.37E+08	5.00E-04	
					-23.8	1375568.2	238940.4	238940.4	3000.6	2009.7	4.58E-04	7.96E-05	7.96E-05	6.84E+08	2.08E+08	2.08E+08	5.00E-04	
					-24.8	2580960.6	580850.2	580850.2	3000.6	2009.7	8.60E-04	1.94E-04	1.94E-04	1.28E+09	4.32E+08	4.32E+08	5.00E-04	
					-25.7	4346273.4	999157.3	999157.3	3000.6	2009.7	1.45E-03	3.33E-04	3.33E-04	2.16E+09	7.34E+08	7.34E+08	5.00E-04	
					-26.7	6865523.5	1235295.4	1235295.4	3000.6	2009.7	2.29E-03	4.12E-04	4.12E-04	3.42E+09	1.05E+09	1.05E+09	5.00E-04	
					-27.7	10527824.9	2689349.5	2689349.5	3000.6	2009.7	3.51E-03	8.96E-04	8.96E-04	5.24E+09	1.87E+09	1.87E+09	5.00E-04	
					-28.7	15716374.5	4737031.5	4737031.5	3000.6	2009.7	5.24E-03	1.58E-03	1.58E-03	7.82E+09	3.06E+09	3.06E+09	5.00E-04	
					-29.7	22620297.1	5589395.1	5589395.1	3000.6	2009.7	7.54E-03	1.86E-03	1.86E-03	1.13E+10	3.96E+09	3.96E+09	5.00E-04	
					-30.8	31271034.1	5782433.8	5782433.8	3000.6	2009.7	1.04E-02	1.93E-03	1.93E-03	1.56E+10	4.84E+09	4.84E+09	5.00E-04	
					-31.9	41190182.6	7950271.1	7950271.1	3000.6	2009.7	1.37E-02	2.65E-03	2.65E-03	2.05E+10	6.47E+09	6.47E+09	5.00E-04	
					-32.6	52574730.2	13702445.5	13702445.5	3000.6	2009.7	1.75E-02	4.57E-03	4.57E-03	2.62E+10	9.45E+09	9.45E+09	5.00E-04	
					-33.6	63428467.5	19670944.1	19670944.1	3000.6	2009.7	2.11E-02	6.56E-03	6.56E-03	3.16E+10	1.26E+10	1.26E+10	5.00E-04	
					-34.5	83140508.4	21883261.0	21883261.0	3000.6	2009.7	2.77E-02	7.29E-03	7.29E-03	4.14E+10	1.50E+10	1.50E+10	5.00E-04	
					-35.8	105887447.1	0.0	0.0	3000.6	2009.7	3.53E-02	0.00E+00	0.00E+00	5.27E+10	1.32E+10	1.32E+10	5.00E-04	
			M-AL	Shared impinger	-10.7	84.8	19.7	19.7	3000.6	2009.7	2.83E-08	6.57E-09	6.57E-09	4.22E+04	1.44E+04	1.44E+04	4.2	
					-11.7	182.8	43.6	43.6	3000.6	2009.7	6.09E-08	1.45E-08	1.45E-08	9.09E+04	3.14E+04	3.14E+04	4.2	
					-12.7	353.9	86.9	86.9	3000.6	2009.7	1.18E-07	2.90E-08	2.90E-08	1.76E+05	6.17E+04	6.17E+04	4.2	
					-13.7	568.2	132.0	132.0	3000.6	2009.7	1.89E-07	4.40E-08	4.40E-08	2.83E+05	9.65E+04	9.65E+04	4.2	
					-14.7	859.2	220.7	220.7	3000.6	2009.7	2.86E-07	7.36E-08	7.36E-08	4.28E+05	1.53E+05	1.53E+05	4.2	
					-15.7	1548.2	407.3	407.3	3000.6	2009.7	5.16E-07	1.36E-07	1.36E-07	7.70E+05	2.80E+05	2.80E+05	4.2	
					-16.7	3907.1	1137.8	1137.8	3000.6	2009.7	1.30E-06	3.79E-07	3.79E-07	1.94E+06	7.46E+05	7.46E+05	4.2	
					-17.7	9810.2	6567.6	6567.6	3000.6	2009.7	3.27E-06	2.19E-06	2.19E-06	4.88E+06	3.49E+06	3.49E+06	4.2	

			NCSU-CS	Shared impinger	-10.2	221.4	0.0	0.0	3000.6	2009.7	7.38E-08	0.00E+00	0.00E+00	1.10E+05	2.75E+04	2.75E+04	1	binned
					-11.2	253.4	0.0	0.0	3000.6	2009.7	8.44E-08	0.00E+00	0.00E+00	1.26E+05	3.15E+04	3.15E+04	1	binned
					-12.2	285.4	0.0	0.0	3000.6	2009.7	9.51E-08	0.00E+00	0.00E+00	1.42E+05	3.55E+04	3.55E+04	1	binned
					-13.2	317.4	0.0	0.0	3000.6	2009.7	1.06E-07	0.00E+00	0.00E+00	1.58E+05	3.95E+04	3.95E+04	1	binned
					-14.2	349.4	0.0	0.0	3000.6	2009.7	1.16E-07	0.00E+00	0.00E+00	1.74E+05	4.35E+04	4.35E+04	1	binned
					-15.2	375.0	12.5	12.5	3000.6	2009.7	1.25E-07	4.17E-09	4.17E-09	1.87E+05	4.71E+04	4.71E+04	1	binned
					-16.2	513.9	102.1	102.1	3000.6	2009.7	1.71E-07	3.40E-08	3.40E-08	2.56E+05	8.17E+04	8.17E+04	1	binned
					-17.2	872.1	145.9	145.9	3000.6	2009.7	2.91E-07	4.86E-08	4.86E-08	4.34E+05	1.31E+05	1.31E+05	1	binned
					-18.2	1918.2	738.6	738.6	3000.6	2009.7	6.39E-07	2.46E-07	2.46E-07	9.54E+05	4.38E+05	4.38E+05	1	binned
					-19.2	3979.6	1621.4	1621.4	3000.6	2009.7	1.33E-06	5.40E-07	5.40E-07	1.98E+06	9.47E+05	9.47E+05	1	binned
					-20.2	28784.8	18985.6	18985.6	3000.6	2009.7	9.59E-06	6.33E-06	6.33E-06	1.43E+07	1.01E+07	1.01E+07	1	binned
					-21.2	202251.8	0.0	0.0	3000.6	2009.7	6.74E-05	0.00E+00	0.00E+00	1.01E+08	2.52E+07	2.52E+07	1	binned
					-22.2	417740.3	0.0	0.0	3000.6	2009.7	1.39E-04	0.00E+00	0.00E+00	2.08E+08	5.20E+07	5.20E+07	1	binned
					-23.2	934105.7	0.0	0.0	3000.6	2009.7	3.11E-04	0.00E+00	0.00E+00	4.65E+08	1.16E+08	1.16E+08	1	binned
					-24.2	1708670.7	0.0	0.0	3000.6	2009.7	5.69E-04	0.00E+00	0.00E+00	8.50E+08	2.13E+08	2.13E+08	1	binned
					-25.2	4228140.8	0.0	0.0	3000.6	2009.7	1.41E-03	0.00E+00	0.00E+00	2.10E+09	5.26E+08	5.26E+08	1	binned
			NIPI	Shared impinger	-13.0	219.6	219.6	109.8	3000.6	2009.7	7.32E-08	7.32E-08	3.66E-08	1.09E+05	1.13E+05	6.11E+04	1	binned
					-14.0	328.8	730.4	226.7	3000.6	2009.7	1.10E-07	2.43E-07	7.56E-08	1.64E+05	3.66E+05	1.20E+05	1	binned
					-15.0	492.3	2062.4	397.5	3000.6	2009.7	1.64E-07	6.87E-07	1.32E-07	2.45E+05	1.03E+06	2.07E+05	1	binned
					-16.0	731.3	2571.3	569.3	3000.6	2009.7	2.44E-07	8.57E-07	1.90E-07	3.64E+05	1.28E+06	2.98E+05	1	binned
					-17.0	1879.7	3850.8	1263.1	3000.6	2009.7	6.26E-07	1.28E-06	4.21E-07	9.35E+05	1.93E+06	6.71E+05	1	binned
					-18.0	5788.7	13113.1	4015.9	3000.6	2009.7	1.93E-06	4.37E-06	1.34E-06	2.88E+06	6.56E+06	2.12E+06	1	binned
					-19.0	20307.2	53212.5	14698.1	3000.6	2009.7	6.77E-06	1.77E-05	4.90E-06	1.01E+07	2.66E+07	7.74E+06	1	binned
					-20.0	143624.5	391800.7	105098.1	3000.6	2009.7	4.79E-05	1.31E-04	3.50E-05	7.15E+07	1.96E+08	5.53E+07	1	binned
					-21.0	602343.1	1183357.8	399163.9	3000.6	2009.7	2.01E-04	3.94E-04	1.33E-04	3.00E+08	5.94E+08	2.12E+08	1	binned
					-22.0	1503195.9	2672706.6	962091.8	3000.6	2009.7	5.01E-04	8.91E-04	3.21E-04	7.48E+08	1.34E+09	5.14E+08	1	binned
					-23.0	3183939.9	4825696.8	1918280.3	3000.6	2009.7	1.06E-03	1.61E-03	6.39E-04	1.58E+09	2.43E+09	1.03E+09	1	binned
					-24.0	3183939.9	3957796.8	1764471.0	3000.6	2009.7	1.06E-03	1.32E-03	5.88E-04	1.58E+09	2.01E+09	9.63E+08	1	binned
			VODCA	Shared impinger	-35.2	204207501.3	81975685.0	81975685.0	3000.6	2009.7	6.81E-02	2.73E-02	2.73E-02	1.02E+11	4.81E+10	4.81E+10	0.000004 - 0.000036	selected points
					-34.7	191370025.1	52055718.2	52055718.2	3000.6	2009.7	6.38E-02	1.73E-02	1.73E-02	9.52E+10	3.52E+10	3.52E+10	0.000004 - 0.000036	selected points
					-34.2	169471282.2	58495479.5	58495479.5	3000.6	2009.7	5.65E-02	1.95E-02	1.95E-02	8.43E+10	3.59E+10	3.59E+10	0.000004 - 0.000036	selected points
					-33.7	101481161.1	34437457.1	34437457.1	3000.6	2009.7	3.38E-02	1.15E-02	1.15E-02	5.05E+10	2.13E+10	2.13E+10	0.000004 - 0.000036	selected points
					-33.2	64805529.4	28924211.8	28924211.8	3000.6	2009.7	2.16E-02	9.64E-03	9.64E-03	3.22E+10	1.65E+10	1.65E+10	0.000004 - 0.000036	selected points
					-32.7	50157669.8	26749088.8	26749088.8	3000.6	2009.7	1.67E-02	8.91E-03	8.91E-03	2.50E+10	1.47E+10	1.47E+10	0.000004 - 0.000036	selected points
					-32.2	25881469.4	17620409.9	17620409.9	3000.6	2009.7	8.63E-03	5.87E-03	5.87E-03	1.29E+10	9.34E+09	9.34E+09	0.000004 - 0.000036	selected points
			WISDOM	Shared impinger	-25.2	1528997.7	336379.5	336379.5	3000.6	2009.7	5.10E-04	1.12E-04	1.12E-04	7.61E+08	2.53E+08	2.53E+08	0.000014 - 0.000034	binned
					-26.2	1912206.6	305953.1	305953.1	3000.6	2009.7	6.37E-04	1.02E-04	1.02E-04	9.51E+08	2.82E+08	2.82E+08	0.000014 - 0.000034	binned
					-27.2	1912206.6	305953.1	305953.1	3000.6	2009.7	6.37E-04	1.02E-04	1.02E-04	9.51E+08	2.82E+08	2.82E+08	0.000014 - 0.000034	binned
					-28.2	2679781.2	321573.7	321573.7	3000.6	2009.7	8.93E-04	1.07E-04	1.07E-04	1.33E+09	3.70E+08	3.70E+08	0.000014 - 0.000034	binned
					-29.2	4219579.1	632936.9	632936.9	3000.6	2009.7	1.41E-03	2.11E-04	2.11E-04	2.10E+09	6.12E+08	6.12E+08	0.000014 - 0.000034	binned
					-30.2	6929271.9	485049.0	485049.0	3000.6	2009.7	2.31E-03	1.62E-04	1.62E-04	3.45E+09	8.95E+08	8.95E+08	0.000014 - 0.000034	binned
					-31.2	11226632.9	336799.0	336799.0	3000.6	2009.7	3.74E-03	1.12E-04	1.12E-04	5.59E+09	1.41E+09	1.41E+09	0.000014 - 0.000034	binned
					-32.2	13591213.4	951384.9	951384.9	3000.6	2009.7	4.53E-03	3.17E-04	3.17E-04	6.76E+09	1.76E+09	1.76E+09	0.000014 - 0.000034	binned
					-33.2	17165794.2	686631.8	686631.8	3000.6	2009.7	5.72E-03	2.29E-04	2.29E-04	8.54E+09	2.16E+09	2.16E+09	0.000014 - 0.000034	binned
					-34.2	23604502.8	472090.1	472090.1	3000.6	2009.7	7.87E-03	1.57E-04	1.57E-04	1.17E+10	2.95E+09	2.95E+09	0.000014 - 0.000034	binned
					-35.2	36817405.3	2209044.3	2209044.3	3000.6	2009.7	1.23E-02	7.36E-04	7.36E-04	1.83E+10	4.71E+09	4.71E+09	0.000014 - 0.000034	binned
					-36.2	70163698.0	2104910.9	2104910.9	3000.6	2009.7	2.34E-02	7.02E-04	7.02E-04	3.49E+10	8.79E+09	8.79E+09	0.000014 - 0.000034	binned
18-Mar-15	AIDA-07	SDT01	FRIDGE-STD	16	-20	1330	1030	1030	270	131	1.02E-05	7.86E-06	7.86E-06	2.09E+07	1.70E+07	1.70E+07	N/A	N/A
					-25	146000	115000	115000	270	131	1.11E-03	8.78E-04	8.78E-04	2.30E+09	1.90E+09	1.90E+09	N/A	N/A

					-30	733000	576000	576000	270	131	5.60E-03	4.40E-03	4.40E-03	1.15E+10	9.51E+09	9.51E+09	N/A	N/A
20-Mar-15	AIDA-12	SDT01	FRIDGE-STD	31	-20	46100	36200	36200	291	119	1.58E-04	1.24E-04	1.24E-04	3.87E+08	3.19E+08	3.19E+08	N/A	N/A
					-25	698000	548000	548000	291	119	2.40E-03	1.88E-03	1.88E-03	5.87E+09	4.83E+09	4.83E+09	N/A	N/A
					-30	4380000	3440000	3440000	291	119	1.51E-02	1.18E-02	1.18E-02	3.68E+10	3.03E+10	3.03E+10	N/A	N/A
			DFPC-ISAC		-20.2	25000	7500	7500	290	116	1.00E-04	3.00E-05	3.00E-05	2.50E+08	9.76E+07	9.76E+07	N/A	N/A
18-Mar-15	AIDA-08	FS02	FRIDGE-STD	21	-20	48300	47800	47800	380	155	1.27E-04	1.26E-04	1.26E-04	3.12E+08	3.18E+08	3.18E+08	N/A	N/A
					-25	677000	669000	669000	380	155	1.78E-03	1.76E-03	1.76E-03	4.37E+09	4.45E+09	4.45E+09	N/A	N/A
			DFPC-ISAC		-20.2	87	26.1	26.1	380	155	2.49E-04	7.46E-05	7.46E-05	6.09E+08	2.38E+08	2.38E+08	N/A	N/A
19-Mar-15	APC-13	FS02	BINARY	Shared impinger	-14.2	2190.0	330.0	330.0	7750.2	3703.1	2.83E-07	4.26E-08	4.26E-08	5.91E+05	8.91E+04	8.91E+04	0.6	binned
					-15.2	6150.0	8650.0	3630.0	7750.2	3703.1	7.94E-07	1.12E-06	4.68E-07	1.66E+06	2.34E+06	9.80E+05	0.6	binned
					-16.2	17300.0	24900.0	10900.0	7750.2	3703.1	2.23E-06	3.21E-06	1.41E-06	4.67E+06	6.72E+06	2.94E+06	0.6	binned
					-17.2	30900.0	31000.0	17000.0	7750.2	3703.1	3.99E-06	4.00E-06	2.19E-06	8.34E+06	8.37E+06	4.59E+06	0.6	binned
					-18.2	54800.0	69200.0	29600.0	7750.2	3703.1	7.07E-06	8.93E-06	3.82E-06	1.48E+07	1.87E+07	7.99E+06	0.6	binned
					-19.2	86700.0	375000.0	61500.0	7750.2	3703.1	1.12E-05	4.84E-05	7.94E-06	2.34E+07	1.01E+08	1.66E+07	0.6	binned
					-20.2	202000.0	1170000.0	115000.0	7750.2	3703.1	2.61E-05	1.51E-04	1.48E-05	5.45E+07	3.16E+08	3.11E+07	0.6	binned
					-21.2	615000.0	2130000.0	362000.0	7750.2	3703.1	7.94E-05	2.75E-04	4.67E-05	1.66E+08	5.75E+08	9.78E+07	0.6	binned
					-22.2	2960000.0	10700000.0	2420000.0	7750.2	3703.1	3.82E-04	1.38E-03	3.12E-04	7.99E+08	2.89E+09	6.54E+08	0.6	binned
					-23.2	11500000.0	18100000.0	8760000.0	7750.2	3703.1	1.48E-03	2.34E-03	1.13E-03	3.11E+09	4.89E+09	2.37E+09	0.6	binned
					-24.2	42200000.0	44500000.0	36900000.0	7750.2	3703.1	5.45E-03	5.74E-03	4.76E-03	1.14E+10	1.20E+10	9.96E+09	0.6	binned
					-25.2	173000000.0	177000000.0	103000000.0	7750.2	3703.1	2.23E-02	2.28E-02	1.33E-02	4.67E+10	4.78E+10	2.78E+10	0.6	binned
					-26.2	422000000.0	344000000.0	169000000.0	7750.2	3703.1	5.45E-02	4.44E-02	2.18E-02	1.14E+11	9.29E+10	4.56E+10	0.6	binned
					-27.2	692000000.0	74000000.0	74000000.0	7750.2	3703.1	8.93E-02	9.55E-03	9.55E-03	1.87E+11	2.00E+10	2.00E+10	0.6	binned
			FRIDGE-IMM	Filter 6	-15.6	3420.0	15680.0	3333.5	6535.1	2613.9	5.23E-07	2.40E-06	5.10E-07	1.31E+06	6.01E+06	1.32E+06	0.5	selected points
					-16.6	24000.0	25500.0	14350.0	6535.1	2613.9	3.67E-06	3.90E-06	2.20E-06	9.18E+06	1.00E+07	5.95E+06	0.5	selected points
					-17.5	219000.0	62000.0	51000.0	6535.1	2613.9	3.35E-05	9.49E-06	7.80E-06	8.38E+07	3.16E+07	2.86E+07	0.5	selected points
					-18.5	981000.0	129000.0	119000.0	6535.1	2613.9	1.50E-04	1.97E-05	1.82E-05	3.75E+08	1.06E+08	1.04E+08	0.5	selected points
					-19.5	2560000.0	240000.0	220000.0	6535.1	2613.9	3.92E-04	3.67E-05	3.37E-05	9.79E+08	2.61E+08	2.59E+08	0.5	selected points
					-20.5	3970000.0	340000.0	310000.0	6535.1	2613.9	6.07E-04	5.20E-05	4.74E-05	1.52E+09	4.01E+08	3.98E+08	0.5	selected points
					-21.5	6140000.0	530000.0	490000.0	6535.1	2613.9	9.40E-04	8.11E-05	7.50E-05	2.35E+09	6.21E+08	6.16E+08	0.5	selected points
					-22.5	10300000.0	1100000.0	1030000.0	6535.1	2613.9	1.58E-03	1.68E-04	1.58E-04	3.94E+09	1.07E+09	1.06E+09	0.5	selected points
					-23.5	16100000.0	3100000.0	2500000.0	6535.1	2613.9	2.46E-03	4.74E-04	3.83E-04	6.16E+09	1.94E+09	1.81E+09	0.5	selected points
					-24.1	19500000.0	6800000.0	4000000.0	6535.1	2613.9	2.98E-03	1.04E-03	6.12E-04	7.46E+09	3.20E+09	2.41E+09	0.5	selected points
			IS	Filter	-7.4	1.7	7.4	1.4	7750.2	3703.1	2.18E-10	9.58E-10	1.80E-10	2.01E+03	8.83E+03	1.73E+03	50	selected points
					-8.0	11.1	12.1	6.1	7750.2	3703.1	1.43E-09	1.57E-09	7.87E-10	3.28E+03	3.69E+03	1.98E+03	50	selected points
					-9.0	22.4	16.3	10.3	7750.2	3703.1	2.89E-09	2.10E-09	1.32E-09	4.40E+03	3.39E+03	2.30E+03	50	selected points
					-10.0	47.9	24.7	18.7	7750.2	3703.1	6.19E-09	3.19E-09	2.41E-09	6.68E+03	3.83E+03	3.10E+03	50	selected points
					-11.0	184.4	92.1	86.1	7750.2	3703.1	2.38E-08	1.19E-08	1.11E-08	2.49E+04	1.39E+04	1.32E+04	50	selected points
					-11.0	68.7	170.8	50.1	7750.2	3703.1	8.86E-09	2.20E-08	6.47E-09	4.61E+04	1.15E+05	3.56E+04	50	selected points
					-12.0	500.3	343.7	223.0	7750.2	3703.1	6.45E-08	4.43E-08	2.88E-08	9.28E+04	6.78E+04	4.74E+04	50	selected points
					-13.0	2519.6	1130.9	1010.2	7750.2	3703.1	3.25E-07	1.46E-07	1.30E-07	3.05E+05	1.57E+05	1.44E+05	50	selected points
					-14.0	7030.2	5842.1	3428.6	7750.2	3703.1	9.07E-07	7.54E-07	4.42E-07	1.58E+06	1.37E+06	8.65E+05	50	selected points
					-15.0	27004.0	12595.5	10182.0	7750.2	3703.1	3.48E-06	1.63E-06	1.31E-06	3.40E+06	1.80E+06	1.54E+06	50	selected points
					-16.0	27477.8	68313.0	20043.3	7750.2	3703.1	3.55E-06	8.81E-06	2.59E-06	1.84E+07	4.61E+07	1.42E+07	50	selected points
					-17.0	88404.2	97037.3	48767.7	7750.2	3703.1	1.14E-05	1.25E-05	6.29E-06	2.62E+07	2.95E+07	1.59E+07	50	selected points
					-18.0	221946.5	144774.3	96504.7	7750.2	3703.1	2.86E-05	1.87E-05	1.25E-05	3.91E+07	2.73E+07	1.96E+07	50	selected points
					-19.0	647078.6	291771.0	243501.4	7750.2	3703.1	8.35E-05	3.76E-05	3.14E-05	7.88E+07	4.06E+07	3.56E+07	50	selected points
					-20.0	1180452.9	546618.6	498349.0	7750.2	3703.1	1.52E-04	7.05E-05	6.43E-05	1.48E+08	7.77E+07	7.24E+07	50	selected points
					-20.0	2449661.1	2204489.7	1239096.9	7750.2	3703.1	3.16E-04	2.84E-04	1.60E-04	5.95E+08	5.56E+08	3.36E+08	50	selected points
					-21.0	5386035.6	3207894.2	2242501.3	7750.2	3703.1	6.95E-04	4.14E-04	2.89E-04	8.66E+08	5.60E+08	4.21E+08	50	selected points

					-21.5	20156454.4	9046884.8	8081491.9	7750.2	3703.1	2.60E-03	1.17E-03	1.04E-03	2.44E+09	1.26E+09	1.15E+09	50	selected points
					-22.0	20117609.3	36555799.6	13386370.3	7750.2	3703.1	2.60E-03	4.72E-03	1.73E-03	9.87E+09	1.81E+10	7.02E+09	50	selected points
					-23.0	96051832.7	65983680.5	42814251.2	7750.2	3703.1	1.24E-02	8.51E-03	5.52E-03	1.78E+10	1.30E+10	9.11E+09	50	selected points
					-23.5	193957920.7	99980683.9	76105883.3	7750.2	3703.1	2.50E-02	1.29E-02	9.82E-03	2.70E+10	1.55E+10	1.26E+10	50	selected points
					-24.0	304109414.2	139768480.5	115893679.9	7750.2	3703.1	3.92E-02	1.80E-02	1.50E-02	3.77E+10	1.97E+10	1.72E+10	50	selected points
					-24.5	372872234.2	167901435.2	144026634.6	7750.2	3703.1	4.81E-02	2.17E-02	1.86E-02	4.53E+10	2.34E+10	2.09E+10	50	selected points
					-25.0	560129094.8	262310481.4	238435680.8	7750.2	3703.1	7.23E-02	3.38E-02	3.08E-02	7.08E+10	3.76E+10	3.50E+10	50	selected points
			KIT-CS	Shared impinger	-17.2	103041.9	0.0	0.0	7750.2	3703.1	1.33E-05	0.00E+00	0.00E+00	2.78E+07	6.96E+06	6.96E+06	5.00E-04	
					-19.0	236433.9	0.0	0.0	7750.2	3703.1	3.05E-05	0.00E+00	0.00E+00	6.38E+07	1.60E+07	1.60E+07	5.00E-04	
					-19.9	694568.6	669207.1	669207.1	7750.2	3703.1	8.96E-05	8.63E-05	8.63E-05	1.88E+08	1.87E+08	1.87E+08	5.00E-04	
					-20.8	3430083.6	1683764.0	1683764.0	7750.2	3703.1	4.43E-04	2.17E-04	2.17E-04	9.26E+08	5.10E+08	5.10E+08	5.00E-04	
					-21.8	13193135.0	5221145.2	5221145.2	7750.2	3703.1	1.70E-03	6.74E-04	6.74E-04	3.56E+09	1.67E+09	1.67E+09	5.00E-04	
					-22.6	38530923.3	13869037.5	13869037.5	7750.2	3703.1	4.97E-03	1.79E-03	1.79E-03	1.04E+10	4.56E+09	4.56E+09	5.00E-04	
					-23.6	86551949.0	30485073.2	30485073.2	7750.2	3703.1	1.12E-02	3.93E-03	3.93E-03	2.34E+10	1.01E+10	1.01E+10	5.00E-04	
					-24.6	117883563.8	30916919.7	30916919.7	7750.2	3703.1	1.52E-02	3.99E-03	3.99E-03	3.18E+10	1.15E+10	1.15E+10	5.00E-04	
			M-AL	Shared impinger	-15.2	219.1	66.8	66.8	7750.2	3703.1	2.83E-08	8.62E-09	8.62E-09	5.92E+04	2.33E+04	2.33E+04	4.2	
					-16.2	2171.3	768.6	768.6	7750.2	3703.1	2.80E-07	9.92E-08	9.92E-08	5.86E+05	2.54E+05	2.54E+05	4.2	
					-17.2	5966.8	2121.4	2121.4	7750.2	3703.1	7.70E-07	2.74E-07	2.74E-07	1.61E+06	7.00E+05	7.00E+05	4.2	
					-18.2	11395.2	4204.5	4204.5	7750.2	3703.1	1.47E-06	5.43E-07	5.43E-07	3.08E+06	1.37E+06	1.37E+06	4.2	
			NCSU-CS	Shared impinger	-16.2	1222.0	235.3	235.3	7750.2	3703.1	1.58E-07	3.04E-08	3.04E-08	3.30E+05	1.04E+05	1.04E+05	1	binned
					-17.2	3456.8	2837.0	2837.0	7750.2	3703.1	4.46E-07	3.66E-07	3.66E-07	9.33E+05	8.01E+05	8.01E+05	1	binned
					-18.2	8477.1	7615.8	7615.8	7750.2	3703.1	1.09E-06	9.83E-07	9.83E-07	2.29E+06	2.13E+06	2.13E+06	1	binned
					-19.2	21362.7	16532.9	16532.9	7750.2	3703.1	2.76E-06	2.13E-06	2.13E-06	5.77E+06	4.69E+06	4.69E+06	1	binned
					-20.2	32641.4	10277.6	10277.6	7750.2	3703.1	4.21E-06	1.33E-06	1.33E-06	8.81E+06	3.54E+06	3.54E+06	1	binned
					-21.2	115375.4	0.0	0.0	7750.2	3703.1	1.49E-05	0.00E+00	0.00E+00	3.12E+07	7.79E+06	7.79E+06	1	binned
					-22.2	379011.2	0.0	0.0	7750.2	3703.1	4.89E-05	0.00E+00	0.00E+00	1.02E+08	2.56E+07	2.56E+07	1	binned
					-23.2	1236963.3	0.0	0.0	7750.2	3703.1	1.60E-04	0.00E+00	0.00E+00	3.34E+08	8.35E+07	8.35E+07	1	binned
					-24.2	2119253.1	0.0	0.0	7750.2	3703.1	2.73E-04	0.00E+00	0.00E+00	5.72E+08	1.43E+08	1.43E+08	1	binned
					-25.2	5306940.2	0.0	0.0	7750.2	3703.1	6.85E-04	0.00E+00	0.00E+00	1.43E+09	3.58E+08	3.58E+08	1	binned
			NIPI	Shared impinger	-8.0	257.2	257.2	128.6	7750.2	3703.1	3.32E-08	3.32E-08	1.66E-08	6.94E+04	7.16E+04	3.88E+04	1	binned
					-9.0	337.0	702.1	227.7	7750.2	3703.1	4.35E-08	9.06E-08	2.94E-08	9.10E+04	1.91E+05	6.56E+04	1	binned
					-10.0	337.0	499.9	201.3	7750.2	3703.1	4.35E-08	6.45E-08	2.60E-08	9.10E+04	1.37E+05	5.89E+04	1	binned
					-11.0	337.0	337.0	168.5	7750.2	3703.1	4.35E-08	4.35E-08	2.17E-08	9.10E+04	9.38E+04	5.09E+04	1	binned
					-12.0	353.6	622.3	225.5	7750.2	3703.1	4.56E-08	8.03E-08	2.91E-08	9.55E+04	1.70E+05	6.54E+04	1	binned
					-13.0	522.4	1467.4	385.2	7750.2	3703.1	6.74E-08	1.89E-07	4.97E-08	1.41E+05	3.98E+05	1.10E+05	1	binned
					-14.0	928.6	2041.1	638.2	7750.2	3703.1	1.20E-07	2.63E-07	8.24E-08	2.51E+05	5.55E+05	1.83E+05	1	binned
					-15.0	3310.9	7374.6	2285.0	7750.2	3703.1	4.27E-07	9.52E-07	2.95E-07	8.94E+05	2.00E+06	6.56E+05	1	binned
					-16.0	11201.5	23195.1	7553.7	7750.2	3703.1	1.45E-06	2.99E-06	9.75E-07	3.02E+06	6.31E+06	2.18E+06	1	binned
					-17.0	30031.1	51565.6	18978.4	7750.2	3703.1	3.87E-06	6.65E-06	2.45E-06	8.11E+06	1.41E+07	5.51E+06	1	binned
					-18.0	34878.9	44023.2	19460.6	7750.2	3703.1	4.50E-06	5.68E-06	2.51E-06	9.42E+06	1.21E+07	5.76E+06	1	binned
					-19.0	34878.9	39310.3	18481.1	7750.2	3703.1	4.50E-06	5.07E-06	2.38E-06	9.42E+06	1.09E+07	5.52E+06	1	binned
			VODCA	Shared impinger	-25.2	77000000.0	61600000.0	61600000.0	7750.2	3703.1	9.94E-03	7.95E-03	7.95E-03	2.08E+10	1.74E+10	1.74E+10	0.000004 - 0.000036	selected points
					-26.2	228000000.0	123000000.0	123000000.0	7750.2	3703.1	2.94E-02	1.59E-02	1.59E-02	6.16E+10	3.66E+10	3.66E+10	0.000004 - 0.000036	selected points
					-27.2	522000000.0	200000000.0	200000000.0	7750.2	3703.1	6.74E-02	2.58E-02	2.58E-02	1.41E+11	6.45E+10	6.45E+10	0.000004 - 0.000036	selected points
					-28.2	667000000.0	117000000.0	117000000.0	7750.2	3703.1	8.61E-02	1.51E-02	1.51E-02	1.80E+11	5.50E+10	5.50E+10	0.000004 - 0.000036	selected points
					-29.2	769000000.0	102000000.0	102000000.0	7750.2	3703.1	9.92E-02	1.32E-02	1.32E-02	2.08E+11	5.88E+10	5.88E+10	0.000004 - 0.000036	selected points
					-30.2	900000000.0	96700000.0	96700000.0	7750.2	3703.1	1.16E-01	1.25E-02	1.25E-02	2.43E+11	6.61E+10	6.61E+10	0.000004 - 0.000036	selected points
					-31.2	979000000.0	175000000.0	175000000.0	7750.2	3703.1	1.26E-01	2.26E-02	2.26E-02	2.64E+11	8.13E+10	8.13E+10	0.000004 - 0.000036	selected points
					-32.2	1050000000.0	234000000.0	234000000.0	7750.2	3703.1	1.35E-01	3.02E-02	3.02E-02	2.84E+11	9.50E+10	9.50E+10	0.000004 - 0.000036	selected points

					-33.2	1150000000.0	320000000.0	320000000.0	7750.2	3703.1	1.48E-01	4.13E-02	4.13E-02	3.11E+11	1.16E+11	1.16E+11	0.000004 - 0.000036	selected points
					-34.2	1290000000.0	381000000.0	381000000.0	7750.2	3703.1	1.66E-01	4.92E-02	4.92E-02	3.48E+11	1.35E+11	1.35E+11	0.000004 - 0.000036	selected points
					-35.2	1380000000.0	199000000.0	199000000.0	7750.2	3703.1	1.78E-01	2.57E-02	2.57E-02	3.73E+11	1.08E+11	1.08E+11	0.000004 - 0.000036	selected points
			WISDOM	Shared impinger	-24.2	5365858.9	173650.0	1072052.0	7750.2	3703.1	6.92E-04	2.24E-05	1.38E-04	1.45E+09	3.65E+08	4.64E+08	0.000014 - 0.000034	binned
					-25.2	42895869.5	1134923.6	6952817.1	7750.2	3703.1	5.53E-03	1.46E-04	8.97E-04	1.16E+10	2.91E+09	3.45E+09	0.000014 - 0.000034	binned
					-26.2	108726562.1	1866015.9	11365519.9	7750.2	3703.1	1.40E-02	2.41E-04	1.47E-03	2.94E+10	7.36E+09	7.96E+09	0.000014 - 0.000034	binned
					-27.2	283021580.9	10001570.3	57286533.6	7750.2	3703.1	3.65E-02	1.29E-03	7.39E-03	7.64E+10	1.93E+10	2.46E+10	0.000014 - 0.000034	binned
					-28.2	460306250.1	3638784.2	21857829.3	7750.2	3703.1	5.94E-02	4.70E-04	2.82E-03	1.24E+11	3.11E+10	3.16E+10	0.000014 - 0.000034	binned
					-29.2	580311767.4	2857494.3	17269331.7	7750.2	3703.1	7.49E-02	3.69E-04	2.23E-03	1.57E+11	3.92E+10	3.95E+10	0.000014 - 0.000034	binned
					-30.2	662990737.3	36833803.3	5681290.6	7750.2	3703.1	8.55E-02	4.75E-03	7.33E-04	1.79E+11	4.59E+10	4.48E+10	0.000014 - 0.000034	binned
					-31.2	724320788.1	16535423.1	2617775.9	7750.2	3703.1	9.35E-02	2.13E-03	3.38E-04	1.96E+11	4.91E+10	4.89E+10	0.000014 - 0.000034	binned
					-32.2	731176449.7	13953352.0	2216390.4	7750.2	3703.1	9.43E-02	1.80E-03	2.86E-04	1.97E+11	4.95E+10	4.94E+10	0.000014 - 0.000034	binned
					-33.2	742842908.9	8542736.6	1366508.9	7750.2	3703.1	9.58E-02	1.10E-03	1.76E-04	2.01E+11	5.02E+10	5.02E+10	0.000014 - 0.000034	binned
					-34.2	747596607.4	5738312.7	921263.2	7750.2	3703.1	9.65E-02	7.40E-04	1.19E-04	2.02E+11	5.05E+10	5.05E+10	0.000014 - 0.000034	binned
					-35.2	764646731.0	27492783.8	4291489.1	7750.2	3703.1	9.87E-02	3.55E-03	5.54E-04	2.06E+11	5.22E+10	5.16E+10	0.000014 - 0.000034	binned
					-36.2	808999815.5	6594769.2	1057584.4	7750.2	3703.1	1.04E-01	8.51E-04	1.36E-04	2.18E+11	5.46E+10	5.46E+10	0.000014 - 0.000034	binned
					-37.2	2354924984.2	35702856.9	173403670.6	7750.2	3703.1	3.04E-01	4.61E-03	2.24E-02	6.36E+11	1.59E+11	1.66E+11	0.000014 - 0.000034	binned
20-Mar-15	AIDA-11	FS02	FRIDGE-STD	28	-20	411000	406000	406000	380	155	1.08E-03	1.07E-03	1.07E-03	2.65E+09	2.70E+09	2.70E+09	N/A	N/A
					-25	7880000	7800000	7800000	380	155	2.07E-02	2.05E-02	2.05E-02	5.08E+10	5.19E+10	5.19E+10	N/A	N/A
					-30	25800000	25500000	25500000	380	155	6.79E-02	6.71E-02	6.71E-02	1.66E+11	1.70E+11	1.70E+11	N/A	N/A
17-Mar-15	AIDA-06	SM04	FRIDGE-STD	6	-10	648000	297000	297000	260	25	2.59E-03	1.19E-03	1.19E-03	2.70E+10	1.41E+10	1.41E+10	N/A	N/A
					-15	1150000	530000	530000	260	25	4.60E-03	2.12E-03	2.12E-03	4.78E+10	2.51E+10	2.51E+10	N/A	N/A
					-20	1350000	621000	621000	260	25	5.40E-03	2.48E-03	2.48E-03	5.62E+10	2.94E+10	2.94E+10	N/A	N/A
20-Mar-15	APC-15	SM04	BINARY	Shared impinger	-4.2	16300.0	31900.0	14000.0	27802.0	4028.0	5.86E-07	1.15E-06	5.04E-07	4.05E+06	7.98E+06	3.62E+06	0.6	binned
					-5.2	110000.0	170000.0	67600.0	27802.0	4028.0	3.96E-06	6.11E-06	2.43E-06	2.73E+07	4.28E+07	1.81E+07	0.6	binned
					-6.2	348000.0	283000.0	165000.0	27802.0	4028.0	1.25E-05	1.02E-05	5.93E-06	8.64E+07	7.35E+07	4.63E+07	0.6	binned
					-7.2	1400000.0	1820000.0	804000.0	27802.0	4028.0	5.04E-05	6.55E-05	2.89E-05	3.48E+08	4.60E+08	2.18E+08	0.6	binned
					-8.2	10500000.0	31400000.0	7810000.0	27802.0	4028.0	3.78E-04	1.13E-03	2.81E-04	2.61E+09	7.82E+09	2.05E+09	0.6	binned
					-9.2	56000000.0	49100000.0	26800000.0	27802.0	4028.0	2.01E-03	1.77E-03	9.64E-04	1.39E+10	1.27E+10	7.51E+09	0.6	binned
					-10.2	129000000.0	69000000.0	50300000.0	27802.0	4028.0	4.64E-03	2.48E-03	1.81E-03	3.20E+10	1.89E+10	1.48E+10	0.6	binned
					-11.2	177000000.0	71500000.0	62500000.0	27802.0	4028.0	6.37E-03	2.57E-03	2.25E-03	4.39E+10	2.09E+10	1.90E+10	0.6	binned
					-12.2	239000000.0	53000000.0	105000000.0	27802.0	4028.0	8.60E-03	1.91E-03	3.78E-03	5.93E+10	1.98E+10	3.00E+10	0.6	binned
					-13.2	305000000.0	13000000.0	159000000.0	27802.0	4028.0	1.10E-02	4.68E-04	5.72E-03	7.57E+10	1.92E+10	4.38E+10	0.6	binned
					-14.2	157000000.0	0.0	0.0	27802.0	4028.0	5.65E-03	0.00E+00	0.00E+00	3.90E+10	9.74E+09	9.74E+09	0.6	binned
					-15.2	170000000.0	0.0	0.0	27802.0	4028.0	6.11E-03	0.00E+00	0.00E+00	4.22E+10	1.06E+10	1.06E+10	0.6	binned
					-16.2	183000000.0	0.0	0.0	27802.0	4028.0	6.58E-03	0.00E+00	0.00E+00	4.54E+10	1.14E+10	1.14E+10	0.6	binned
					-19.2	198000000.0	0.0	0.0	27802.0	4028.0	7.12E-03	0.00E+00	0.00E+00	4.92E+10	1.23E+10	1.23E+10	0.6	binned
					-25.2	230000000.0	118000000.0	17000000.0	27802.0	4028.0	8.27E-03	4.24E-03	6.11E-04	5.71E+10	3.26E+10	1.49E+10	0.6	binned
					-26.2	259000000.0	10500000.0	10500000.0	27802.0	4028.0	9.32E-03	3.78E-04	3.78E-04	6.43E+10	1.63E+10	1.63E+10	0.6	binned
					-28.2	292000000.0	0.0	0.0	27802.0	4028.0	1.05E-02	0.00E+00	0.00E+00	7.25E+10	1.81E+10	1.81E+10	0.6	binned
					-29.2	318000000.0	0.0	0.0	27802.0	4028.0	1.14E-02	0.00E+00	0.00E+00	7.89E+10	1.97E+10	1.97E+10	0.6	binned
					-30.2	366000000.0	17500000.0	17500000.0	27802.0	4028.0	1.32E-02	6.29E-04	6.29E-04	9.09E+10	2.31E+10	2.31E+10	0.6	binned
					-31.2	383000000.0	43000000.0	35000000.0	27802.0	4028.0	1.38E-02	1.55E-03	1.26E-03	9.51E+10	2.61E+10	2.53E+10	0.6	binned
					-32.2	522000000.0	39500000.0	39500000.0	27802.0	4028.0	1.88E-02	1.42E-03	1.42E-03	1.30E+11	3.38E+10	3.38E+10	0.6	binned
			CMU-CS	Shared impinger	-4.0	11174.5	15143.2	15143.2	27802.0	4028.0	4.01929E-07	5.44677E-07	5.45E-07	2.77E+06	3.82E+06	3.82E+06	0.1	binned, scan1
					-5.0	134214.0	23188.9	23188.9	27802.0	4028.0	4.82746E-06	8.34068E-07	8.34E-07	3.33E+07	1.01E+07	1.01E+07	0.1	binned, scan1
					-6.0	343715.0	12007.2	12007.2	27802.0	4028.0	1.23629E-05	4.3188E-07	4.32E-07	8.53E+07	2.15E+07	2.15E+07	0.1	binned, scan1
					-6.0	1671760.0	0.0	0.0	27802.0	4028.0	6.01306E-05	0	0.00E+00	4.15E+08	1.04E+08	1.04E+08	0.1	binned, scan2

					-7.0	13561700.0	1620220.0	1620220.0	27802.0	4028.0	0.000487793	5.82767E-05	5.83E-05	3.37E+09	9.33E+08	9.33E+08	0.1	binned, scan2
					-8.0	86400900.0	25160200.0	25160200.0	27802.0	4028.0	0.003107703	0.000904972	9.05E-04	2.15E+10	8.23E+09	8.23E+09	0.1	binned, scan2
					-9.0	118748000.0	24566400.0	24566400.0	27802.0	4028.0	0.004271177	0.000883614	8.84E-04	2.95E+10	9.57E+09	9.57E+09	0.1	binned, scan2
					-10.0	178996000.0	17619000.0	17619000.0	27802.0	4028.0	0.006438202	0.000633727	6.34E-04	4.44E+10	1.19E+10	1.19E+10	0.1	binned, scan2
					-11.0	213774000.0	37345300.0	37345300.0	27802.0	4028.0	0.007689111	0.001343251	1.34E-03	5.31E+10	1.62E+10	1.62E+10	0.1	binned, scan2
					-12.0	234104000.0	0.0	0.0	27802.0	4028.0	0.008420349	0	0.00E+00	5.81E+10	1.45E+10	1.45E+10	0.1	binned, scan2
					-13.0	264820000.0	0.0	0.0	27802.0	4028.0	0.009525155	0	0.00E+00	6.57E+10	1.64E+10	1.64E+10	0.1	binned, scan2
					-14.0	382300000.0	0.0	0.0	27802.0	4028.0	0.013750724	0	0.00E+00	9.49E+10	2.37E+10	2.37E+10	0.1	binned, scan2
					-15.0	460110000.0	0.0	0.0	27802.0	4028.0	0.016549426	0	0.00E+00	1.14E+11	2.86E+10	2.86E+10	0.1	binned, scan2
					-3.0	14278.2	0.0	0.0	27802.0	4028.0	5.13564E-07	0	0.00E+00	3.54E+06	8.86E+05	8.86E+05	0.1	binned, first freeze
					-4.0	169419.0	18058.5	18058.5	27802.0	4028.0	6.09373E-06	6.49536E-07	6.50E-07	4.21E+07	1.14E+07	1.14E+07	0.1	binned, first freeze
					-5.0	490146.0	51065.3	51065.3	27802.0	4028.0	1.76298E-05	1.83674E-06	1.84E-06	1.22E+08	3.30E+07	3.30E+07	0.1	binned, first freeze
					-6.0	1055580.0	0.0	0.0	27802.0	4028.0	3.79675E-05	0	0.00E+00	2.62E+08	6.55E+07	6.55E+07	0.1	binned, first freeze
			IS	Shared impinger	-3.7	161.3	73.5	108.1	27802.0	4028.0	5.80E-09	3.89E-09	2.64E-09	4.01E+04	2.86E+04	2.08E+04	50	
					-4.3	848.8	527.0	1218.2	27802.0	4028.0	3.05E-08	4.38E-08	1.90E-08	2.11E+05	3.07E+05	1.41E+05	50	
					-4.5	3227.0	1470.6	2161.8	27802.0	4028.0	1.16E-07	7.78E-08	5.29E-08	8.01E+05	5.73E+05	4.16E+05	50	
					-4.7	7302.7	3091.4	3782.6	27802.0	4028.0	2.63E-07	1.36E-07	1.11E-07	1.81E+06	1.04E+06	8.91E+05	50	
					-5.0	12433.2	8297.7	22122.5	27802.0	4028.0	4.47E-07	7.96E-07	2.98E-07	3.09E+06	5.55E+06	2.20E+06	50	
					-5.3	50186.2	24058.9	37883.7	27802.0	4028.0	1.81E-06	1.36E-06	8.65E-07	1.25E+07	9.91E+06	6.74E+06	50	
					-5.6	64539.2	29411.1	43235.9	27802.0	4028.0	2.32E-06	1.56E-06	1.06E-06	1.60E+07	1.15E+07	8.33E+06	50	
					-6.0	72640.9	32423.6	46248.4	27802.0	4028.0	2.61E-06	1.66E-06	1.17E-06	1.80E+07	1.23E+07	9.23E+06	50	
					-6.5	146054.4	61827.9	75652.6	27802.0	4028.0	5.25E-06	2.72E-06	2.22E-06	3.63E+07	2.09E+07	1.78E+07	50	
					-6.8	231370.6	105402.5	119227.3	27802.0	4028.0	8.32E-06	4.29E-06	3.79E-06	5.74E+07	3.29E+07	2.98E+07	50	
					-6.8	435039.3	254399.2	530895.1	27802.0	4028.0	1.56E-05	1.91E-05	9.15E-06	1.08E+08	1.35E+08	6.87E+07	50	
					-7.0	642164.5	341393.6	617889.5	27802.0	4028.0	2.31E-05	2.22E-05	1.23E-05	1.59E+08	1.58E+08	9.37E+07	50	
					-7.5	1630304.3	714872.6	991368.4	27802.0	4028.0	5.86E-05	3.57E-05	2.57E-05	4.05E+08	2.66E+08	2.04E+08	50	
					-7.8	4627411.4	2108049.8	2384545.7	27802.0	4028.0	1.66E-04	8.58E-05	7.58E-05	1.15E+09	6.58E+08	5.97E+08	50	
					-7.8	3666316.6	2439587.6	6662080.5	27802.0	4028.0	1.32E-04	2.40E-04	8.77E-05	9.10E+08	1.67E+09	6.47E+08	50	
					-8.0	12299570.0	5998562.2	10221055.1	27802.0	4028.0	4.42E-04	3.68E-04	2.16E-04	3.05E+09	2.65E+09	1.67E+09	50	
					-8.5	30788938.4	12180145.7	16402638.5	27802.0	4028.0	1.11E-03	5.90E-04	4.38E-04	7.64E+09	4.50E+09	3.58E+09	50	
					-9.0	43320559.9	16421872.1	20644364.9	27802.0	4028.0	1.56E-03	7.43E-04	5.91E-04	1.08E+10	5.79E+09	4.88E+09	50	
					-9.5	56604614.0	21300817.3	25523310.1	27802.0	4028.0	2.04E-03	9.18E-04	7.66E-04	1.41E+10	7.25E+09	6.35E+09	50	
					-10.0	77447026.8	30127708.5	34350201.3	27802.0	4028.0	2.79E-03	1.24E-03	1.08E-03	1.92E+10	9.79E+09	8.89E+09	50	
					-10.5	77447026.8	30127708.5	34350201.3	27802.0	4028.0	2.79E-03	1.24E-03	1.08E-03	1.92E+10	9.79E+09	8.89E+09	50	
					-10.0	99465256.7	61492523.7	145942381.3	27802.0	4028.0	3.58E-03	5.25E-03	2.21E-03	2.47E+10	3.68E+10	1.65E+10	50	
					-10.5	126554894.6	73584166.6	158034024.3	27802.0	4028.0	4.55E-03	5.68E-03	2.65E-03	3.14E+10	4.00E+10	1.99E+10	50	
					-11.0	126554894.6	73584166.6	158034024.3	27802.0	4028.0	4.55E-03	5.68E-03	2.65E-03	3.14E+10	4.00E+10	1.99E+10	50	
					-11.5	154667021.1	85321178.5	169771036.1	27802.0	4028.0	5.56E-03	6.11E-03	3.07E-03	3.84E+10	4.32E+10	2.33E+10	50	
					-12.0	183881861.4	96879452.2	181329309.8	27802.0	4028.0	6.61E-03	6.52E-03	3.48E-03	4.57E+10	4.64E+10	2.66E+10	50	
					-13.0	183881861.4	96879452.2	181329309.8	27802.0	4028.0	6.61E-03	6.52E-03	3.48E-03	4.57E+10	4.64E+10	2.66E+10	50	
					-14.0	183881861.4	96879452.2	181329309.8	27802.0	4028.0	6.61E-03	6.52E-03	3.48E-03	4.57E+10	4.64E+10	2.66E+10	50	
					-15.0	183881861.4	96879452.2	181329309.8	27802.0	4028.0	6.61E-03	6.52E-03	3.48E-03	4.57E+10	4.64E+10	2.66E+10	50	
					-16.0	183881861.4	96879452.2	181329309.8	27802.0	4028.0	6.61E-03	6.52E-03	3.48E-03	4.57E+10	4.64E+10	2.66E+10	50	
					-17.0	183881861.4	96879452.2	181329309.8	27802.0	4028.0	6.61E-03	6.52E-03	3.48E-03	4.57E+10	4.64E+10	2.66E+10	50	

					-18.0	183881861.4	96879452.2	181329309.8	27802.0	4028.0	6.61E-03	6.52E-03	3.48E-03	4.57E+10	4.64E+10	2.66E+10	50	
					-19.0	183881861.4	96879452.2	181329309.8	27802.0	4028.0	6.61E-03	6.52E-03	3.48E-03	4.57E+10	4.64E+10	2.66E+10	50	
					-20.0	214289468.8	108392712.4	192842570.0	27802.0	4028.0	7.71E-03	6.94E-03	3.90E-03	5.32E+10	4.97E+10	3.00E+10	50	
					-21.0	245991399.7	119971244.2	204421101.8	27802.0	4028.0	8.85E-03	7.35E-03	4.32E-03	6.11E+10	5.30E+10	3.35E+10	50	
					-22.0	245991399.7	119971244.2	204421101.8	27802.0	4028.0	8.85E-03	7.35E-03	4.32E-03	6.11E+10	5.30E+10	3.35E+10	50	
					-23.0	245991399.7	119971244.2	204421101.8	27802.0	4028.0	8.85E-03	7.35E-03	4.32E-03	6.11E+10	5.30E+10	3.35E+10	50	
					-24.0	245991399.7	119971244.2	204421101.8	27802.0	4028.0	8.85E-03	7.35E-03	4.32E-03	6.11E+10	5.30E+10	3.35E+10	50	
					-25.0	255453695.6	124732417.0	211753270.4	27802.0	4028.0	9.19E-03	7.62E-03	4.49E-03	6.34E+10	5.49E+10	3.48E+10	50	
					-26.0	255453695.6	124732417.0	211753270.4	27802.0	4028.0	9.19E-03	7.62E-03	4.49E-03	6.34E+10	5.49E+10	3.48E+10	50	
					-27.0	302024043.1	154455824.1	265054162.5	27802.0	4028.0	1.09E-02	9.53E-03	5.56E-03	7.50E+10	6.84E+10	4.27E+10	50	
			KIT-CS	Shared impinger	-4.5	61593.2	0.0	0.0	27802.0	4028.0	2.22E-06	0.00E+00	0.00E+00	1.53E+07	3.82E+06	3.82E+06	5.00E-04	
					-6.0	152162.0	0.0	0.0	27802.0	4028.0	5.47E-06	0.00E+00	0.00E+00	3.78E+07	9.44E+06	9.44E+06	5.00E-04	
					-7.0	238969.7	100093.8	100093.8	27802.0	4028.0	8.60E-06	3.60E-06	3.60E-06	5.93E+07	2.89E+07	2.89E+07	5.00E-04	
					-8.0	1749105.9	897594.5	897594.5	27802.0	4028.0	6.29E-05	3.23E-05	3.23E-05	4.34E+08	2.48E+08	2.48E+08	5.00E-04	
					-8.7	18916879.2	2942698.3	2942698.3	27802.0	4028.0	6.80E-04	1.06E-04	1.06E-04	4.70E+09	1.38E+09	1.38E+09	5.00E-04	
					-9.6	67659429.6	4210943.9	4210943.9	27802.0	4028.0	2.43E-03	1.51E-04	1.51E-04	1.68E+10	4.33E+09	4.33E+09	5.00E-04	
					-10.5	125300935.4	10843885.1	10843885.1	27802.0	4028.0	4.51E-03	3.90E-04	3.90E-04	3.11E+10	8.23E+09	8.23E+09	5.00E-04	
			NCSU-CS	Shared impinger	-5.2	15611.4	14676.3	14676.3	27802.0	4028.0	5.62E-07	5.28E-07	5.28E-07	3.88E+06	3.77E+06	3.77E+06	1	binned
					-6.2	121527.3	102695.9	102695.9	27802.0	4028.0	4.37E-06	3.69E-06	3.69E-06	3.02E+07	2.66E+07	2.66E+07	1	binned
					-7.2	326734.6	258366.4	258366.4	27802.0	4028.0	1.18E-05	9.29E-06	9.29E-06	8.11E+07	6.73E+07	6.73E+07	1	binned
					-8.2	2843331.0	2843330.0	3240235.0	27802.0	4028.0	1.02E-04	1.17E-04	1.02E-04	7.06E+08	8.24E+08	7.28E+08	1	binned
					-9.2	64464901.3	19194131.3	19194131.3	27802.0	4028.0	2.32E-03	6.90E-04	6.90E-04	1.60E+10	6.22E+09	6.22E+09	1	binned
					-10.2	145302193.0	39137536.4	39137536.4	27802.0	4028.0	5.23E-03	1.41E-03	1.41E-03	3.61E+10	1.33E+10	1.33E+10	1	binned
					-11.2	178558020.6	18673608.4	18673608.4	27802.0	4028.0	6.42E-03	6.72E-04	6.72E-04	4.43E+10	1.20E+10	1.20E+10	1	binned
					-12.2	196487719.5	7985649.3	7985649.3	27802.0	4028.0	7.07E-03	2.87E-04	2.87E-04	4.88E+10	1.24E+10	1.24E+10	1	binned
					-13.2	217005649.5	5940382.1	5940382.1	27802.0	4028.0	7.81E-03	2.14E-04	2.14E-04	5.39E+10	1.35E+10	1.35E+10	1	binned
					-14.2	243388759.6	20119427.8	20119427.8	27802.0	4028.0	8.75E-03	7.24E-04	7.24E-04	6.04E+10	1.59E+10	1.59E+10	1	binned
					-15.2	263478270.2	36340286.2	36340286.2	27802.0	4028.0	9.48E-03	1.31E-03	1.31E-03	6.54E+10	1.87E+10	1.87E+10	1	binned
					-16.2	278572841.2	31995682.1	31995682.1	27802.0	4028.0	1.00E-02	1.15E-03	1.15E-03	6.92E+10	1.90E+10	1.90E+10	1	binned
					-17.2	285888521.3	39605092.2	39605092.2	27802.0	4028.0	1.03E-02	1.42E-03	1.42E-03	7.10E+10	2.03E+10	2.03E+10	1	binned
					-18.2	291147767.1	43183891.1	43183891.1	27802.0	4028.0	1.05E-02	1.55E-03	1.55E-03	7.23E+10	2.10E+10	2.10E+10	1	binned
					-19.2	296407012.9	46762689.9	46762689.9	27802.0	4028.0	1.07E-02	1.68E-03	1.68E-03	7.36E+10	2.18E+10	2.18E+10	1	binned
					-20.2	301666258.7	50341488.7	50341488.7	27802.0	4028.0	1.09E-02	1.81E-03	1.81E-03	7.49E+10	2.25E+10	2.25E+10	1	binned
					-21.2	306925504.5	53920287.6	53920287.6	27802.0	4028.0	1.10E-02	1.94E-03	1.94E-03	7.62E+10	2.33E+10	2.33E+10	1	binned
					-22.2	316369189.6	61887263.0	61887263.0	27802.0	4028.0	1.14E-02	2.23E-03	2.23E-03	7.85E+10	2.49E+10	2.49E+10	1	binned
					-23.2	333245685.2	64402593.1	64402593.1	27802.0	4028.0	1.20E-02	2.32E-03	2.32E-03	8.27E+10	2.61E+10	2.61E+10	1	binned
					-24.2	368610535.1	30680748.6	30680748.7	27802.0	4028.0	1.33E-02	1.10E-03	1.10E-03	9.15E+10	2.41E+10	2.41E+10	1	binned
			NIPI	Shared impinger	-3.0	2.6	10777.9	2104.5	27802.0	4028.0	9.41E-08	3.88E-07	7.57E-08	6.49E+05	5.47E+05	5.47E+05	1	binned
					-4.0	19.9	98536.9	16560.0	27802.0	4028.0	7.16E-07	3.54E-06	5.96E-07	4.94E+06	4.29E+06	4.29E+06	1	binned
					-5.0	3856.7	5094304.0	2194974.3	27802.0	4028.0	1.39E-04	1.83E-04	7.89E-05	9.57E+08	5.95E+08	5.95E+08	1	binned
					-6.0	3856.7	10442819.4	2816519.7	27802.0	4028.0	1.39E-04	3.76E-04	1.01E-04	9.57E+08	7.39E+08	7.39E+08	1	binned
					-7.0	5371.5	12079489.3	3718112.4	27802.0	4028.0	1.93E-04	4.34E-04	1.34E-04	1.33E+09	9.81E+08	9.81E+08	1	binned
					-8.0	28888.9	79343201.5	21177976.9	27802.0	4028.0	1.04E-03	2.85E-03	7.62E-04	7.17E+09	5.56E+09	5.56E+09	1	binned
					-9.0	100054.5	154602061.8	60743095.7	27802.0	4028.0	3.60E-03	5.56E-03	2.18E-03	2.48E+10	1.63E+10	1.63E+10	1	binned
					-10.0	161682.8	246889543.2	97700677.1	27802.0	4028.0	5.82E-03	8.88E-03	3.51E-03	4.01E+10	2.62E+10	2.62E+10	1	binned
					-11.0	161682.8	161682812.9	80841406.5	27802.0	4028.0	5.82E-03	5.82E-03	2.91E-03	4.01E+10	2.24E+10	2.24E+10	1	binned
					-12.0	183655.8	183655794.1	91827897.0	27802.0	4028.0	6.61E-03	6.61E-03	3.30E-03	4.56E+10	2.55E+10	2.55E+10	1	binned
					-13.0	202787.8	202787800.4	101393900.2	27802.0	4028.0	7.29E-03	7.29E-03	3.65E-03	5.03E+10	2.81E+10	2.81E+10	1	binned
					-14.0	223912.8	223912848.5	111956424.3	27802.0	4028.0	8.05E-03	8.05E-03	4.03E-03	5.56E+10	3.11E+10	3.11E+10	1	binned

			VODCA	Shared impinger	-10.2	76704112.5	7478069.5	7478069.5	27802.0	4028.0	2.76E-03	2.69E-04	2.69E-04	1.90E+10	5.11E+09	5.11E+09	0.000004 - 0.000036	selected points
					-11.2	84512762.3	15771703.5	15771703.5	27802.0	4028.0	3.04E-03	5.67E-04	5.67E-04	2.10E+10	6.55E+09	6.55E+09	0.000004 - 0.000036	selected points
					-12.2	95141425.5	15379330.1	15379330.1	27802.0	4028.0	3.42E-03	5.53E-04	5.53E-04	2.36E+10	7.03E+09	7.03E+09	0.000004 - 0.000036	selected points
					-13.2	131549740.0	2422324.1	2422324.1	27802.0	4028.0	4.73E-03	8.71E-05	8.71E-05	3.27E+10	8.19E+09	8.19E+09	0.000004 - 0.000036	selected points
					-14.2	160878067.6	7707190.2	7707190.2	27802.0	4028.0	5.79E-03	2.77E-04	2.77E-04	3.99E+10	1.02E+10	1.02E+10	0.000004 - 0.000036	selected points
					-15.2	205659593.9	19651144.4	19651144.4	27802.0	4028.0	7.40E-03	7.07E-04	7.07E-04	5.11E+10	1.37E+10	1.37E+10	0.000004 - 0.000036	selected points
					-16.2	215581389.0	28008951.3	28008951.3	27802.0	4028.0	7.75E-03	1.01E-03	1.01E-03	5.35E+10	1.51E+10	1.51E+10	0.000004 - 0.000036	selected points
					-17.2	233260669.0	42968859.6	42968859.6	27802.0	4028.0	8.39E-03	1.55E-03	1.55E-03	5.79E+10	1.80E+10	1.80E+10	0.000004 - 0.000036	selected points
					-18.2	248696385.5	56112968.0	56112968.0	27802.0	4028.0	8.95E-03	2.02E-03	2.02E-03	6.17E+10	2.08E+10	2.08E+10	0.000004 - 0.000036	selected points
					-19.2	275384883.8	79119616.9	79119616.9	27802.0	4028.0	9.91E-03	2.85E-03	2.85E-03	6.84E+10	2.60E+10	2.60E+10	0.000004 - 0.000036	selected points
					-20.2	295377656.5	96475374.6	96475374.6	27802.0	4028.0	1.06E-02	3.47E-03	3.47E-03	7.33E+10	3.02E+10	3.02E+10	0.000004 - 0.000036	selected points
					-21.2	314595379.9	113015724.0	113015724.0	27802.0	4028.0	1.13E-02	4.06E-03	4.06E-03	7.81E+10	3.42E+10	3.42E+10	0.000004 - 0.000036	selected points
					-22.2	306109465.4	104824512.7	104824512.7	27802.0	4028.0	1.10E-02	3.77E-03	3.77E-03	7.60E+10	3.22E+10	3.22E+10	0.000004 - 0.000036	selected points
					-23.2	295743619.5	93346341.9	93346341.9	27802.0	4028.0	1.06E-02	3.36E-03	3.36E-03	7.34E+10	2.96E+10	2.96E+10	0.000004 - 0.000036	selected points
					-24.2	290769318.9	82749566.4	82749566.4	27802.0	4028.0	1.05E-02	2.98E-03	2.98E-03	7.22E+10	2.73E+10	2.73E+10	0.000004 - 0.000036	selected points
					-25.2	282853327.8	69869168.6	69869168.6	27802.0	4028.0	1.02E-02	2.51E-03	2.51E-03	7.02E+10	2.47E+10	2.47E+10	0.000004 - 0.000036	selected points
					-26.2	273283509.9	63141047.8	63141047.8	27802.0	4028.0	9.83E-03	2.27E-03	2.27E-03	6.78E+10	2.31E+10	2.31E+10	0.000004 - 0.000036	selected points
					-27.2	263713692.0	56536059.0	56536059.0	27802.0	4028.0	9.49E-03	2.03E-03	2.03E-03	6.55E+10	2.16E+10	2.16E+10	0.000004 - 0.000036	selected points
					-28.2	250955100.3	47935618.1	47935618.1	27802.0	4028.0	9.03E-03	1.72E-03	1.72E-03	6.23E+10	1.96E+10	1.96E+10	0.000004 - 0.000036	selected points
					-29.2	241385282.4	41651089.0	41651089.0	27802.0	4028.0	8.68E-03	1.50E-03	1.50E-03	5.99E+10	1.82E+10	1.82E+10	0.000004 - 0.000036	selected points
					-30.2	247815276.9	48691126.5	48691126.5	27802.0	4028.0	8.91E-03	1.75E-03	1.75E-03	6.15E+10	1.96E+10	1.96E+10	0.000004 - 0.000036	selected points
					-31.2	250009889.9	50565122.2	50565122.2	27802.0	4028.0	8.99E-03	1.82E-03	1.82E-03	6.21E+10	2.00E+10	2.00E+10	0.000004 - 0.000036	selected points
					-32.2	264433963.2	44950395.9	44950395.9	27802.0	4028.0	9.51E-03	1.62E-03	1.62E-03	6.56E+10	1.98E+10	1.98E+10	0.000004 - 0.000036	selected points
					-33.2	275252018.3	40689482.0	40689482.0	27802.0	4028.0	9.90E-03	1.46E-03	1.46E-03	6.83E+10	1.98E+10	1.98E+10	0.000004 - 0.000036	selected points
					-34.2	262942139.2	32674451.3	32674451.3	27802.0	4028.0	9.46E-03	1.18E-03	1.18E-03	6.53E+10	1.82E+10	1.82E+10	0.000004 - 0.000036	selected points
			WISDOM	Shared impinger	-8.2	37870409.8	354694.0	86729.6	27802.0	4028.0	1.36E-03	1.28E-05	3.12E-06	9.40E+09	2.35E+09	2.35E+09	0.000014 - 0.000034	binned
					-9.2	109349118.6	23004923.3	24533815.0	27802.0	4028.0	3.93E-03	8.27E-04	8.82E-04	2.71E+10	8.87E+09	9.12E+09	0.000014 - 0.000034	binned
					-10.2	143767561.7	23555829.2	24807570.7	27802.0	4028.0	5.17E-03	8.47E-04	8.92E-04	3.57E+10	1.07E+10	1.08E+10	0.000014 - 0.000034	binned
					-11.2	180821284.2	30846117.9	31125827.6	27802.0	4028.0	6.50E-03	1.11E-03	1.12E-03	4.49E+10	1.36E+10	1.36E+10	0.000014 - 0.000034	binned
					-12.2	217327717.8	28167395.2	28202110.5	27802.0	4028.0	7.82E-03	1.01E-03	1.01E-03	5.40E+10	1.52E+10	1.52E+10	0.000014 - 0.000034	binned
					-13.2	256612873.3	15327839.3	16980741.1	27802.0	4028.0	9.23E-03	5.51E-04	6.11E-04	6.37E+10	1.64E+10	1.65E+10	0.000014 - 0.000034	binned
					-14.2	298180888.9	28421498.9	29738879.5	27802.0	4028.0	1.07E-02	1.02E-03	1.07E-03	7.40E+10	1.98E+10	1.99E+10	0.000014 - 0.000034	binned
					-15.2	315743875.0	61855536.7	55785715.6	27802.0	4028.0	1.14E-02	2.22E-03	2.01E-03	7.84E+10	2.49E+10	2.40E+10	0.000014 - 0.000034	binned
					-16.2	315743875.0	61855536.7	55785715.6	27802.0	4028.0	1.14E-02	2.22E-03	2.01E-03	7.84E+10	2.49E+10	2.40E+10	0.000014 - 0.000034	binned
					-17.2	321289842.4	50550458.8	46693172.2	27802.0	4028.0	1.16E-02	1.82E-03	1.68E-03	7.98E+10	2.36E+10	2.31E+10	0.000014 - 0.000034	binned
					-18.2	348078692.9	111585496.0	84792013.3	27802.0	4028.0	1.25E-02	4.01E-03	3.05E-03	8.64E+10	3.51E+10	3.02E+10	0.000014 - 0.000034	binned
					-19.2	363326211.9	116195545.9	88164997.0	27802.0	4028.0	1.31E-02	4.18E-03	3.17E-03	9.02E+10	3.66E+10	3.14E+10	0.000014 - 0.000034	binned
					-20.2	370188828.5	99778696.5	78250798.5	27802.0	4028.0	1.33E-02	3.59E-03	2.81E-03	9.19E+10	3.38E+10	3.01E+10	0.000014 - 0.000034	binned
					-21.2	387059852.7	103733430.2	81596947.2	27802.0	4028.0	1.39E-02	3.73E-03	2.93E-03	9.61E+10	3.52E+10	3.14E+10	0.000014 - 0.000034	binned
					-22.2	387059852.7	103733430.2	81596947.2	27802.0	4028.0	1.39E-02	3.73E-03	2.93E-03	9.61E+10	3.52E+10	3.14E+10	0.000014 - 0.000034	binned
					-23.2	395991394.2	84770704.3	71244549.6	27802.0	4028.0	1.42E-02	3.05E-03	2.56E-03	9.83E+10	3.24E+10	3.03E+10	0.000014 - 0.000034	binned
					-24.2	395991394.2	84770704.3	71244549.6	27802.0	4028.0	1.42E-02	3.05E-03	2.56E-03	9.83E+10	3.24E+10	3.03E+10	0.000014 - 0.000034	binned
					-25.2	395991394.2	84770704.3	71244549.6	27802.0	4028.0	1.42E-02	3.05E-03	2.56E-03	9.83E+10	3.24E+10	3.03E+10	0.000014 - 0.000034	binned
					-26.2	395991394.2	84770704.3	71244549.6	27802.0	4028.0	1.42E-02	3.05E-03	2.56E-03	9.83E+10	3.24E+10	3.03E+10	0.000014 - 0.000034	binned
					-27.2	395991394.2	84770704.3	71244549.6	27802.0	4028.0	1.42E-02	3.05E-03	2.56E-03	9.83E+10	3.24E+10	3.03E+10	0.000014 - 0.000034	binned
					-28.2	395991394.2	84770704.3	71244549.6	27802.0	4028.0	1.42E-02	3.05E-03	2.56E-03	9.83E+10	3.24E+10	3.03E+10	0.000014 - 0.000034	binned
					-29.2	403937789.2	109084045.3	82856140.1	27802.0	4028.0	1.45E-02	3.92E-03	2.98E-03	1.00E+11	3.69E+10	3.24E+10	0.000014 - 0.000034	binned
					-30.2	443612583.2	71560768.7	61752108.7	27802.0	4028.0	1.60E-02	2.57E-03	2.22E-03	1.10E+11	3.28E+10	3.15E+10	0.000014 - 0.000034	binned
					-31.2	443612583.2	71560768.7	61752108.7	27802.0	4028.0	1.60E-02	2.57E-03	2.22E-03	1.10E+11	3.28E+10	3.15E+10	0.000014 - 0.000034	binned

					-32.2	443612583.2	71560768.7	61752108.7	27802.0	4028.0	1.60E-02	2.57E-03	2.22E-03	1.10E+11	3.28E+10	3.15E+10	0.000014 - 0.000034	binned
					-33.2	443612583.2	71560768.7	61752108.7	27802.0	4028.0	1.60E-02	2.57E-03	2.22E-03	1.10E+11	3.28E+10	3.15E+10	0.000014 - 0.000034	binned
					-34.2	443612583.2	71560768.7	61752108.7	27802.0	4028.0	1.60E-02	2.57E-03	2.22E-03	1.10E+11	3.28E+10	3.15E+10	0.000014 - 0.000034	binned
					-35.2	443612583.2	71560768.7	61752108.7	27802.0	4028.0	1.60E-02	2.57E-03	2.22E-03	1.10E+11	3.28E+10	3.15E+10	0.000014 - 0.000034	binned
					-36.2	519164891.9	24140515.5	23840216.5	27802.0	4028.0	1.87E-02	8.68E-04	8.57E-04	1.29E+11	3.28E+10	3.28E+10	0.000014 - 0.000034	binned

*: FRIDGE-STD and DFPC-ISAC data are diffusion chamber data processed at 101% relative humidity.